Pretreatment of Asphaltenes as Precursors for Carbon Fiber Production

by

Yuna Kim

A thesis submitted in partial fulfillment of the requirements for the degree of

Master of Science

in

Chemical Engineering

Department of Chemical and Materials Engineering
University of Alberta

ABSTRACT

Oilsands bitumen produced from Alberta, Canada contains 14–20 wt.% *n*-pentane insoluble asphaltenes. Separation of asphaltenes from the bitumen by solvent deasphalting has the benefit of improving the properties of the deasphalted oil compared to the bitumen, for example, by decreasing its viscosity and increasing its hydrogen-to-carbon ratio. Due to the low hydrogen-to-carbon ratio and high aromatic content of the asphaltenes, the asphaltenes fraction potentially is a good feedstock for carbon fiber production.

The processing path for converting asphaltenes to carbon fibers involves the following steps. First, melt-spinning is used to convert the asphaltenes into fibrous form. Then the precursor fibers are oxidatively stabilized to render them infusible for the final carbonation step, during which the fibers are subjected to high temperatures, up to 1500 °C, in an inert atmosphere.

When using asphaltenes as a precursor for carbon fibers production, the production process can benefit from pretreatment of the asphaltenes to increase its softening point temperature. Low softening point is undesirable as it can lead to a lengthy stabilization process as well as potential fusing of the fibers during stabilization and carbonization steps. In this study, industrially pentane solvent deasphalted asphaltenes was pretreated in three ways to increase its softening point temperature: (i) solvent deasphalting / solvent extraction with *n*-pentane and *n*-heptane as solvent (ii) autoxidation and (iii) halogenation/dehalogenation. From this investigation, it was found that all three treatments were effective in increasing the softening point. Additionally, all three pretreatments were also effective in improving the melt spin productivity during the melt-spinning process. One exception was noted, namely, when removing the *n*-heptane soluble materials by rigorous solvent deasphalting, it did not improve melt spin productivity.

Keywords: Asphaltenes, Carbon Fibers, Pretreatment, Solvent Deasphalting, Autoxidation, Halogenation, Dehalogenation

PREFACE

Chapter 3, 4 and **5** will be submitted to be published as "Kim, Y.; Leistenschneider, D.; De Klerk, A.; Chen, W. Autoxidation and halogenation as pretreatment of oilsands bitumen derived asphaltenes to improve carbon fiber production." I was responsible for data collection and analysis as well as the manuscript composition. Desiree Leistenschneider was involved with data collection and analysis. Arno de Klerk and Weixing Chen were the supervisory authors and were involved with concept formation, data analysis and manuscript composition.

Acknowledgements

I would like to thank my two supervisors – Dr. Arno de Klerk and Dr. Weixing Chen – for extending me the opportunity to work on this fascinating project, as well as for their support and guidance during these two years. I greatly improved my critical reading and thinking skills from discussions with Dr. Arno de Klerk and broadened my perspective and knowledge with Dr. Weixing Chen's suggestions during our meetings.

I also want to thank my carbon fiber group, Desiree, Peiyuan, Zahra, and Dr. Ivey and my laboratory group, especially Felix and Natalia, for their help and advice during this research project. This work could not have been done without their help.

In addition, I want to express my gratitude to Alberta Innovates and Natural Sciences and Engineering Research Council (NSERC) of Canada for the financial support for this project.

Last, but not least, I want to thank my family and friends for their unconditional love and support.

TABLE OF CONTENTS

LIST OF TABLES

LIST OF FIGURES

CHAPTER 1:
INTRODUCTION TO ASPHALTENES AND CARBON FIBERS

(1.1) Background

Asphaltenes is material present in oil that is defined as the portion soluble in toluene and insoluble in excess *n*-alkane[1]. The definition is based on its solubility and hence, the separated asphaltenes encompasses a wide range of compounds that is the least soluble in paraffinic solvents, "owing either to flocculation of aggregations or to insolubility"[2]. Therefore, depending on the precipitant and precipitation conditions, yield as well as composition of asphaltenes can vary.

Nevertheless, there are three physical properties that distinguish asphaltenes from the other fractions of heavy oil or bitumen: insolubility in light *n*-alkanes, tendency to form multicomponent aggregates both in the crude oil and strong solvents, and lastly, strong adherence to a range of surfaces[2]. Apart from these three physical properties, asphaltenes is also known to contain the least favorable composition of the crude oil solubility fractions: high aromaticity, ash content, molecular weight as well as NOS content, Ni and V content[1]. These asphaltenes properties are responsible for many problems they cause in the oil industry such as well bore plugging and pipeline deposition, emulsion stabilization, and coke formation[3]. Therefore, some upgrading operations choose to remove asphaltenes by solvent deasphalting due to the benefits from the improvement in the properties of the deasphalted oil, or from the value gained in removing the asphaltenes and solid impurities from the bitumen stream[2].

After asphaltenes is removed from crude oil by a solvent deasphalting process, it can be used as a road packing material[4], gasified to integrate the energy with other operations[2], or treated by cracking and converted to feedstocks for other conversion processes[5]. On the other hand, in a recent investigation from the Bitumen Beyond Combustion (BBC) program, another potential use for asphaltene was identified: feedstock for carbon fibers[6]. This is a topic of particular interest in Alberta, Canada, because Alberta bitumen contains a high asphaltenes content of up to 20% *n*-pentane insoluble material. Given the Alberta crude bitumen production in 2019[7] –

490,000 m^3/d – there is almost 100,000 m^3/d of asphaltenes that can potentially be separated and utilized as feedstock for carbon fibers.

Carbon fibers are stiff, black synthetic fibers with long aromatic molecular chains with at least 92 to 100 wt.% carbon[8,9]. As a "material of the future," carbon fibers are used in various industries due to its high stiffness, high tensile strength, high chemical resistance, and temperature tolerance with low thermal expansion while keeping its lightweight properties. These characteristics allow carbon fibers to be broadly used in industries such as aerospace, building materials, military, motorsports and sporting goods industries[10].

Carbon fibers are produced by the controlled pyrolysis of a carbonaceous material in fibrous form. The processing path for asphaltenes precursors to carbon fibers is illustrated in Figure 1-1 and the steps include:

1. **Melt Spinning**

   The objective of melt spinning step is to convert the solid form precursor into fibrous forms. The process includes melting the asphaltenes precursor, extruding through the spinneret and drawing the fibers as they cool[8]. The resulting fibers from the melt spinning step is referred to as 'precursor fibers.'

2. **Stabilization / Oxidative Stabilization**

   After spinning, the precursor fibers proceed to the stabilization process to be converted into stable, non-fusible fibers, in preparation for the subsequent high heat carbonization process[8]. Stabilization can occur by oxidation procedures and is performed at relatively low temperatures of 200 – 400°C[11]. Stabilization temperatures must be chosen so they are below the precursor fiber softening point, so its fiber shape is preserved during stabilization. During this process, precursor fibers are most commonly stabilized through oxidative cross-linking reactions[12–15].

3. **Carbonization and Graphitization**

   Finally, the stabilized fibers are converted to carbon fibers through the carbonization process. This step includes subjecting the stabilized fibers to high temperature up to

1500°C in an inert environment to remove the non-carbon impurities[8,16,17]. During this step, rapid evolution of volatiles can occur with removal of the heteroatoms and can result in defects in the final carbon fiber. Optionally, further heat treatment up to 3000°C can be performed to obtain carbon fibers with higher modulus via graphitization process[8,18].

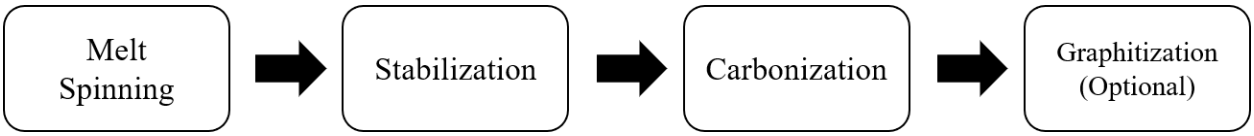

Figure 1-1: Block Flow Diagram for Carbon Fiber Production Process

Right now, 95% of all carbon fibers are produced from polyacrylonitrile (PAN) precursor where the remaining 5% are produced from pitch and rayon[19]. Using asphaltenes instead of using conventional PAN precursor are expected to offer the following advantages[10]:

- PAN feedstock has a cost of 3 – 6 US dollar/lb (9 – 17 CAD/kg) compared to asphaltenes, which costs 0.02 US dollar/lb (0.05 CAD/kg). Both costs are reported by Stantec[10] based on their costs in 2017 for comparative purposes. Using asphaltenes can reduce feedstock costs by a significant amount, which can be used towards the pretreatment of asphaltenes.
- The asphaltenes fraction of bitumen has a high carbon content and rich in aromatics[6]. One of the key considerations for carbon fiber precursor selection is the final carbon yield after the fibers are carbonized. As seen in Table 1-1, pitch precursor is reported to give the highest carbon yield. Asphaltenes, which is reported to have aromatic carbon of around 40 – 50 %[1], is expected to provide a high carbon yield, suggesting asphaltenes can be a good quality precursor for fiber production.
- Economic diversification for non-combustion related products from bitumen in the Alberta oilsands industry.

When using asphaltenes as a precursor for carbon fibers production, the production process can benefit from pretreatment of the asphaltenes to increase its softening point temperature. Industrially produced asphaltenes from *n*-pentane solvent deasphalting has a softening point <200°C and its low softening point is undesirable as it can lead to a more lengthy stabilization

process and fusing of the fibers during stabilization and carbonization step compared to PAN or pitch derived fibers.

Table 1-1: Carbon Yield for Various Raw Materials for CF Production [10]

Carbon Fiber Raw Material	Carbon Yield
PAN	40 – 50%
Pitch	80 – 90%
Rayon	10 – 30%

(1.2) Objectives

The objective of this project is to find asphaltenes pretreatment methods that will increase the softening point of asphaltenes. The pretreatment method should be suitable for practical, large-scale applications.

In the production sequence leading to carbon fibers, the pretreatment step takes place before melt-spinning. One advantage of having a pretreatment step is that the material can be processed as a fluid instead of a solid material. A related benefit is that the release of volatile products does not affect the morphology or integrity of the fiber, because the fiber is produced only after the pretreatment step.

(1.3) Scope of Work

Chapter 2 addresses the current carbon fiber production process, previously studied pretreatment methodologies on the commercialized carbon fiber precursors as well as literature on the effects of solvent extraction, autoxidation and halogenation/ dehalogenation on oilsands products.

Three different asphaltenes pretreatment methods for producing an asphaltenes precursor materials were considered. Chapter 3 presents a study on solvent extraction, or solvent deasphalting (physical pretreatment), followed by Chapter 4, which presents autoxidation (conventional reactive pretreatment) and lastly, Chapter 5 for discussing halogenation/ dehalogenation (newly suggested pretreatment) method for asphaltene precursor. In each chapter

the effects of the three pretreatments on the asphaltene chemistry, softening point and the spinnability were explored.

(1.4) References

(1) Strausz, O.; Lown, E. M., *The chemistry of Alberta oil sands, bitumens and heavy oil*. Alberta Energy Research Inst., Calgary, AB (Canada): Canada, 2003.

(2) Gray, M. R., *Upgrading Oilsands Bitumen and Heavy Oil*. University of Alberta Press: 2015.

(3) Speight, J., Petroleum Asphaltenes - Part 1: Asphaltenes, Resins and the Structure of Petroleum. *Oil & Gas Science and Technology-revue De L Institut Francais Du Petrole - OIL GAS SCI TECHNOL* **2004**, *59*, 467-477.

(4) Lee, J. M.; Shin, S.; Ahn, S.; Chun, J. H.; lee, K. B.; Mun, S.; Jeon, S. G.; Na, J. G.; Nho, N. S., Separation of solvent and deasphalted oil for solvent deasphalting process. *Fuel Processing Technology* **2014**, *119*, 7.

(5) Speight, J. G., *Fouling in refineries*. 2015; p 1-538.

(6) Meisen, A. *Bitumen Beyond Combusion (BBC) Project Phase 1 Report*; Alberta Innovates: 2017; p 112.

(7) Alberta Energy Regulator. Crude Bitumen Production https://www.aer.ca/providing-information/data-and-reports/statistical-reports/st98/crude-bitumen/production (accessed Dec 23, 2020).

(8) Park, S.-J., *Carbon Fibers*. Springer Nature Pte Ltd. : Incheon, Korea (Republic of), 2018; Vol. 210, p 366.

(9) Frank, E.; Hermanutz, F.; Buchmeiser, M. R., Carbon Fibers: Precursors, Manufacturing, and Properties. *Macromol. Mater. Eng.* **2012**, *297 (6),* 493-501.

(10) Harding, K. *Bitumen Beyond Combustion- Phase 2 Report*; Stantec: 2018; p 112.

(11) Chawla, K., *Fibrous Materials*. 2nd ed.; Cambridge University Press: Cambridge, 2016.

(12) Dhami, T. L.; Manocha, L. M.; Bahl, O. P., Oxidation behaviour of pitch based carbon fibers. *Carbon* **1991**, *29 (1),* 51-60.

(13) Matsumoto, T.; Mochida, I., A structural study on oxidative stabilization of mesophase pitch fibers derived from coaltar. *Carbon* **1992**, *30 (7),* 1041-1046.

(14) Yuan, G.; Li, X.; Xiong, X.; Dong, Z.; Westwood, A.; Li, B.; Ye, C.; Ma, G.; Cui, Z.; Cong, Y.; Zhang, J.; Li, Y., A comprehensive study on the oxidative stabilization of mesophase pitch-based tape-shaped thick fibers with oxygen. *Carbon* **2017**, *115*, 59-76.

(15) Senda, T.; Yamada, Y.; Morimoto, M.; Nono, N.; Sogabe, T.; Kubo, S.; Sato, S., Analyses of oxidation process for isotropic pitch-based carbon fibers using model compounds. *Carbon* **2019**, *142*, 311-326.

(16) Huang, X., Fabrication and Properties of Carbon Fibers. *Materials* **2009***, 2 (4),* 2369-2403.

(17) Burnsell, A. R., *Fibre Reinforcements for Composite Materials.* Elsevier Science Publishers: Amsterdam, Nethernalnds, 1988; Vol. 2.

(18) Chung, D. D. L., *Carbon Fiber Composites*. Butterworth-Heinemann: Newton, MA, 1994; p 215.

(19) Bhat, G., *Structure and Properties of High-Performance Fibers*. Matthew Deans: Duxford, UK, Cambridge, MA, Kidlington, UK, 2017; Vol. 187, p 438.

CHAPTER 2:
LITERATURE REVIEW

(2.1) Introduction

For this study, the focus is on investigating practically relevant modification chemistry of industrial asphaltenes (asphaltenes industrially obtained by *n*-pentane solvent deasphalting) that are low cost, can be applied at large scale, and that will not unnecessarily increase the emission footprint of the overall process. To develop the suitable pretreatment methods, the following needs to be considered and hence, is included in this chapter:

- Feed materials currently used for producing carbon fibers
- Effect of composition and properties of precursors in each carbon fiber production process
- Different pretreatments used for the polyacrylonitrile (PAN), rayon and pitch precursors in literature
- Chemistry, relevant process variables and pretreatment literature on solvent deasphalting / solvent extraction, autoxidation, and halogenation/ dehalogenation modification methods, which are the methods investigated in this study

(2.2) Feed Materials Used for Carbon Fiber Production

Many carbonaceous precursors have been investigated to evaluate their feasibility to become high quality carbon fibers. Earliest commercial use of carbon fibers was by Thomas Alva Edison in the 1880s, where the bamboo fibers were carbonized and the resulting fire-resistant carbon fibers were used for light bulbs[1,2]. Subsequently, pitch and PAN based carbon fibers started to be produced from 1963 and 1971, respectively[3]. Carbon fibers are now mainly produced from PAN, rayon, and pitch, with PAN being the dominating precursor in the market. In this section, carbon fiber production process for PAN, rayon, and pitch, and differences between pitch and asphaltenes are discussed.

(2.2.1) Precursor I: Polyacrylonitrile (PAN)

Polyacrylonitrile (PAN) fibers, also known as acrylic fibers, are synthetic fibers made from a polymer that contains > 85% acrylonitrile monomer[2]. Acrylic fibers were developed from the

1950s for textile applications and hence, it is not surprising that manufacture of PAN precursor fibers for the carbon fiber production process originated from companies that produced acrylic fibers. Currently, manufacturers such as Hexcel, Mitsubishi, Toho Belson, Toray and Zoltek produce their own special grade PAN fibers[4]. Since the PAN precursor fiber compositions and properties dictate the final carbon fiber properties, the specific compositions and manufacturing processes for the precursor fibers are not disclosed to the public.

Figure 2-1 outlines the basic processing steps for PAN-based precursor fibers. The processing step for PAN-based carbon fibers starts with the precursor synthesis, which includes polymerization process followed by fiber spinning. Depending on the final application of the carbon fibers, the choice, and the amount of comonomer, as well as the polymerization method is carefully selected[2]. The produced polymer then proceeds to the fiber spinning stage to form the fibrous shapes. Due to the tendency of PAN to undergo thermally induced cyclization reaction before melting, solution spinning method is used instead of melt spinning[5].

The spun fibers are then subjected to stabilization, where the fibers are subjected to heating at 200 – 300°C in air often with stretching to apply tension to the fibers. During this step, three reactions occur concurrently– cyclization reaction, incorporation of O-containing groups and dehydrogenation reaction – to convert the thermoplastic PAN into a non-plastic compound[1,5,6]. Finally, the stabilized fibers are subjected to high heat of 1000 – 1500 °C during the 'carbonization' step in an inert atmosphere to carbonize the stabilized fibers. Further heat treatment process, 'graphitization', can be performed for production of high modulus carbon fibers.

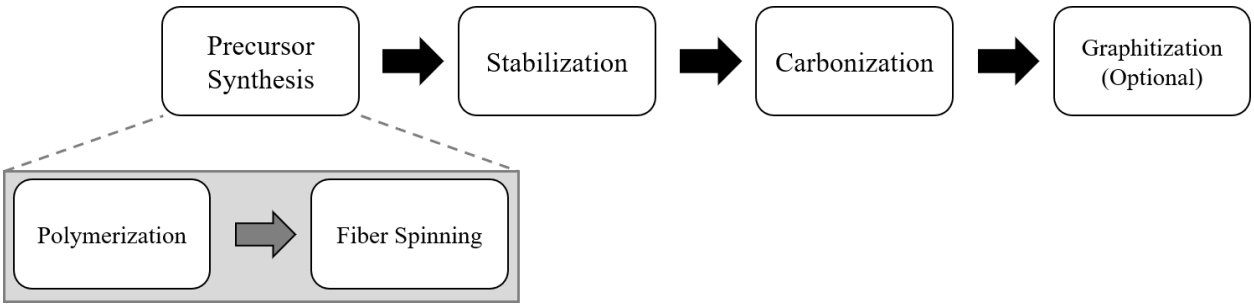

Figure 2-1: Carbon Fiber Processing Steps for PAN-based Precursors

(2.2.2) Precursor II: Rayon

Rayon is manufactured textile fibers and filaments composed of regenerated cellulose. Various types and grades of rayon fibers exist in the market and majority are used for textile applications. Then, from 1959, the National Carbon Company (a division of Union Carbide) introduced a carbon cloth from rayon precursor, then carbon yarn in 1961 and finally Thornel range of carbon fibers in 1965[4]. However, in 1978, they discontinued the process and replaced it with PAN and pitch-based carbon fibers. Since then, a niche market for carbon fibers from cellulosic precursor were maintained by a handful of manufacturers. Some of the most common end uses for rayon-based carbon fibers are ablative shields and high temperature packing materials.

The general processing steps to convert rayon fibers to carbon fibers is shown in Figure 2-2 below. The regenerated cellulose fiber precursors used to make carbon fibers are viscose, cuprammonium rayon or textile-grade rayon[2]. According to Morgan[4], the availability of suitable precursor fibers have fallen over the years and several manufacturers have phased out such products. The author also notes that one of the causes include specific end-users such as NASA and the atomic energy industry superimpose their own purchasing specifications. Similar to PAN-based carbon fibers, there is little information available on the production process or the specifics of the precursor fibers.

Since the rayon precursor fibers can withstand high temperature without softening, they are not required to go through an oxidative stabilization process like for PAN precursor fibers. Instead, they proceed to the pyrolysis stage to facilitate dehydration reactions and break down the polymeric structure[2]. To increase the final yield of the carbon fiber and decrease the flammability of cellulose, use of compounds that act as flame retardants can be used, which will be discussed in Section 2.4.2. The pyrolyzed fibers are then subjected to carbonization step, where the depolymerized structure is converted into graphite-like layers through repolymerization[2]. To improve the orientation of the graphitic layers, further heat treatment – graphitization step – can be performed under tension.

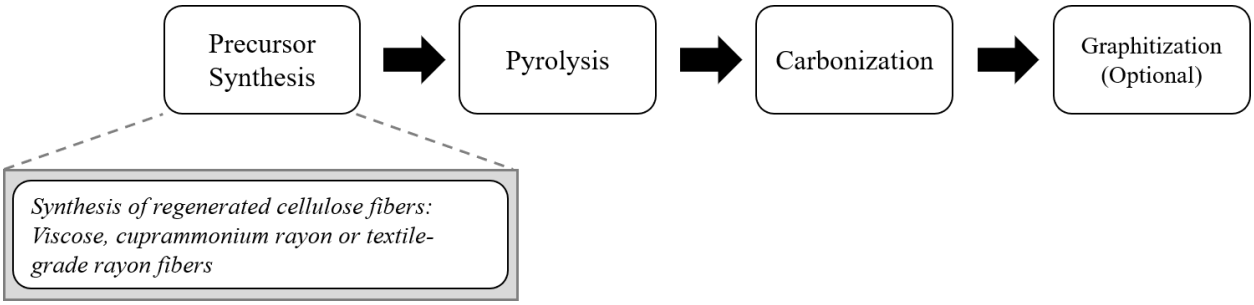

Figure 2-2: Carbon Fiber Processing Steps for Rayon-based Precursors

(2.2.3) Precursor III: Pitch

Pitch is complex blends of polyaromatic molecules and heterocyclic compounds. Depending on the source tar and processing conditions, composition can vary. For natural pitches, it can be obtained from petroleum refining processes, destructive distillation of coal, or natural asphalt, e.g. from Trinidad Lake. Natural pitches are isotropic and hence, are amorphous and not graphitic[2]. Isotropic pitches can be used to produce low-cost general-purpose carbon fibers for concrete reinforcement applications or to produce activated carbon fibers.

Isotropic pitches can be further treated to be converted into mesophase pitch, which contains liquid crystalline material consisting of large polynuclear aromatic hydrocarbons. With proper processing techniques, carbon fibers with oriented fibrous microstructure can be obtained from mesophase pitch. The general processing steps of pitch precursors to convert them into carbon fibers is the same as asphaltenes processing steps, which was illustrated previously in Section 1.1.

(2.2.4) Relationship between Pitch and Asphaltenes

Asphaltenes is one of the components of pitch defined by SARA (saturates, aromatics, resins, asphaltenes) fractionation technique. The technique attempts to separate the pitch into four main classes based on their solubility and adsorption characteristics, as illustrated in Figure 2-3. As the technique is operational based, it does not offer a clear insight on the chemical or molecular nature of the material. Hence, composition and properties of a SARA class, asphaltenes for example, from different pitches may vary. On the other hand, according to Park[2], several

researchers confirmed that the asphaltenes-rich precursors were the most suitable for production of carbon fibers.

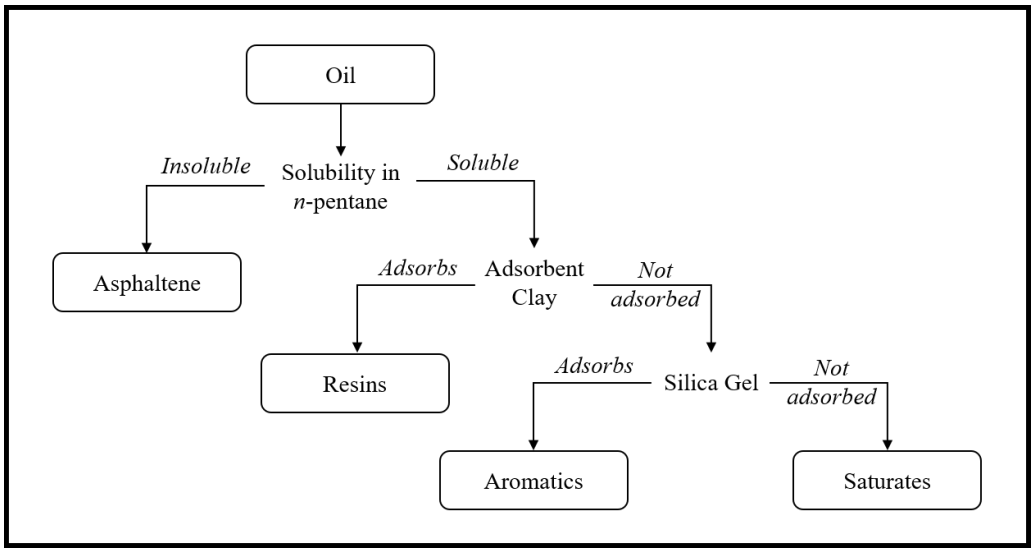

Figure 2-3: Process Diagram of SARA Fractionation as per ASTM D2007[7]

(2.3) Effect of Precursor Properties on Each Fiber Production Process

Regardless of which precursor is used, all precursors go through the three main steps – spinning of the fibers, stabilization and finally, carbonization/ graphitization – to be converted to carbon fibers. However, different processing conditions are required depending on the precursors to obtain good quality carbon fibers[2]. The major considerations in the processing and economics of carbon fiber technology include minimizing precursor weight loss and retention of orientation of the graphitic planes[1]. This section will outline the effect of precursor compositions and properties on the design of each carbon fiber production process steps, specifically for isotropic pitch-based precursors.

(2.3.1) Effect of Precursor Properties and Composition on the Melt Spinning Process

The spinnability of pitch is greatly influenced by the viscosity of the pitch, and hence, the temperature dependency of the pitch can play a major role. For isotropic pitches that exhibit Newtonian flow properties, softening point measurements are used to estimate the optimum spinning temperature[8]. Often, suitable spinning temperature is 30 – 50°C above the softening point temperature of the precursor.

Other than the viscosity of the pitch, the solid content, volatile matter as well as molecular weight distribution of the precursor can affect the spinnability. Solids present in the pitch, such as primary quinoline insoluble (QI) in coal-tar pitches or toluene insoluble (TI) in petroleum pitches, disturb the continuous spinning process[4,10,11]. Hence, typically, QI and TI are removed from the pitches prior to carbon fiber production process to improve the spinnability of the pitch. Similarly, precursors with high volatile matter can suffer from poor spinnability because the high volume of volatile matter content generated during the melt spinning and lead to frequent fiber breakage[4,12]. As poor spinnability leads to low production rate as well as lead to fibers with non-uniform fiber diameters, pitches may be pre-treated to remove the solids, and reduce the volatile content of the isotropic pitch.

(2.3.2) Effect of Precursor Properties and Composition on the Stabilization Process

Softening point of the precursor and its volatiles content have a major effect on the stabilization process. Stabilization temperatures must be below the precursor softening point, so its fiber shape is preserved during stabilization. Higher stabilization temperatures increase the stabilization reaction rate and decreases the required stabilization time[5,10,13]. Hence, for the pitch precursor fibers, a precursor with higher softening point is desirable as it permits shorter oxidation time[5]. Since the stabilization step is a costly step in the overall process, it is desirable to increase the softening temperature of the precursor even it if means its spinnability is negatively impacted[5,10]. Derbyshire *et al.*[10] reports increasing the softening temperature to 220 – 260°C as a compromise between the spinnability and the reduction of the time spent in the stabilization process. Furthermore, volatile matter present in the precursors can lead to fiber fusing during the stabilization process and lead to negative impact on the fiber integrity and the mechanical properties of the fibers[10].

(2.3.3) Effect of Precursor Properties and Composition on the Carbonization/ Graphitization Process

The precursor properties that affect the carbonization/graphitization process the most is the amount of volatiles produced at high temperatures. During the carbonization process, much of the remaining heteroatoms are eliminated and is accompanied by the evolution of volatiles[5]. Precursor with higher heteroatom content suffer greater loss of material during carbonization and

lead to low carbon yield[10]. This is undesirable as excessive volatile evolution can result in defect formation and negatively affect the fiber performance. Furthermore, more significant diameter reduction can result for the fibers with high volatile release. Hence, precursors with low heteroatom content is desired, or are pre-carbonized at 700 – 900°C[2,3] to remove volatiles in the early stage and avoid defect formation.

(2.4) Previous Work on Pretreatment Methods

Because many carbon fiber manufacturers have not publicly disclosed the specific compositions and process conditions, it is hard to determine the pretreatment methods used in the commercial processes today. However, by reviewing patents and literature, insight on various pretreatment methods used for various precursors can be obtained. This section reviews different types of precursor fiber pretreatment methods for the three commercialized precursors – PAN, rayon and pitch.

(2.4.1) Precursor Pretreatment Methods Used for PAN Precursor Fibers

Since PAN precursor fibers are synthetic polymer fibers, precursor composition is often modified at the precursor manufacturing step for the commercialized processes. However, some manufacturers choose to do precursor modification after precursor synthesis step because there is an upper limit to the amount of comonomer they can add during polymerization step; PAN precursor fiber must have acrylonitrile content higher than 85% for producing carbon fibers with good mechanical properties[4] and therefore, maximum comonomer they can add must be lower than 15%. Furthermore, pretreatment is particularly important for when using textile-grade PAN fibers for carbon fiber production because they suffer from uncontrollable oxidation and extremely long stabilization step[3]. Some of the reported treatment methods for improving the stabilization time and/or the final carbon fiber properties include:

1) **Modification via Surface Coating**

   Surface coating of the acrylic fibers at the pre-stabilization stage reduces the entangling, fusion, and fiber to fiber adhesion[14–16]. In addition, some resin coatings suppress possible thermal runaway reactions during the stabilization step, making stabilization at higher temperature possible[17]. The suppression of exotherm can improve the mechanical properties

of the produced carbon fiber[18,19]. The commonly used coating material include silicone-based oil, fatty acid derivatives, polyoxyethylene, and guar gum[14,16]. These surface coatings are removed during later stage of stabilization or early stage of carbonization, as they are oxidatively decomposed and becomes volatile[4].

2) **Catalytical Modification via Impregnation of PAN Precursor Fibers**

Impregnation of PAN precursor fiber with proper chemicals can catalyze the cyclization reaction in PAN and shorten the overall stabilization time[4,11,12,16]. Moreover, the stabilization exotherm can be reduced with catalytical modification, leading to the fibers becoming uniformly stabilized and improve final mechanical properties of the fibers[16]. Some of the commonly used impregnation agents include inorganic or organic acids, Lewis acids and bases, oxidizing compounds and transition metal compounds[4,15,20]. However, despite the improvement in the stabilization process, impregnation of PAN precursor fibers with chemicals is not always a commercially viable solution[4].

3) **Post Spinning Stretching Using Different Plasticizers**

Another pretreatment method includes stretching the PAN-precursor fibers in order to improve the orientation of the molecular chains, improve the stabilization step as well as the final carbon fiber mechanical properties[4]. Stretching is often completed in the presence of plasticizers to reduce the dipolar interactions that makes PAN stretching difficult[16]. Some of the plasticizers that can be used are steam, hot CuCl solution, ethylene glycol, H_2O, KOH or NaOH[15,16].

4) **Irradiation of PAN-Precursor Fibers**

Pretreatment by irradiation have been shown to be an efficient and technically feasible way to shorten and improve stabilization step for both conventional special grade PAN precursor fibers as well as low cost homopolymer and textile-grade PAN fibers[21–23]. Modification of polymer materials through radiation from radioactive sources or highly accelerated electrons have been studied extensively in the polymer industry[24,25]. Through irradiation of polymeric materials, reactive intermediates, free radicals, ions and excited states can be formed, which goes on to induce various modification reactions, including cross-linking reactions[24,26]. In a

similar manner, by exposing the PAN precursor fibers to electron beams before the stabilization process, free radicals are formed to accelerate the stabilization process as well as regulate the exothermic heat through acting as an initiation seed for cyclization reactions[22].

(2.4.2) Precursor Pretreatment Methods Used for Rayon Precursor Fibers

Despite the theoretical carbon yield of 44.4% based on its chemical formula, carbon fibers produced from rayon precursor fibers in practice have a carbon yield of 10 – 30% due to the significant release of volatiles during pyrolysis[27,28]. Hence, pretreatment of rayon precursor fibers aim to improve the subsequent pyrolysis process and, therefore, the carbon yield[27,28]. The main pretreatment used for rayon as well as other cellulosic precursor fibers is through:

Impregnation with Flame Retardants or Impregnants

Before pyrolysis, by impregnating the rayon precursor fibers in the aqueous dispersions of flame retardants, dehydration reactions can be promoted while suppressing the levoglucosan formation reaction[2,27]. This is important because during the pyrolysis step, sufficient H_2O dehydration reactions need to take place and stabilize the fiber before depolymerization reaction takes place. If pyrolysis is completed too quickly or at a too high temperature, formation of levoglucosan is favored, which is to be avoided because it reduces the carbon yield. Hence, by using the flame retardants, it allows for pyrolysis to take place at a faster rate, but with less levoglucosan produced. Some of the fire retardants that can be used include Lewis acids (e.g. – zinc and calcium chloride), bases, strong acids and halides[27,28].

(2.4.3) Precursor Pretreatment Methods Used for Pitch

Depending on the final application of the carbon fiber, isotropic pitch can be modified in two main pathways – be converted to mesophase pitch or be modified to become a better isotropic pitch precursor. The focus on this section is on the pretreatment methods for improving isotropic pitch and hence, methods for forming mesophase will not be discussed.

Research on isotropic pitch modification methods have centered on preparation of spinnable pitches, shortening the stabilization/ carbonization process and enhancement of mechanical properties. The modification methods aim to remove impurities, modify the precursor to have

high molecular weight, narrow molecular distribution and to have high softening point[3]. Some of the investigated modification methods in the literature include:

1) **Modification via Heat Treatment (Thermal Treatment)**

   With heat treatment, volatiles are released, and dehydrogenation, crosslinking and condensation reactions occur to increase the molecular weight of the precursor[4,29]. For isotropic precursor modification purposes, heat treatment is usually conducted at < 350°C to avoid mesophase formation[9].

2) **Oxidation of Pitch Precursor**

   Pitch oxidation is one of the widely investigated modification methods used to increase the softening point of the pitches[30–37]. This method involves heat treatment of pitch in presence of oxidizing gas, usually low-cost air. Other oxidizing gases such as NO_2, and SO_2 can also be used[38]. During this process, pitch undergoes dehydrogenative polymerization reactions, which increases the molecular weight of the components without significantly introducing oxygen into the precursor[30]. Pitch oxidation have been widely used for preparing pitches as it effectively increases the softening point while hindering mesophase formation[34,37]. This has been a particular interest for low softening point isotropic pitch, as it can turn the low softening point pitch into a spinnable isotropic pitch with a sufficiently high softening point for carbon fiber production[31–34].

3) **Wiped Film Evaporation (Thin Film Evaporation)**

   Wiped film evaporator method aims to efficiently remove the volatile components with minimal exposure of pitch to high temperatures[4,38]. In this design, a thin layer of molten pitch is spread on the heating surface and is continuously wiped over the heating surface. Pitch is exposed to high temperature for only a few seconds, and hence, this method efficiently removes the volatile without the risk of forming mesophase regions[38].

4) **Solvent Extraction**

   For natural pitch that encompasses a wide range of molecular species, constituents with the desired properties – such as molecular weight or softening point – can be separated from the

rest of the material by a proper solvent. One of the extraction methods that have been widely studied for purifying pitch precursors is supercritical fluid extraction (SCF) method. SCF method exploits the unique property of a compressed fluid approaching its critical point, where the solvent strength can be varied with the operating temperature and pressure[39]. By adjusting the extraction temperature and pressure, the portion with the desired molecular weight and hence, the portion with the desired softening point, can be extracted from the pitch[38,40]. In addition, inorganic or coke particulates can be removed with the suitable solvent. SCF method is widely used for producing high quality mesophase pitch as well because this process allows for extracting a portion with narrow molecular weight distribution and the separation process is more reproducible[40].

(2.5) Solvent Extraction / Solvent Deasphalting

Solvent extraction is a physical separation process where compounds are separated based on their relative solubilities. It is a technique used in various industries ranging from food industries for decaffeination of coffee beans, as well as pharmaceutical and petrochemical industries. For materials that do not readily become volatile, solvent extraction process has a clear advantage compared to other commonly used fractionation techniques like distillation. One of the widely used solvent extraction method is the solvent deasphalting (SDA) process in the oil industry. As mentioned earlier, asphaltenes is a fraction in heavy oil or bitumen that is characterized by its insolubility in *n*-alkane solvents, often *n*-pentane or *n*-heptane. In an industrial SDA process, heavy oil or bitumen is mixed with the chosen solvent to remove the *n*-alkane insoluble asphaltenes portion.

To better understand the feed material for this study – industrial asphaltenes – and the effects of the solvent extraction process, the separation chemistry, and the relevant process variables for an SDA process will be discussed in Section 2.5.1 and 2.5.2, respectively. In addition, Section 2.5.3 will discuss some of the previous literature on using solvent extraction process as a pretreatment method for carbon fiber production.

(2.5.1) Separation Chemistry

The chemistry of the solvent extraction technique can be explained by solubility parameters. The term 'solubility parameter' was first coined by Hildebrand and Scott and this parameter helps predict solubility relations of various materials. Consistent with the popular phrase, "like dissolves like," liquids with similar solubility parameters will be miscible and polymers will be dissolved in solvents with similar solubility parameters of their own[41].

Hildebrand Solubility Parameter

The Hildebrand solubility parameter for a liquid at temperature well below its normal boiling point is expressed as[42]:

$$\delta = \sqrt{c} = \sqrt{\frac{H_{vap} - RT}{V}} \quad (2.5.1)$$

where c is the cohesive energy density, H_{vap} is the molar vaporization enthalpy, R is the universal gas constant (8.314 J K^{-1} mol^{-1}), V is the molar volume and T is the temperature.

As seen in Equation 2.5.1, Hildebrand solubility parameter uses the energy of vaporization as a direct reflection of the forces holding the molecules of the liquid together. Since the solubility of two materials is likely when their intermolecular attractive forces are similar, comparing the cohesive energy density values of the two materials allow us to estimate their mixing behaviour. Two materials with similar solubility parameter will be miscible whereas two materials with a significant difference in solubility parameter is likely to be immiscible.

However, using the Hildebrand solubility parameter has a limitation and that is this parameter was developed for nonpolar, non-associating systems[42]. It does not account for association between molecules, such as polar and hydrogen-bonding interactions. For polar molecules, three-dimensional solubility parameters such as Hansen solubility parameter is more widely used.

Hansen Solubility Parameter

Similar to Hildebrand solubility parameters, Hansen solubility parameter was developed based on the energy of vaporization. However, the main difference is that the total energy of vaporization is split into three individual parts – dispersion, polar and hydrogen bonding

components – to account for the interactions in the molecular level. The basic equation for determining the Hansen solubility parameter is as follows[41]:

$$\delta^2 = \delta_D^2 + \delta_P^2 + \delta_H^2 \quad (2.5.2)$$

where δ_D represents the nonpolar dispersion forces, δ_P represents the polar forces and finally, δ_H represents the attractions among molecules due to hydrogen bonds. By comparing the Hansen solubility parameters, the interaction between two materials can be predicted, even for the materials with high polarity or with hydrogen bonding.

Due to the more descriptive nature of the contributions in Hansen solubility parameters, this formulation will be used for the discussion[41]. Table 2-1 shows a list of Hansen solubility parameters and the three-dimensional solubility parameters for various materials including asphaltenes. As seen in Table 2-1, the materials with similar parameter as asphaltenes due to high London dispersion forces, such as toluene, or has high polar or H-bonding interactions, such as methylene chloride, are the commonly used solvents to dissolve asphaltenes. It is worthwhile noting that asphaltenes in Table 2-1 is a product of analytical determination of asphaltenes in labs, which uses more rigorous separation processes. Hence, for the industrially precipitated asphaltenes, it will contain asphaltenes as well as residual products that are soluble in *n*-alkane.

Table 2-1: Hansen and the Three-Dimensional Solubility Parameters for Various Materials

Material	Three-dimensional solubility parameters [$MPa^{1/2}$]			Hansen solubility parameter (δ) [$MPa^{1/2}$]
	δ_D	δ_P	δ_H	
Asphaltenes[43]	20.2	2.0	4.0	20.7
Asphaltenes[50]				20.3
Benzene[50]	18.4	0	2.0	18.5
Methylene chloride[50]	13.4	11.7	9.6	20.2
Chloroform[50]	17.8	3.1	5.7	19.0
Toluene[44]	18.0	1.4	2.0	18.2
1-Methyl naphthalene[41]	20.6	0.8	4.7	21.1
Quinoline[41]	19.8	5.6	5.7	21.4
Propane[44]	13.4	0	0	13.4
Pentane[44]	14.5	0	0	14.5
Heptane[44]	15.3	0	0	15.3
Octane[44]	15.5	0	0	15.5

(2.5.2) Relevant Process Variables

Various process variables can affect the dissolution process and affect the yield and quality of the products obtained from the solvent extraction process. Some of the process variables that have a significant effect on the separation include the solvent, solvent-to-feed ratio, and contact time.

The choice of solvent affects the final yield, as well as the properties of the separated portion. For example, in a SDA process, *n*-pentane and *n*-heptane insoluble have different yields and as seen in Figure 2-4, they have vastly different properties. With the increase in the carbon number of *n*-alkane solvent, the yield of asphaltenes fraction decreases and the molecular weight and aromaticity of the precipitated asphaltenes increase[45]. This observation makes sense by looking at the solubility parameters as seen in Table 2-1; pentane has a solubility parameter of

14.5 $MPa^{1/2}$ and heptane with 15.3 $MPa^{1/2}$ when asphaltenes have the solubility parameter around 20 – 21 $MPa^{1/2}$. Heptane has a closer solubility parameter compared to pentane and therefore, it can dissolve more pentane insoluble asphaltenes and more molecular species that are bulkier (high dispersion force) or has higher polar interaction or H-bonding.

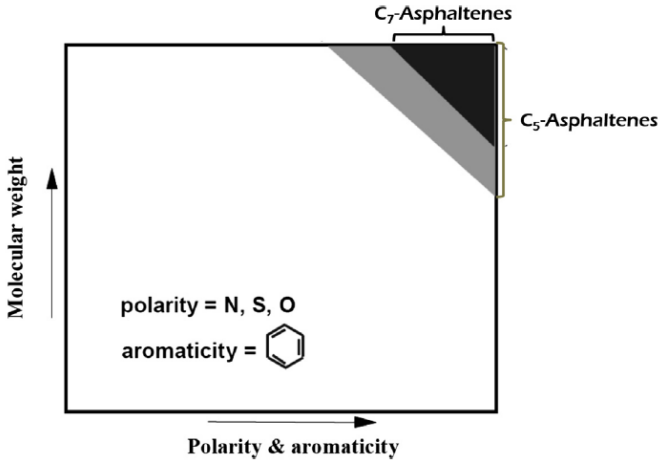

Figure 2-4: Asphaltenes Properties Variation with Different Solvent Employed[45,46]

In addition, solvent-to-feed ratio ($ml_{solvent}$:g_{feed}) have a significant effect on the yield until the saturation point is reached. Specifically, for the SDA process, the saturation point for *n*-pentane and bitumen mixture is 30:1[47]. After this point, there are no notable changes in the obtained insoluble yield. On the other hand, the increase in the solvent-to-feed ratio until the saturation point leads to an increase in the yield of insoluble material obtained from the bitumen-alkane mixture. Due to the cost implications, a typical industrial SDA process uses a low solvent-to-feed ratio of 3:1 to 10:1[48], which is not as rigorous as high solvent-to-feed ratio laboratory separation as seen in literature for analytical determination of asphaltenes content. Hence, as discussed previously, the industrial asphaltenes contains some material that is soluble in *n*-alkanes.

Contact time between the solvent and feed can also have a significant effect on the yield and quality of the precipitated material. According to Speight *et al.*[47], contact times of the order of 12 – 16 hours is recommended to ensure reproducible yields. Shorter contact time will result in higher insoluble yields, and result in *n*-alkane insoluble material that exhibit more semi-solid like appearance.

(2.5.3) Solvent Extraction as a Pretreatment Method in Previous Literature

Precursors such as natural pitches comprise of a variety of molecular species often with a wide range of molecular weight (MW) distribution. Through utilization of solvent extraction with a proper solvent and the extraction conditions, the portion with the desirable properties for carbon fiber production can be obtained. For example, Li and colleagues[49,50] extensively studied the use of solvent extraction as a method to separate low-rank coal and biomass into three solid fractions with distinct properties. One of their investigations found that the 1-methylnaphthalene (MN) soluble portion is a suitable precursor for carbon fiber production, with its high carbon content of 80 – 85%, ash content of lower than 1.0% and the softening and melting points ranging in 100 – 300°C[51]. Moreover, with a further extraction of the MN-soluble fraction with cyclohexane, a portion with a high softening point was obtained. Similarly, Yang *et al.*[12] used solvent extraction with MN at 60 and 100°C on hyper-coal to obtain the fraction with desirable molecular weight range for carbon fiber production. The MN soluble fraction obtained at 60°C showed excellent spinnability and the resulting carbon fibers showed good mechanical properties compared to the extracted portion at 100°C.

(2.6) Autoxidation

Autoxidation is the oxidation of organic compound with molecular O_2 in air in the absence of added catalyst[52]. It is employed as a stabilization step after carbon fiber melt-spinning, but it can also be applied at milder conditions as pretreatment to produce a more viscous product. In a similar manner, autoxidation is routinely used to increase viscosity of road paving asphalt and make them more resistant to weather and changes in temperature[53,54].

Autoxidation, or oxidation in air, is a free radical chain process and can produce various final products like oxygenated compounds – peroxides, alcohols, carbonyl compounds, acids, esters – and/or cross-linked molecules[55]. The final products and their selectivity depend significantly on the reaction conditions and, therefore, it is important to understand the reaction mechanism. The autoxidation mechanism chemistry and the relevant process variables are covered in Section 2.6.1 and 2.6.2, followed by Section 2.6.3 to discuss literature on autoxidation used as a pretreatment method for carbon fiber production.

(2.6.1) Oxidation Chemistry

Mechanism of liquid phase oxidation of hydrocarbons with molecular oxygen is described in literature as follows[52,55]:

Initiation:

First, the oxygen abstracts hydrogen from the hydrocarbon, thereby creating free radicals.

$$RH, O_2 \rightarrow \dot{R} \tag{2.6.1}$$

Propagation:

The produced radicals can interact with another oxygen to further convert into the peroxy radical.

$$\dot{R} + O_2 \rightarrow R\dot{O}_2 \tag{2.6.2}$$

This peroxy radical can further abstract a hydrogen from a hydrocarbon to form a hydroperoxide and a free radical.

$$R\dot{O}_2 + RH \rightarrow ROOH + \dot{R} \tag{2.6.3}$$

Degenerate branching:

During the oxidation process, hydroperoxide can decompose into radicals and increase the free radicals by the reaction:

$$ROOH \rightarrow R\dot{O} + \dot{O}H \tag{2.6.4}$$

Termination:

The formed free radicals are highly reactive and rapidly disappear by the reactions below:

$$\dot{R} + \dot{R} \rightarrow R - R \tag{2.6.5}$$

$$R\dot{O}_2 + \dot{R} \rightarrow ROOR \tag{2.6.6}$$

$$R\dot{O}_2 + R\dot{O}_2 \rightarrow ROH + R_1COR_2 + O_2 \tag{2.6.7}$$

Depending on the free radicals available at termination, different termination reactions (2.6.5 – 2.6.7) take place. Reaction (2.6.5) is desired for using oxidation as a pretreatment method for carbon fiber production purpose. This is because unnecessary incorporation of oxygen in the pretreatment stage can lead to high evolution of volatiles during carbonization, leading to defect formation in the final carbon fibers.

Several studies of bitumen autoxidation reported hardening of bitumen at various autoxidation conditions[56–60]. For one of the studies, the authors[57,58] investigated autoxidation of model compounds to understand oxidative bitumen hardening and noticed that naphthenic-aromatic compounds, furanic O-containing compounds and pyrrolic N-containing compounds were susceptible to form addition products. From this observation, asphaltenes fraction from bitumen, which has high heteroatoms and aromatic compounds compared to its source oil, is predicted to be more prone to oxidative addition.

Furthermore, the previously outlined autoxidation mechanism without an added initiator is slow and is marked by an induction period. This is due to formation of alkyl radicals in Reaction (2.6.1) being thermodynamically and kinetically unfavorable[61]. The rate of the reaction can be improved through addition of initiators capable of forming free radicals, such as peroxides or radical initiators[55,61]. On the other hand, oilsands derived asphaltenes have high free radical contents, of the order 10^{18} spins/g[62]. It is postulated that the free radicals in asphaltenes will act as an initiator and a chain-transfer agent during autoxidation to improve the reaction rate.

(2.6.2) Relevant Process Variables

By a combination of the three main variables – autoxidation temperature, oxygen availability and reaction time – autoxidation selectivity of hydrocarbons can be controlled[52]. De Klerk[52] outlined the product selectivity at different autoxidation regimes for reaction temperatures of 75 – 475 °C and changes in the oxygen availability.

The autoxidation regime of interest is at the medium temperature (180°C – 300°C), the regime used in processes such as asphalt oxidation to achieve asphalt hardening. At these temperatures, through manipulating the oxygen availability and exposure time, asphalt conversion can be regulated[52]. For the pretreatment for carbon fiber production purposes, formation of $\dot{R}$ is crucial and can be achieved through limiting oxygen availability after the initiation reaction. This is because if there is low concentration of dissolved oxygen available after Reaction (2.6.1), formation of $\dot{R}$ radicals are preferred over $R\dot{O}$, leading to chain termination by Reaction (2.6.5) to be more likely.

(2.6.3) Oxidation as a Pretreatment Method in Previous Literature

As previously discussed in Section 2.4.3, there are several works in literature that use autoxidation at temperature ranging 250 – 400°C as a modification method to increase the softening point of the isotropic pitches[30–37]. For example, Barr and Lewis[30] performed air blowing of coal tar and petroleum pitches at temperatures up to 250°C to advance their softening points from 110°C to 174°C for coal tar pitch and 122°C to 181°C for petroleum pitch while introducing < 1wt.% oxygen. In a similar setup, another investigation[36] performed air blowing at temperatures between 250 – 300°C for two industrial coal tar pitches and reported a softening point temperature increase from 72°C to 151 – 223°C and 54°C to 148 – 219°C. They also observed small oxygen incorporation of the order < 2 wt.% and credited the softening point temperature increase to the formation of cross-linked oligomers. Often, oxidation is used for pretreating isotropic pitches because presence of oxygen can hinder the formation of graphitic structure[34,37]. However, for air-blowing pretreatment which facilitated cross-linking reactions with minimum oxygen incorporation, the authors noted no significant effect on the subsequent graphitic development[30,31].

(2.7) Halogenation/ Dehalogenation

Halogenation is a method used widely in the industry for the synthesis of chlorinated intermediates, chloro- and fluoro- containing monomers, chloro-organic solvents, and halogen-containing pesticides[63]. Typically, non-catalytic halogenation occurs by free radical chemistry, in a similar reaction fashion as autoxidation outlined in Section 2.6. Through halogenation and dehalogenation, it is also possible to facilitate addition reactions via free radical reaction chemistry. Section 2.7.1 outlines the mechanism of halogenation and dehalogenation reactions, then the relevant process variables are reviewed in Section 2.7.2. Finally, literature on using halogenation and dehalogenation as a pretreatment method for carbon fiber production is discussed in Section 2.7.3.

(2.7.1) Halogenation/ Dehalogenation Chemistry

Halogenation and dehalogenation of asphaltenes, which possess high free radical content, is proposed as follows[64]. The proposed halogenation reaction will be illustrated with Br, and a similar reaction chemistry is anticipated when using other halogens such as chlorine or iodine.

Halogenation reaction starts with Reaction (2.7.1), where bromine dissociates to form two radicals. Dissociation can occur by heat, irradiation, or chemical initiators[63].

$$Br_2 \rightarrow 2Br^{\bullet} \quad (2.7.1)$$

Then, the radical bromine reacts with asphaltenes molecule, as represented by 2-ethylnaphthalene in Reaction (2.7.2) below, to form brominated asphaltenes.

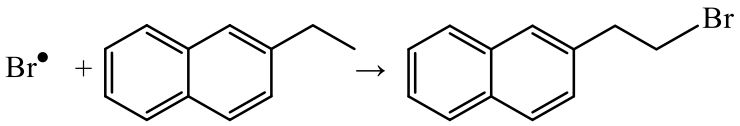

(2.7.2)

After bromination, debromination reaction can be facilitated through heat. This will eliminate the attached bromine with aliphatic hydrogen on the adjacent carbon to form HBr and an olefin.

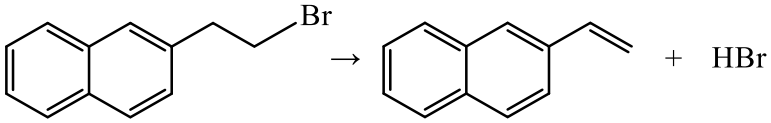

(2.7.3)

The formed olefin intermediates will readily participate in free radical addition reactions meanwhile leaving the free radical to remain to further react with other reactive species present in asphaltenes as seen in Reaction (2.7.4). The reaction will be terminated only when the two free radical species combine. Theoretically, this will lead to formation of products as depicted in Reaction (2.7.5), where the resulting asphaltenes product will be bigger and bulkier due to the free radical addition reactions.

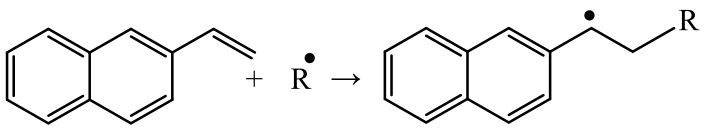

(2.7.4)

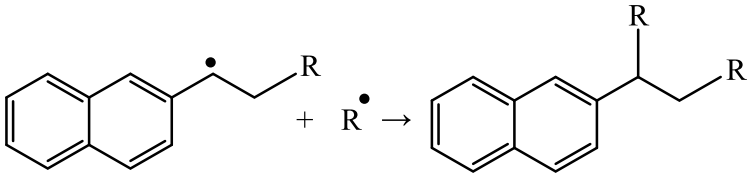

(2.7.5)

(2.7.2) Relevant Process Variables

Like autoxidation, halogenation occurs through free radical chemistry. Hence, the most relevant process variables for halogenation without initiators are expected to be similar to autoxidation and the variables include reaction temperature, time and halogen availability.

Halogenation should occur at sufficiently high temperatures to facilitate thermal dissociation of the diatomic halogens to start the radical reactions. Halogenation at low temperatures require utilization of initiators or irradiation[63]. At too high temperatures, it will lead to dehalogenation. Furthermore, to facilitate halogenation at a sufficiently short reaction times, liquid-phase halogenation will be preferred to reduce the mass-transfer limitation present in solid phase reactions. This can be achieved by dissolving asphaltenes in a solvent or by performing halogenation at temperatures where asphaltenes is softened (>150 – 160°C). Previous literature on asphaltenes halogenation[65,66] reported successful halogenation at temperatures as low as room temperatures by performing the reactions with asphaltenes-solvent mixture.

Furthermore, with the longer reaction time, increased halogen incorporation is expected. Interestingly, a previous study[66] reported chlorine uptake by the asphaltenes molecules ceased after about 4 hours and reached a plateau. In the same study, asphaltenes bromination at 8 hours under heat resulted in the same degree of Br incorporation (37.4 wt.% Br) as bromination at 24 hours at room temperature (38.0 wt.% Br). It is not clear from the study if this observation was due to the increased reaction rate with the higher bromination temperature or if Br incorporation reached a plateau at 8 hours as observed for Cl incorporation.

Halogen availability can be controlled by adjusting the amount of halogen added to the reaction. As outlined in Section 2.7.1, only a small amount of halogen is required in the beginning of the reaction to kickstart the olefin formation. Previous study on asphaltenes halogenation[65] reported mild bromination as low as 1 – 3wt.% Br incorporation caused observable changes in the bulk asphaltenes that was consistent with observation for asphaltenes halogenation with higher bromine content (37 – 38 wt.% Br incorporation)[66].

On the other hand, debromination should occur at higher temperatures than bromination to eliminate halogens from the molecule. As a reference, it was reported that heating PVC between 230°C and 310°C generated polyene-type radicals[67].

(2.7.3) Halogenation/ Dehalogenation as a Pretreatment Method in Previous Literature

Using halogenation and dehalogenation as a pretreatment method for carbon fiber production was not studied extensively as much as autoxidation and solvent extraction in the carbon fiber industry. However, there are literatures by Kim and his colleagues[26,68] where they synthesized carbon fiber precursor through bromination and subsequent dehydrobromination to produce spinnable pitches. In one of their investigations[68], naphtha-cracked oil was brominated with 20 wt.% Br then subsequently dehydrobrominated by heat. This produced isotropic pitch composed of linear methylene chains of polycondensed aromatic molecules, denoted as NB pitch, and they also prepared an isotropic pitch through distillation of the naphtha-cracked oil for comparison (ND pitch). They found the NB pitch to have viscosity almost 10-fold higher than ND pitch, and the produced carbon fibers had strength that was 2.1-fold higher than from ND pitch. They attributed the observed high strength in the carbon fibers to the linear chains of the NB pitch, which resulted in more homogeneous fibers and a greater degree of molecular orientation during spinning. In a similar manner, facilitating chlorination-dehydrochlorination through pyrolysis of PVC[69,70] and pyrolysis of PVC and pitch mixture[67] to produce high softening pitch for carbon fiber production have been previously reported.

(2.8) References

(1) Mortensen, A., *Concise Encyclopedia of Composite Materials*. 2nd ed.; Elsevier: Oxford, UK, 2007.

(2) Park, S.-J., *Carbon Fibers*. Springer Nature Pte Ltd.: Incheon, Korea (Republic of), 2018; Vol. 210, p 366.

(3) Choi, D.; Kil, H.-S.; Lee, S., Fabrication of low-cost carbon fibers using economical precursors and advanced processing technologies. *Carbon* **2019**, *142*, 610-649.

(4) Morgan, P., *Carbon Fibers and Their Composites*. 1st ed.; CRC Press: Boca Raton, 2005.

(5) Chung, D. D. L., *Carbon Fiber Composites*. Butterworth-Heinemann: Newton, MA, 1994; p 215.

(6) Burnsell, A. R., *Fibre Reinforcements for Composite Materials*. Elsevier Science Publishers: Amsterdam, Nethernalnds, 1988; Vol. 2.

(7) ASTM D2007-19: Standard Test Method for Characteristic Groups in Rubber Extender 29 and Processing Oils and Other Petroleum-Derived Oils by the Clay-Gel Absorption Chromatographic Method. ASTM International. 2019, pp 1–9

(8) Berrueco, C.; Álvarez, P.; Díez, N.; Granda, M.; Menéndez, R.; Blanco, C.; Santamaria, R.; Millan, M., Characterisation and feasibility as carbon fibre precursors of isotropic pitches derived from anthracene oil. *Fuel* **2012**, *101*, 9-15.

(9) Huson, M. G., *High-performance pitch-based carbon fibers*. 2017; pp 31-78.

(10) Derbyshire, F.; Andrews, R.; Jacques, D.; Jagtoyen, M.; Kimber, G.; Rantell, T., Synthesis of isotropic carbon fibers and activated carbon fibers from pitch precursors. *Fuel* **2001**, *80 (3),* 345-356.

(11) Bahl, O. P.; Shen, Z.; Lavin, J. G.; Ross, R. A., *Carbon Fibers* Third Edition, Revised and Expanded. Marcel Dekker: New York, 1998.

(12) Yang, J.; Nakabayashi, K.; Miyawaki, J.; Yoon, S.-H., Preparation of pitch based carbon fibers using Hyper-coal as a raw material. *Carbon* **2016**, *106*, 28-36.

(13) Buckley, J. D.; Edie, D. D., *Carbon-Carbon Materials and Composites*. William Andrew: 1993; p 294.

(14) Gupta, A. K.; Paliwal, D. K.; Bajaj, P., Acrylic Precursors for Carbon Fibers. *JMS, Polym. Rev.*, Part C **1991**, *31 (1)*, 1-89.

(15) Yusof, N.; Ismail, A. F., Post spinning and pyrolysis processes of polyacrylonitrile (PAN)-based carbon fiber and activated carbon fiber: A review. *J. Anal. Appl. Pyrolysis* **2012**, *93*, 1-13.

(16) Mittal, J.; Mathur, R. B.; Bahl, O. P., Post spinning modification of PAN fibres — a review. *Carbon* **1997**, *35 (12),* 1713-1721.

(17) Harland, W.; King, M.; Phillips, L. Improvements in or Relating to Fibrous Materials. 1,431,883, 1976.

(18) Yamazaki, K.; Yamane, S.; Fukuhara, M. Production of Acrylic Precursor Fiber Bundle. 6183373, 1986.

(19) Saruyama, H.; Yamazaki, K. Production of Precursor Yarn for Producing Carbon Yarn. 63135510, 1988.

(20) Maghe, M.; Creighton, C.; Henderson, L. C.; Huson, M. G.; Nunna, S.; Atkiss, S.; Byrne, N.; Fox, B. L., Using ionic liquids to reduce energy consumption for carbon fibre production. *J. Mater. Chem. A* **2016**, *4 (42),* 16619-16626.

(21) Yoo, S. H.; Park, S.; Park, Y.; Lee, D.; Joh, H.-I.; Shin, I.; Lee, S., Facile method to fabricate carbon fibers from textile-grade polyacrylonitrile fibers based on electron-beam irradiation and its effect on the subsequent thermal stabilization process. *Carbon* **2017**, *118*, 106-113.

(22) Park, S.; Yoo, S. H.; Kang, H. R.; Jo, S. M.; Joh, H.-I.; Lee, S. Comprehensive stabilization mechanism of electron-beam irradiated polyacrylonitrile fibers to shorten the conventional thermal treatment *Scientific reports* [Online], 2016, p. 27330. PubMed. https://doi.org/10.1038/srep27330

(23) Dietrich, J.; Hirt, P.; Herlinger, H., Electron-beam-induced cyclisation to obtain C-fibre precursors from polyacrylonitrile homopolymers. *Eur. Polym. J.* **1996**, *32 (5)*, 617-623.

(24) Chmielewski, A. G.; Haji-Saeid, M.; Ahmed, S., Progress in radiation processing of polymers. *Nucl. Instrum. Methods Phys. Res., Sect. B* **2005,** *236*, 44-54.

(25) Clough, R. L., High-energy radiation and polymers: A review of commercial processes and emerging applications. *Nucl. Instrum. Methods Phys. Res., Sect. B* **2001**, *185*, 8.

(26) Kim, B.-J.; Kotegawa, T.; Eom, Y.; An, J.; Hong, I.-P.; Kato, O.; Nakabayashi, K.; Miyawaki, J.; Kim, B. C.; Mochida, I.; Yoon, S.-H., Enhancing the tensile strength of isotropic pitch-based carbon fibers by improving the stabilization and carbonization properties of precursor pitch. *Carbon* **2016**, *99*, 649-657.

(27) Huang, X., Fabrication and Properties of Carbon Fibers. *Materials* **2009**, *2(4),* 2369-2403.

(28) Dumanlı, A. G.; Windle, A. H., Carbon fibres from cellulosic precursors: a review. *J. Mater. Sci.* **2012**, *47 (10)*, 4236-4250.

(29) Lewis, I. C., Thermal polymerization of aromatic hydrocarbons. *Carbon* **1980**, *18 (3),* 191-196.

(30) Barr, J. B.; Lewis, I. C., Chemical changes during the mild air oxidation of pitch. *Carbon* **1978**, *16 (6),* 439-444.

(31) Maeda, T.; Ming Zeng, S.; Tokumitsu, K.; mondori, J.; Mochida, I., Preparation of isotropic pitch precursors for general purpose carbon fibers (GPCF) by air blowing—I.

Preparation of spinnable isotropic pitch precursor from coal tar by air blowing. *Carbon* **1993**, *31 (3)*, 407-412.

(32) Zeng, S. M.; Maeda, T.; Mondori, J.; Tokumitsu, K.; Mochida, I., Preparation of isotropic pitch precursors for general purpose carbon fibers (GPCF) by air blowing—III. Air blowing of isotropic naphthalene and hydrogenated coal tar pitches with addition of 1,8-dinitronaphthalene. *Carbon* **1993**, *31 (3),* 421-426.

(33) Zeng, S. M.; Maeda, T.; Tokumitsu, K.; Mondori, J.; Mochida, I., Preparation of isotropic pitch precursors for general purpose carbon fibers (GPCF) by air blowing—II. Air blowing of coal tar, hydrogenated coal tar, and petroleum pitches. *Carbon* **1993**, *31 (3),* 413-419.

(34) Alcañiz-Monge, J.; Cazorla-Amorós, D.; Linares-Solano, A.; Oya, A.; Sakamoto, A.; Hosm, K., Preparation of general purpose carbon fibers from coal tar pitches with low softening point. *Carbon* **1997**, *35 (8),* 1079-1087.

(35) Fernández, J. J.; Figueiras, A.; Granda, M.; Bermejo, J.; Menéndez, R., Modification of coal-tar pitch by air-blowing — I. Variation of pitch composition and properties. *Carbon* **1995**, *33 (3),* 295-307.

(36) Fernández, J. J.; Figueiras, A.; Granda, M.; Bermejo, J.; Parra, J. B.; Menéndez, R., Modification of coal-tar pitch by air-blowing II. Influence on coke structure and properties. *Carbon* **1995**, *33 (9),* 1235-1245.

(37) Blanco, C.; Santamaría, R.; Bermejo, J.; Menéndez, R., A comparative study of air-blown and thermally treated coal-tar pitches. *Carbon* **2000**, *38 (4),* 517-523.

(38) Sawran, W.; Turrill, F.; Newman, J.; Hall, N.; Ward, C. Process for the Manufacture of Carbon Fibers and Feedstock Therefor. 4,671,864, 1987.

(39) McHugh, M.; Krukonis, V., *Supercritical Fluid Extraction*, 2nd Ed. Elsevier: Butterworth-Heinemann, 2013; p 608.

(40) Hutchenson, K. W.; Roebers, J. R.; Thies, M. C., Fractionation of petroleum pitch by supercritical fluid extraction. *Carbon* **1991**, *29 (2),* 215-223.

(41) Hansen, C., *Hansen Solubility Parameters: A User's Handbook*, 2nd Ed. CRC Press: Boca Raton, 2012; p 546.

(42) Barton, A. F. M., *CRC Handbook of Solubility Parameters and Other Cohesion Parameters*. Routledge as part of the Taylor and Francis group: New York, 2017.

(43) Mannistu, K. D.; Yarranton, H. W.; Masliyah, J. H., Solubility Modeling of Asphaltenes in Organic Solvents. *Energy Fuels* **1997**, *11 (3),* 615-622.

(44) Strausz, O.; Lown, E. M.*, The chemistry of Alberta oil sands, bitumens and heavy oil.* Alberta Energy Research Inst., Calgary, AB (Canada): Canada, 2003.

(45) Ramírez-Corredores, M. M., *The science and technology of unconventional oils: finding refining opportunities*. Academic Press: London, 2017.

(46) Long, R., Concept of Asphaltenes. In *Chemistry of Asphaltenes*; Division of Petroleum Chemistry. Bunger, J., Li, N., Eds.; American Chemical Society, 1982.

(47) Speight, J. G.; Long, R. B.; Trowbridge, T. D. Factors Influencing the Separation of Asphaltenes from Heavy Petroleum Feedstocks. *Fuel* **1984**, *63(5)*, 616-620.

(48) Gray, M. *Upgrading Oilsands Bitumen and Heavy Oil*. University of Alberta Press: 2015.

(49) Li, X.; Ashida, R.; Miura, K. Preparation of High-Grade Carbonaceous Materials Having Similar Chemical and Physical Properties from Various Low-Rank Coals by Degradative Solvent Extraction. *Energy Fuels* **2012**, *26(11)*, 6897-6904.

(50) Li, X.; Zhu, X. Q.; Xiao, L.; Ryuichi, A.; Kouichi, M.; Luo, G. Q.; Yao, H. Degradative Solvent Extraction of Demineralized and Ion-Exchanged Low-Rank Coals. *J. Fuel Chem. Technol. (Beijing, China).* **2014**, *42(8)*, 897-904.

(51) Li, X.; Zhu, X. Q.; Okuda, K.; Zhang, Z.; Ashida, R.; Yao, H.; Miura, K. Preparation of Carbon Fibers from Low-Molecular-Weight Compounds Obtained from Low-Rank Coal and Biomass by Solvent Extraction. *New Carbon Mater.* **2017**, *32(1)*, 41-47.

(52) de Klerk, A. *Fischer-Tropsch Refining*; 1st ed. Wiley VCH: Weinheim, 2011.

(53) Mallick, R. B.; El-Korchi, T. *Pavement Engineering: Principles and Practice*; 3rd Edition; CRC Press: Boca Raton, Florida, 2013; pp 228.

(54) Kett, I. *Asphalt Materials and Mix Design Manual*; Noyes Publications: New Jersey, 1998; pp 8.

(55) Emanuel, Nikolai; Denisov, Evgenii; Maizus, Z. *Liquid-Phase Oxidation of Hydrocarbons*; Plenum Press: New York, 1967; pp 37-39.

(56) García Zapata, J. L.; De Klerk, A. Viscosity Changes during Mild Oxidation of Oilsands-Derived Bitumen: Solvent Effects and Selectivity. *Energy Fuels* **2014**. *28*, 6242-6248.

(57) Siddiquee, M. N.; De Klerk, A. Hydrocarbon Addition Reactions during Low-Temperature Autoxidation of Oilsands Bitumen. *Energy and Fuels* **2014**. *Energy Fuels*

2014. 28 (11), 6848-6859.

(58) Siddiquee, M. N.; De Klerk, A. Heterocyclic Addition Reactions during Low Temperature Autoxidation. *Energy Fuels* **2015**. *29(7)*, 4236-4244.

(59) Babu, D. R.; Cormack, D. E. Effect of Low-Temperature Oxidation on the Composition of Athabasca Bitumen. *Fuel* **1984**, *64*, 858-861.

(60) Babu, D. R.; Cormack, D. E. Effect of Oxidation on the Viscosity of Athabasca Bitumen. *Can. J. Chem. Eng.* **1983**. *61*, 575-580.

(61) Molnár, Á.; Olah, G. A.; Prakash, G. K. S. *Hydrocarbon Chemistry, Two Volume Set*, 3rd Ed.; Hoboken, New Jersey, 2017; pp 593 – 691.

(62) Niizuma, S.; Steele, C. T.; Gunning, H. E.; Strausz, O. P. Electron Spin Resonance Study of Free Radicals in Athabasca Asphaltene. *Fuel* **1977**. *56(3)*, 249-256.

(63) Murzin, D. Chapter 8: Halogenation. In *Chemical Reaction Technology*, 1st Ed.; De Gruyter: Finland, 2015; pp 197-203.

(64) Prado, G. H. C.; De Klerk, A. Origin of Penetration Hardness Due to Mild Halogenation: A Model Compound Study. *Energy and Fuels* **2015**. *29(11)*, 6935–6947.

(65) Prado, G. H. C.; De Klerk, A. Halogenation of Oilsands Bitumen, Maltenes, and Asphaltenes. *Energy Fuels* **2014**. *28 (7)*, 4458-4468.

(66) Moschopedis, S. E.; Speight, J. G. The Halogenation of Athabasca Asphaltenes with Elemental Halogen. *Fuel* **1971**. *50 (1)*, 58-64

(67) Liu, J.; Shimanoe, H.; Nakabayashi, K.; Miyawaki, J.; Ko, S.; Jeon, Y. P.; Yoon, S. H. Preparation of Isotropic Pitch Precursor for Pitch-Based Carbon Fiber through the Co-Carbonization of Ethylene Bottom Oil and Polyvinyl Chloride. *J. Ind. Eng. Chem.* **2018**. *67*, 276-283.

(68) Kim, B. J.; Eom, Y.; Kato, O.; Miyawaki, J.; Kim, B. C.; Mochida, I.; Yoon, S. H. Preparation of Carbon Fibers with Excellent Mechanical Properties from Isotropic Pitches. *Carbon* **2014**. *77*, 745-755.

(69) Qiao, W. M.; Yoon, S. H.; Korai, Y.; Mochida, I.; Inoue, S.; Sakurai, T.; Shimohara, T. Preparation of Activated Carbon Fibers from Polyvinyl Chloride. *Carbon* **2004**. *42*, 1327-1331.

(70) Otani, S. On the Carbon Fiber from the Molten Pyrolysis Products. *Carbon* **1965**. *3*, 35-38.

CHAPTER 3:
PRETREATMENT I: FURTHER SOLVENT DEASPHALTING/ SOLVENT EXTRACTION OF INDUSTRIAL RAW ASPHALTENES

(3.1) Introduction

The starting material for carbon fiber production is industrially obtained asphaltenes. When asphaltenes are separated industrially, the solvent-to-feed ratio is limited and are in the range of 3 to 10 L/kg in a typical solvent deasphalting process[1]. This ratio is far less than the ratio used in laboratory precipitation procedure to rigorously separate asphaltenes, which is in the range of 10 to 50 L/kg for *n*-pentane and >30 L/kg for *n*-heptane. Hence, the industrially precipitated raw asphaltenes contains other materials that are *n*-alkane soluble, and that could be removed by more rigorous solvent deasphalting. These *n*-alkane soluble materials have lower softening point temperatures and hence, decrease the softening point of the industrially precipitated asphaltenes. For example, heptane insoluble Athabasca asphaltenes is reported to melt at the temperature range of 205 – 234°C[1], which is far higher than 150 – 160 °C when the industrial asphaltenes starts to soften. Low softening point temperature of the industrial asphaltenes can cause the fibers to fuse during the stabilization/ oxidation step, which takes place at temperature ranges of 200 – 400 °C and destroy the fiber integrity.

This study investigated the effect of removing alkane soluble materials on the chemical composition, softening point, which was indirectly measured by its hardness at elevated temperatures, and its behavior during the melt spinning process. The industrial raw asphaltenes from an industrial pentane solvent deasphalting process was further precipitated by 5:1, 10:1 and 40:1 solvent-to-feed ratio with *n*-pentane and *n*-heptane and the products were characterized.

(3.2) Experimental

(3.2.1) Materials

The raw asphaltenes were obtained from CNOOC Ltd. (previously Nexen Energy) from an industrial *n*-pentane solvent deasphalting process at the Long Lake Upgrader, AB, Canada in 2014. The properties of the asphaltenes used for the experiments are shown below in Table 3-1. Standard

deviation values reported correspond to repeatability of the measurements, which were performed in triplicate.

The solvents used for asphaltenes precipitation were *n*-pentane (99.7% purity), and *n*-heptane (99.6% HPLC grade) supplied by Fisher Scientific.

Table 3-1: Properties and Composition of Long Lake Industrial Asphaltenes [a]

Property	Industrial Asphaltenes
Elemental Composition (wt.%)	
Carbon	82.10 ± 0.17
Hydrogen	8.07 ± 0.04
Nitrogen	1.07 ± 0.03
Sulfur	7.61 ± 0.11
Oxygen[b]	1.15 ± 0.26
H:C Molar ratio	1.2
^{1}H NMR aliphatic H (%)	88.6 ± 1.8
Penetration Values (mm) at 186°C[c]	15.3 ± 0.4
Vanadium content (µg/g)	879 ± 4
Nickel content (µg/g)	530 ± 4

[a] Analysis performed in triplicate, values reported as average ± one sample standard deviation

[b] Oxygen content calculated by difference

[c] Applied load of 100 g for 0.10 s using a Humboldt H-1280 needle; details in Section 3.2.3

(3.2.2) Equipment and Procedure

(3.2.2.1) Solvent Deasphalting/ Solvent Extraction Procedure

The procedure for obtaining the *n*-pentane and *n*-heptane insoluble material from industrial raw asphaltenes is as follows. For each experiment, about 10 g of the raw material was mixed with the *n*-alkane solvent in an Erlenmeyer flask for a given solvent-to-asphaltenes (S/A) ratio ($mL_{solvent}/g_{raw\ material}$). To avoid evaporation of the solvent, a rubber stopper was inserted to the mouth of the flask. The solvent and asphaltenes mixture were stirred for 1 hour at room temperature by a magnetic stirring bar. The stirring speed used was 250 rpm and was controlled

by a Fisherbrand™ Isotemp™ Hot Plate Stirrer. After stirring, the mixture was stored in the dark for the next 24 hours.

The stored mixture was vacuum filtered with a 0.22 µm Millipore nitrocellulose membrane filter to obtain the insoluble products. The filter paper with the product was transferred to an aluminum cup and was dried in the fume hood for 48 hours to evaporate the solvent. The dried products were weighed and the previously weighed membrane filter and the aluminum cup were subtracted to obtain the weight of the product. Mettler Model XP1203S analytical balance with the readability of 1 mg and the capacity of 1210 g was used for weighing the materials. All the experiments were conducted in duplicate.

(3.2.2.2) Melt Spinning Procedure

Melt spinning process to produce as-spun fibers was completed using the AT225 melt spinner from Anytester, China. About 8 – 10 g of the material was pre-weighed and was loaded into the chamber inside the melt spinner machine. The bottom of the chamber contained a melt spinning spinneret hole with a diameter of 0.15 mm. Once the material was loaded, the chamber was heated, and the nitrogen line was opened to provide an inert atmosphere inside the chamber. When the chamber reached the temperature where the molten material started extruding through the spinneret hole and forming a droplet, the outlet gas line was closed to subject the chamber to a nitrogen pressure of 400 kPa gauge. The extruded droplet was pulled to be collected in the fibrous form on the rotating drum. At the same chamber temperature, the rotation speed of the drum was progressively increased starting from 100 rpm and the maximum rotation speed that could be achieved without frequent fiber breakage was recorded.

In this study, the chamber temperature in which the material had low enough viscosity to form a droplet will be referred to as the ‘melt spin temperature’ and the maximum rotation speed of the drum attained for the material without frequent fiber breakage will be denoted as the ‘maximum melt spin productivity.’

(3.2.2.3) Process Conditions

In this study, two process conditions were varied – choice of *n*-alkane solvent and solvent-to-asphaltenes (S/A) ratio. The process conditions evaluated in this study were precipitation with *n*-pentane and *n*-heptane, for S/A ratios (ml/g) of 5:1, 10:1 and 40:1. To avoid confusion, the products obtained from each process conditions will be denoted as seen in Table 3-2 throughout this paper.

Table 3-2: Sample Names for Products Obtained for Individual Process Conditions

Process Conditions		**Sample Name**
Solvent Used	**S/A ratio (mL/g)**	
n-pentane	5:1	*n*C5 5:1 Insoluble
	10:1	*n*C5 10:1 Insoluble
	40:1	*n*C5 40:1 Insoluble
n-heptane	5:1	*n*C7 5:1 Insoluble
	10:1	*n*C7 10:1 Insoluble
	40:1	*n*C7 40:1 Insoluble

(3.2.3) Analyses

The precipitated insoluble products were analyzed by the following techniques and instruments:

(a) Penetrometer Test

The hardness of the obtained products was determined using an electric penetrometer, model H-1240, with the penetration needle H-1280 (Humboldt Mfg. Co.). It was not possible to follow the standard test method as the samples were solid at ambient temperatures and the standard test method required larger sample size than was available. About 8 g of the material was loaded in a small beaker, which was submerged in an oil bath. Due to the solid nature of the products, the samples were in an oil bath at the temperature of 185 – 190 °C, where they were in viscous fluids that appeared homogeneous. The beakers with the samples were submerged in the heated oil bath for 60 minutes to allow for temperature equilibrium. Before the measurement, the samples were stirred and left to settle to a constant liquid level. Then, the hardness values were obtained with an applied load of 100 g for 0.10 s.

(b) Proton Nuclear Magnetic Resonance (^{1}H NMR) Spectroscopy

The proton nuclear magnetic resonance (^{1}H NMR) spectra were measured using a NMReady 60 spectrometer (Nanalysis Corp.). Chloroform-d ($CDCl_3$) (99.96 % deuterium, Sigma) was used for sample preparation. Samples were analyzed using standard 5 mm NMR tubes (NORELL). Experimental conditions were: frequency = 60 MHz, spectral range = 0 - 12 ppm, number of scans = 32. In the ^{1}H NMR spectra, the proton shift-value of δ = 0.15 to 3.50 ppm was assigned to aliphatic hydrogen whereas δ = 6.60 to 8.50 ppm was assigned to aromatic hydrogen.

(c) Elemental (CHNS) Analysis

Elemental analysis was conducted by CHNS-O Flash2000 (Thermo Fisher Scientific) located in the Institute for Oil Sands Innovation (IOSI) lab at University of Alberta. The samples were weighed in tin capsules and were loaded in the autosampler to be placed into oxidation/ reduction reactor heated at 900 – 1000°C. With the addition of small volume of pure oxygen, the samples undergo combustion and the tin capsule at these temperatures facilitate exothermic reaction to raise the temperature to 1800°C. The produced elemental gases go through a separation column and thermal conductivity detector (TCD) and carbon, hydrogen, nitrogen, and sulfur contents were determined as CO_2, H_2O, NO_2, and SO_2 with 2,5-Bis (5-tert-butyl-benzoxazol-2-yl) thiophene (BBOT) as the standard.

(d) Fourier Transform Infrared (FTIR) Spectroscopy

Fourier Transform Infrared (FTIR) spectra of the samples were obtained using an ABB MB3000 analyzer with deuterated-triglycine sulfate (DTGS) detector. A PIKE MIRacle TM Reflection Attenuated Total Reflectance (ATR) accessory, containing a diamond crystal plate and high-pressure clamping, was used to facilitate collection of the spectra. IR spectra were obtained over the wavenumber range 4000 – 600 cm^{-1} at 2 cm^{-1} resolution with an average number of scans of 120. After every measurement, the ATR crystal was cleaned with toluene, followed by acetone, then was left to evaporate acetone for at least 3 minutes. Live spectrum was observed after every cleaning to ensure total evaporation of acetone. Background spectra was collected for every 5 measurements.

(e) X-Ray Fluorescence (XRF) Spectroscopy

Nickel and vanadium content were analyzed by X-Ray Fluorescence spectrometry, using S2 Ranger instrument (Bruker Corp.). The instrument contains a silicon drift detector with Peltier cooling, and a Pd-target X-ray tube. XRF calibration for analysis was performed using Ni(II) Phythalocyanine and V2O5 at different concentrations (5-10-20-50-100-200-300-400-500-600-700 ppm) in a potassium carbonate matrix. The analysis was performed at 40keV and the presence of Ni and V metals was indicated by the $K_{\alpha 1}$ lines.

(3.3) Results

(3.3.1) Physical Properties of *n*-Alkane Insoluble Material at Different Solvent-to-Asphaltenes Ratio

(3.3.1.1) Yield of n-Alkane Insoluble Material at Different Solvent-to-Asphaltenes Ratio

The yield of *n*-alkane insoluble products obtained for each process condition are shown in Table 3-3, expressed in wt.% of the raw industrial asphaltenes. As shown, the yield of *n*-alkane insoluble material decreases with the increase in solvent-to-asphaltenes (S/A) ratio, and for a given S/A ratio, smaller yield is observed for precipitation with *n*-heptane compared to *n*-pentane.

According to other literature[2,3], typically the opposite is observed when starting with bitumen as feed, and lower yield is obtained for *n*C7 insoluble than *n*C5 insoluble. For example, in a study by Turuga[3], she observed C5 asphaltenes at 40:1 solvent-to-bitumen (mL/g) ratio had yield of 19.86 wt.% whereas C7 asphaltenes had a yield of 17.40 wt.%. However, these literatures utilize heavy oil as the feedstock and the feed material utilized for this study is industrial asphaltenes, a product from pentane deasphalting process. The opposite trend should therefore be anticipated because it is a removal of *n*-alkane soluble material from industrial asphaltenes and not *n*-alkane insoluble material from bitumen.

Furthermore, as shown in Figure 3-1, the appearance changed from the black and shiny raw industrial asphaltenes to look browner, and the material became more powder-like solids with the increase in the S/A ratio. This is consistent with the observation made by Speight[2], where he noticed asphaltenes produced from ‘insufficient amount’ of *n*-alkane were black, shiny solids

and he attributed this appearance to resins retained in the bulk asphaltenes. He noted that further deasphalting these materials produced asphaltenes that were browner and powderier, as was observed in this study.

Table 3-3: Yield of *n*-Alkane Insoluble Material Obtained from Raw Industrial Asphaltenes for Each Solvent Deasphalting Process Condition

Process Conditions		***n*-Alkane Insoluble Yield (wt.%)**	
Solvent Used	**S/A ratio (v/w)**	**Run 1**	**Run 2**
*n*C5	5:1	85.6	87.8
	10:1	84.0	83.1
	40:1	81.3	79.8
*n*C7	5:1	84.9	81.7
	10:1	77.2	79.9
	40:1	71.7	72.9

Figure 3-1: Appearance of Raw Asphaltene, *n*C5 and *n*C7 40:1 Insoluble (from left to right)

(3.3.1.2) Viscosity of *n*-Alkane Insoluble Material

Considering that one of the key objectives of this research is to increase the softening point temperature of the industrial raw asphaltenes, penetrometer test was used to indirectly assess the softening point of the products. The penetration depth measured for each samples at the given temperature will be an indirect indication of the viscosity of the sample and hence, give an idea of relative softening point of the products compared to the raw asphaltenes. Table 3-4 shows the

penetrometer test results for the raw asphaltenes and the *n*-alkane insoluble products obtained by further solvent deasphalting. With the increase in S/A ratios of solvent deasphalting, smaller penetration depth was observed and decreased from 15.3 mm to as low as 3.4 mm for *n*C5 insoluble materials and as low as 0.6 mm for *n*C7 insoluble materials. For the given S/A ratio, the *n*C7 insoluble materials exhibited lower penetration values than *n*C5 insoluble materials. A decrease in penetration depth corresponds to an increase in softening point temperature and an increase in viscosity.

Table 3-4: Penetrometer Results for *n*-Pentane and *n*-Heptane Insoluble Products Precipitated from Industrial Raw Asphaltenes

Sample[a]	**Penetration (mm)**[b]
Raw Asphaltenes	15.3 ± 0.4
*n*C5 5:1 Insoluble	9.8 ± 0.8
*n*C5 10:1 Insoluble	8.9 ± 0.3
*n*C5 40:1 Insoluble	3.4 ± 1.1
*n*C7 5:1 Insoluble	8.1 ± 0.5
*n*C7 10:1 Insoluble	3.7 ± 1.4
*n*C7 40:1 Insoluble	0.6 ± 0.6

[a] Insoluble materials from Run 1 and 2 were combined

[b] Analysis performed in triplicate, values reported as average ± one sample standard deviation

The yield of *n*-alkane insoluble materials from raw industrial asphaltenes indicated that there are 20 wt.% to 30 wt.% of the industrial asphaltenes that are still soluble in *n*-pentane and *n*-heptane solvents, respectively. In addition, these soluble materials seem to be responsible for black and shiny appearance in the industrial asphaltenes and removing these caused considerable changes in the softening point, as the penetration values decreased from 15.3 mm to as low as 0.6 mm. To obtain a better insight on the separation chemistry, the chemical composition of *n*-alkane insoluble materials was analyzed by elemental analysis, FTIR, ^{1}H NMR and XRF Spectroscopy as discussed in the next section.

(3.3.2) Chemical Composition of *n*-Alkane Insoluble Material at Different Solvent-to-Asphaltenes Ratio

(3.3.2.1) Elemental Composition and Functional Groups Present in the *n*-Alkane Insoluble Material

Elemental analysis of the insoluble products was conducted, and the results are shown in Table 3-5. From the results, H/C, N/C and S/C atomic ratios were calculated. Comparing the H/C atomic ratio of the raw industrial asphaltenes and the obtained *n*-alkane insoluble materials reveal a decrease in H/C molar ratio from 1.17 to at least 1.13. The observed decreasing trend in the H/C molar ratio can be due to a somewhat larger quantity of aromatic compounds being present and/or longer molecules being present in the insoluble material. To better understand the meaning of the observed decrease in H/C, further analysis with proton nuclear magnetic resonance (^{1}H NMR) was performed in Section 3.3.2.2.

Furthermore, there was a slight increase in the N/C molar ratio, which increased from 0.011 to at most 0.013. There was also an increase in the residual content, i.e. not CHNS, with further deasphalting, as it increased from 1.15 wt.% to as high as 3.84 wt.%. On the other hand, there were no significant changes observed for the S/C ratio and varied in the range of 0.034 – 0.037 without any noticeable trends. Overall, the changes in elemental ratios were minor and may not be significant considering the reported uncertainties.

As the residual content was calculated by difference, the observed increase can mean an increase in the oxygen content or an increase in other elements such as metals, or possibly an error during the measurement. To further analyze the chemical composition changes with deasphalting and find if the observed residual content increase represents increase in the O content, Fourier Transform Infrared (FTIR) spectra was obtained as shown in Figure 3-2.

Table 3-5: Elemental Analysis of *n*-Pentane and *n*-Heptane Insoluble Products Precipitated from Industrial Raw Asphaltenes[a]

	N (wt.%)		C (wt.%)		H (wt.%)		S (wt.%)		Residual [b] (wt.%)		H/C[d]	N/C[d]	S/C[d]
	x	u	x	u	x	u	x	u	x	u			
Raw Asphaltenes	1.07	0.03	82.10	0.17	8.07	0.04	7.61	0.11	1.15	0.26	1.17	0.011	0.035
*n*C5 5:1 Insoluble	1.12	0.02	81.27	0.68	7.80	0.08	7.64	0.08	2.17	0.77	1.14	0.012	0.035
*n*C5 10:1 Insoluble	1.18	0.02	81.97	0.20	7.85	0.03	7.38	0.68	1.62	0.52	1.14	0.012	0.034
*n*C5 40:1 Insoluble[c]	1.18	-	81.37	-	7.75	-	8.00	-	1.70	-	1.13	0.012	0.037
*n*C7 5:1 Insoluble	1.16	0.01	81.49	0.17	7.86	0.05	7.82	0.05	1.67	0.23	1.15	0.012	0.036
*n*C7 10:1 Insoluble	1.20	0.01	81.27	0.30	7.78	0.04	7.76	0.05	1.99	0.36	1.14	0.013	0.036
*n*C7 40:1 Insoluble	1.19	0.04	79.75	3.09	7.62	0.30	7.60	0.33	3.84	3.64	1.13	0.013	0.036

[a] (x) average and (u) standard deviation due to repeatability of 3 measurements

[b] Residual content calculated by difference

[c] Analysis performed once due to limited quantity of the product available

[d] Molar ratio

The spectra in Figure 3-2 of the insoluble materials indicated no clear trends with the changes in the *n*-alkane solvents or with the increasing S/A ratios. There were some changes in the spectra observed at wavelengths 1711 – 1715 cm^{-1}, 1356 – 1360 cm^{-1} and 1217 – 1219 cm^{-1} range, which corresponds to C=O, S=O and C–O stretching, respectively. FTIR is particularly sensitive to oxygen containing functional groups and if the residual content shown in Table 3-5 was reflective of change in O/C content, then these differences should have been seen in the FTIR spectra. As seen in Figure 3-2, the FTIR spectra did not show significant increases in the C-O, S=O and C=O bonds with rigorous deasphalting and suggested that it is unlikely that the increase in the residual content reflects an increase in the oxygen content.

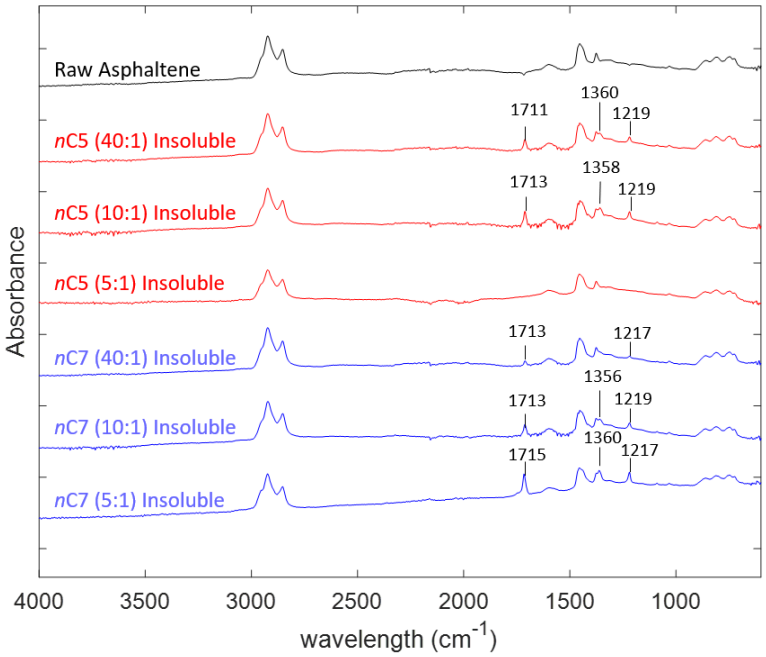

Figure 3-2: FTIR Spectra of *n*-Pentane and *n*-Heptane Insoluble Products Precipitated from Industrial Raw Asphaltenes

However, there is one consideration that needs to be taken into account and that is the heterogeneous nature of the insoluble materials. Although there was a significant increase in the residual content with more rigorous separation as seen in Table 3-5, there was also a very high standard deviation noted for the residual content in the insoluble materials. Similarly, there was a deviation in the FTIR spectra for the subsamples from the same deasphalting conditions and is shown in Figure 3-3. The subsamples obtained from the same batch of *n*C5 (10:1) insoluble materials showed notable differences in 1711 – 1715 cm^{-1}, 1356 – 1360 cm^{-1} and 1217 – 1219 cm^{-1} range, which corresponds to C=O, S=O and C-O stretching, and are coincidentally the peaks attributed to bonds with oxygen. Hence, it is possible that the observed increase in the residual content by elemental analysis represents the increase in the oxygen content, and the insoluble materials exhibit very heterogeneous nature in terms of oxygen functionalities.

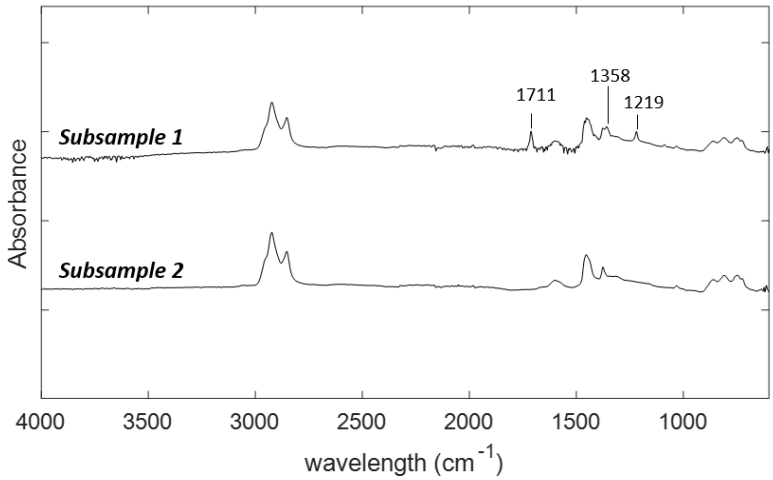

Figure 3-3: FTIR Spectra of Two *n*C5 10:1 Insoluble Subsamples

(3.3.2.2) Aromatic Compounds in the Insoluble Materials (^{1}H NMR and H/C ratios)

As previously observed in Table 3-5, there was a slight decrease in H/C observed with the increase in S/A ratio. The decrease could have been due to higher among of aromatic compounds or longer chains of hydrocarbons present in the bulk material. To further test this, ^{1}H NMR analysis was used to investigate if there were any increases in the aromatic distribution of hydrogen in the precipitated insoluble materials.

Table 3-6 shows % aliphatic H for *n*-pentane and *n*-heptane insoluble, respectively, and its difference represents the % aromatic H. As shown in Table 3-6, there appears to be a slight decreasing trend in % aliphatic H with an increase in the S/A ratios for using *n*-pentane, as it decreased from 88.6% to 87.0%. The *n*-heptane insoluble materials did not show a significant change with the increasing S/A ratio and % aliphatic H were in the range of 87.3% to 87.7%.

In literature, asphaltenes precipitated from higher carbon number (CN) solvents are reported to be more aromatic. For example, Luo *et al.*[4] precipitated C3, C5 and C7 asphaltenes from heavy oil and through performing ^{1}H NMR and ^{13}C NMR, found C7 asphaltenes to be more aromatic compared to C3 and C5 asphaltenes. Furthermore, other literature[5,6] reported that C7 asphaltenes had lower H/C ratio compared to the C5 asphaltenes obtained from the same source oil.

However, this observation is not consistent with % aliphatic H content results presented in Table 3-6 or the H/C ratios presented in Table 3-5, and that is most likely to due to the feed material utilized for this study. In heavy oil, there are C5-soluble but C7-insoluble aromatic compounds present and this will produce C7 asphaltenes to have more aromatic compounds compared to C5 asphaltenes. However, the starting material utilized for this study is C5 asphaltenes from an industrial solvent deasphalting process, and hence, these C5-soluble but C7-insoluble aromatic compounds are mostly removed. Therefore, aliphatic H % and H/C atomic ratio for *n*C7 insoluble materials is observed to be the same as *n*C5 insoluble materials in this study.

Table 3-6: ^{1}H NMR Results for *n*-Pentane and *n*-Heptane Insoluble Products Precipitated from Industrial Raw Asphaltenes [a]

Sample	Aliphatic H (%)
Raw Asphaltenes	88.6 ± 1.8
*n*C5 5:1 Insoluble	88.9 ± 0.3
*n*C5 10:1 Insoluble	87.2 ± 1.6
*n*C5 40:1 Insoluble	87.0 ± 0.8
*n*C7 5:1 Insoluble	87.3 ± 2.3
*n*C7 10:1 Insoluble	87.5 ± 1.2
*n*C7 40:1 Insoluble	87.7 ± 0.8

[a] Analysis performed in triplicate, values reported as average ± one sample standard deviation

(3.3.2.3) Nickel and Vanadium Content in *n*-Alkane Insoluble Material

X-Ray Fluorescence (XRF) spectroscopy was used to quantify nickel (Ni) and vanadium (V) present in the *n*-alkane insoluble materials and the results are shown in Table 3-7. With the increase in the S/A ratio, Ni content did not change considerably whereas vanadium content changed significantly. Specifically, Ni content did not change through further deasphalting with *n*-pentane up to S/A ratio of 10:1. Only at S/A ratio of 40:1, there was a slight increase in the Ni content as it increased from 530 ppm up to 584 ppm. On the other hand, removing the *n*C7-soluble materials seemed to have more effect on the Ni content, as it increased progressively from 530 ppm to 587 ppm. Furthermore, removing the *n*C5 and *n*C7 soluble materials increased

the V content more significantly and their content increased from 879 ppm to as high as 1023 ppm and 1057 ppm, respectively.

Table 3-7: Nickel and Vanadium Content of *n*-Pentane and *n*-Heptane Insoluble Products Precipitated from Industrial Raw Asphaltenes by XRF Spectroscopy [a]

Sample	**Ni (ppm)**		**V (ppm)**	
	x	**u**	**x**	**u**
Raw Asphaltenes	530	4	879	4
*n*C5 5:1 Insoluble	524	5	908	2
*n*C5 10:1 Insoluble	531	8	939	8
*n*C5 40:1 Insoluble	584	21	1023	12
*n*C7 5:1 Insoluble	545	9	929	4
*n*C7 10:1 Insoluble	568	26	978	50
*n*C7 40:1 Insoluble	587	15	1057	7

[a] (x) average and (u) standard deviation due to repeatability of 3 measurements

The observed increase in the Ni and V is indicative of insolubility of Ni- and V-bearing compounds in *n*-alkane solvents. In oilsands-derived bitumen, Ni and V are reported to be present mainly in metalloporphyrin form[1], which is shown in Figure 3-4 below. The bulky metalloporphyrin structure contains Ni^{2+} or VO^{2+} in the core coordinated with nitrogen in the porphyrin ring structure. Interestingly, as seen in Table 3-5 and Table 3-7, removing *n*-alkane soluble materials increased the N/C ratio and Ni and V content. This could suggest that Ni and V in industrial asphaltenes are mostly present as metalloporphyrin compounds, which are retained even with further removing *n*-pentane and *n*-heptane soluble materials.

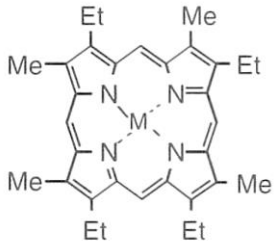

Figure 3-4: Structure of Metalloporphyrin (M = Ni^{2+} or VO^{2+})

To further test this idea, Ni/N and V/N atomic ratios were calculated from the elemental analysis and XRF data and are shown in Table 3-8. If all Ni and V are indeed present in metalloporphyrin structure, Ni/N and V/N ratios of the *n*-alkane insoluble materials will stay relatively the same as raw asphaltenes. Interestingly, Ni/N and V/N atomic ratios of the separated *n*C5 and *n*C7 insoluble materials did remain relatively constant as the raw industrial asphaltenes and all remained in the range of 0.00011-0.00012 for Ni/N and 0.00022-0.00024 for V/N atomic ratios. A study by Freeman and Swahn[7] observed nickel and vanadyl porphyrin compounds to have very low solubility in hexane (<10µg/$mL_{solvent}$). This confirms that most of the Ni and V-bearing compounds in the industrial asphaltenes are most likely in *n*-alkane insoluble metalloporphyrin structures.

Table 3-8: Ni/N and V/N Atomic Ratios in *n*C5 and *n*C7 Insoluble Materials

	Ni/N	**V/N**
Raw Asphaltenes	0.00012	0.00023
*n*C5 5:1 Insoluble	0.00011	0.00022
*n*C5 10:1 Insoluble	0.00011	0.00022
*n*C5 40:1 Insoluble	0.00012	0.00024
*n*C7 5:1 Insoluble	0.00011	0.00022
*n*C7 10:1 Insoluble	0.00011	0.00022
*n*C7 40:1 Insoluble	0.00012	0.00024

(3.3.3) Effect of Removing *n*-Alkane Soluble Material on Melt Spinning Process

The impact of how the solvent deasphalting process by which the asphaltenes were obtained affected the melt spinning of fibers was evaluated. For this purpose, the industrial asphaltenes and *n*C5 and *n*C7 insoluble materials obtained at 40:1 S/A ratio were selected. The results of the melt spinning process are shown in Table 3-9.

Table 3-9: Maximum Melt Spinning Productivity for Different Asphaltenes Feed Materials

Asphaltenes feed material	Melt Spin Temperature (°C)	Maximum Melt Spinning Productivity
Raw asphaltenes	195	200 rpm (126 m/min)
*n*C5 40:1 Insoluble	210	800 rpm (502 m/min)
*n*C7 40:1 Insoluble	223	100 rpm (63 m/min)

As shown in Table 3-9, industrial asphaltenes suffered from poor spinnability and the fibers broke often during the melt spinning process. This had a negative effect on the productivity as well as the resulting fibers. Due to the frequent fiber breakage, the maximum melt spinning speed that could be maintained was 200 rpm (126 m/min).

Of the three asphaltenes, the *n*C7 40:1 insoluble material had the worst spinnability. The highest melt spinning speed that could be maintained was 100 rpm (63 m/min) and the material produced suffered significantly from the fiber breakage. Hence, the fibers produced from *n*C7 40:1 insoluble material often had very broad diameter distribution. The best melt spinning performance was found for the *n*C5 40:1 insoluble material. A melt spinning speed of 800 rpm (502 m/min) could be maintained. There was less fiber breakage for the *n*C5 40:1 insoluble material and the produced fibers were more consistent compared to the fibers from any of the other asphaltenes.

To illustrate the impact of the melt spinning performance and resulting diameter distribution, the fibers obtained from the *n*C7 40:1 insoluble and *n*C5 40:1 insoluble material are compared in Figure 3-5. The large diameter distribution of the fibers prepared from *n*C7 (40:1) insoluble material is immediately apparent.

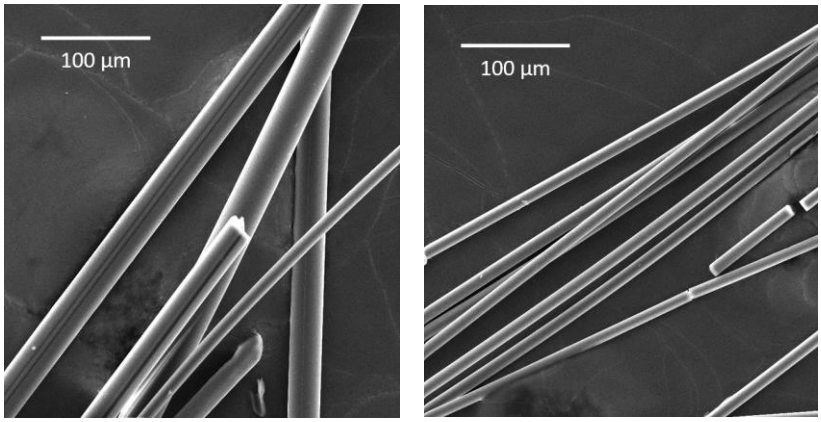

Figure 3-5: As-Spun Precursor Fibers from the *n*C7 (40:1) Insoluble (left) and *n*C5 (40:1) Insoluble (right) Materials

(3.4) Discussion

(3.4.1) What are the Differences Between *n*C7 Insoluble Materials Compared to *n*C5 Insoluble Materials?

Interestingly, behavior of *n*C5 40:1 and *n*C7 40:1 insoluble material during the melt spinning process were vastly different as seen in Section 3.3.3. To find what caused these differences, comparison of *n*C5 and *n*C7 40:1 insoluble material was performed more in detail, and the comparison is organized in Table 3-10 below. As seen, there is about 8.3 wt.% *n*C7 soluble but *n*C5 insoluble material and removing these materials cause significant changes in the viscosity, as seen by the decrease in the penetration value from 3.4 mm to 0.6 mm. However, there were no notable differences observed between *n*C5 and *n*C7 insoluble materials in terms of H/C, N/C, S/C atomic ratio, or the Ni and aliphatic H content.

Table 3-10: Comparison Between *n*C5 and *n*C7 40:1 Insoluble Materials

	***n*C5 (40:1) Insoluble**	***n*C7 (40:1) Insoluble**
Yield (wt.%)[a]	80.6	72.3
Penetration Values (mm)	3.4	0.6
C (wt.%)	81.37 [b]	79.75
H (wt.%)	7.75 [b]	7.62
N (wt.%)	1.18 [b]	1.19
S (wt.%)	8.00 [b]	7.60
Residual (wt.%)[c]	1.70 [b]	3.84
Ni (ppm)	584	587
V (ppm)	1023	1057
H/C	1.13	1.13
N/C	0.012	0.013
S/C	0.037	0.036

[a] Average of Run 1 and Run 2

[b] Only run once due to the limited amount of sample available

[c] Calculated by difference

On the other hand, there was slightly lower C and H content noted for *n*C7 insoluble materials compared to *n*C5 insoluble materials. As well, *n*C7 had slightly higher residual and V content. Slightly lower S content was also noted for C7 (40:1) insoluble materials but as seen in Table 3-5, *n*C7 insoluble at 5:1 and 10:1 S/A ratio typically had higher S content than *n*C5 insoluble at the same S/A ratio. This observation may be just due to having one run of elemental analysis run on C5 (40:1) insoluble materials and hence, will not be compared in detail.

Due to the limited composition changes noted for the two products, *n*C7 (40:1) and *n*C5 (40:1) insoluble materials, strong conclusions regarding the difference between these two products could not be made. Hence, the Hansen solubility parameters were used to get an idea on the differences between *n*C7 (40:1) and *n*C5 (40:1) insoluble materials; what were the *n*C5 insoluble but *n*C7 soluble species?

According to the Hansen solubility parameter as outlined in Section 2.5, pentane and heptane have solubility parameters of 14.5 and 15.3 $MPa^{1/2}$, respectively. With the higher solvent power, heptane will dissolve more compounds with higher solubility parameters than pentane, which includes longer or bulkier hydrocarbons, or heteroatom-bearing species that has strong interactions due to the polar forces or hydrogen bonds. To find if the differences in the physical properties in *n*C5 and *n*C7 insoluble materials are mainly due to more long and bulkier hydrocarbons, or heteroatom-bearing species present, the yield of carbon, hydrogen, sulfur, and nitrogen relative to the feed material were calculated and shown in Table 3-11. The yield was calculated by using the average of the yield (wt.%) for each alkane insoluble materials as was shown in Table 3-3 and using the elemental composition data from Table 3-5.

Since *n*C5 (40:1) insoluble data is based on only one run of elemental analysis, opposed to three runs obtained for the other products, it may not be as accurate. Hence, the yield data of *n*C5 and *n*C7 insoluble materials from S/A ratio of 5:1 and 10:1 are discussed. As shown, both C and H yields for *n*C7 insoluble materials are 3 wt.% lower compared to *n*C5 insoluble materials at 5:1 ratio and are 5 wt.% lower at 10:1 ratio, respectively. On the other hand, yield of nitrogen is relatively the same at 5:1 ratio but at 10:1, *n*C7 insoluble materials show around 4 wt.% lower nitrogen yield compared to *n*C5 insoluble. Yield of sulfur remains relatively the same for S/A ratio of 5:1 and 10:1. These yield values suggest that the materials that are *n*C5 insoluble and *n*C7 soluble are mostly carbon and hydrogen, and possibly some nitrogen containing species.

Table 3-11: Yield of Carbon, Hydrogen, Nitrogen and Sulfur Relative to the Elements Present in the Feed Material

Yield Relative	***n*C5 Insoluble Materials**			***n*C7 Insoluble Materials**		
to Feed Material	**5:1**	**10:1**	**40:1[a]**	**5:1**	**10:1**	**40:1**
C (wt.%)	86%	83%	80%	83%	78%	70%
H (wt.%)	84%	81%	77%	81%	76%	68%
N (wt.%)	91%	92%	89%	90%	88%	80%
S (wt.%)	87%	81%	85%	86%	80%	72%

[a] Only run once due to the limited amount of sample available

(3.4.2) Predicted Improvement in Carbon Fiber Quality by Removing *n*-Alkane Soluble Materials

Other than more consistent fibers with better productivity being produced, removing the *n*-alkane soluble materials are expected to decrease the stabilization time. The *n*-alkane insoluble materials had an increase in the spinning temperature, as it increased from 195°C to 210°C for *n*C5 40:1 insoluble material, and to 223°C for *n*C7 40:1 insoluble material. As previously mentioned in Section 2.3.2, increasing the softening point temperature of the precursor can shorten the time and cost intensive stabilization step.

On the other hand, there are few potential downsides to using this method as pretreatment and that is the cost considerations for commercialization. To obtain the softening point temperature increase of about 15°C, 40 mL of n-pentane solvent had to be utilized for 1 g of asphaltenes. To utilize this amount of solvent in the commercialized process, it will require large equipment for performing the solvation process as well as the solvent recovery process, which can incur large capital investments. In addition, the operating costs for the solvent recovery is expected to be expensive due to the large amount of heat required to recover the large volume of solvents.

One of the big game changers to this assessment is to see how much benefit this pretreatment has on the final carbon fiber quality. From the chemical composition analysis, removing the *n*-alkane soluble materials seemed to remove some carbon and hydrogens, and retain metalloporphyrins and possibly O-containing compounds. As discussed in Section 2.3, having high heteroatom content precursor can lead to defect formation during carbonization stage, and negatively affect the fiber performance. Hence, it was estimated that performing solvent extraction as the pretreatment method may not benefit the final carbon fiber quality. However, as shown in Appendix B, carbon fibers from C5 (40:1) Insoluble materials did not necessarily show deteriorated or improved performance compared to carbon fibers from industrial asphaltenes.

To more properly assess the viability of utilizing solvent deasphalting as a commercialized pretreatment process, more detailed analysis must be completed to quantify how much shortening of the stabilization time is achieved. With this further analysis, better evaluation of

using this solvent extraction/ solvent deasphalting process as a pretreatment method can be performed.

(3.5) Conclusions

Using solvent extraction with *n*-alkane as a pretreatment method for carbon fiber production purposes was evaluated. From this study, the following conclusions were obtained:

a) With higher S/A ratio utilized, more *n*-alkane soluble fractions can be removed from industrially precipitated asphaltenes. Removal of these fractions increase the viscosity as indirectly determined by penetrometer tests; through removing the *n*C5-soluble materials and *n*C7-soluble materials, softening point temperature increase up to 15°C and 28°C was achieved, respectively.

b) Most nickel and vanadium in the oilsands-derived asphaltenes from an industrial pentane deasphalting process are reportedly in metalloporphyrin structures. Metalloporphyrins are not very soluble in *n*-pentane or *n*-heptane and hence, is retained even with further deasphalting.

c) Through further deasphalting procedure, up to about 20 wt.% and 30 wt.% of *n*C5 and *n*C7 soluble materials can be removed from the industrial raw asphaltenes.

d) Removing *n*C7 soluble materials from the industrial asphaltenes from the C5 solvent deasphalting process had a negative effect on the melt spinning process and produced fibers with inconsistent diameters with low melt spin productivity. However, removing *n*C5 soluble materials produced precursor that was able to achieve high melt spin productivity and that produce fibers with more consistent diameters. There must be *n*C7 soluble but *n*C5 insoluble component that is vital for the melt spin process that aid in producing more consistent diameter fibers and improved melt spin productivity.

(3.6) References

(1) Gray, M. R., Upgrading Oilsands Bitumen and Heavy Oil. University of Alberta Press: 2015.

(2) Speight, J. G.; Long, R. B.; Trowbridge, T. D., Factors Influencing the Separation of Asphaltenes from Heavy Petroleum Feedstocks. *Fuel* **1984**, *63*, 616-620.

(3) Turuga, A. S. S. Effect of Solvent Deasphalting Process on the Properties of Deasphalted Oil and Asphaltenes From Bitumen. M.S. Thesis, University of Alberta, 2017.

(4) Luo, P.; Wang, X.; Gu, Y., Characterization of Asphaltenes Precipitated with Three Light Alkanes under Different Experimental Conditions. *Fluid Phase Equilib* **2010**, 291 (2), 103–110.

(5) Ancheyta, J.; Centeno, G.; Trejo, F.; Marroquín, G.; García, J. A.; Tenorio, E.; Torres, A. Extraction and Characterization of Asphaltenes from Different Crude Oils and Solvents. *Energy Fuels* **2002**, 16 (5), 1121–1127.

(6) Speight, J. G. Chemical and Physical Studies of Petroleum Asphaltenes. *Dev. Pet. Sci.* **1994**, 40 (PA), 7–65.

(7) Freeman, D. H.; Swahn, I. D.; Hambright, P. Spectrophotometry and Solubility Properties of Nickel and Vanadyl Porphyrin Complexes. *Energy Fuels* **1990**, 4 (6), 699–704.

CHAPTER 4:
PRETREATMENT II: AUTOXIDATION OF INDUSTRIAL RAW ASPHALTENES

(4.1) Introduction

Autoxidation is a widely used method for road paving industries to achieve asphalt hardening. The process utilizes air to oxidize bulk asphalt to produce more temperature and weather resistant road paving asphalt. In a typical process, air-blowing or oxidation is facilitated at temperatures of 240°C – 320°C and it results in a decrease in penetration, increase in the softening point and decrease in temperature susceptibility[1].

In the bitumen literature, various studies were conducted on bitumen hardening during autoxidation at mild conditions. For example, Babu and Cormack[2] found that autoxidation of Athabasca bitumen at temperatures <100°C caused a significant increase in the viscosity. Similarly, Javadli and de Klerk[3] observed more than six-fold increase in bitumen viscosity after autoxidation of bitumen at 175°C. As significant hardening is observed for autoxidation of bitumen, heteroatom-rich asphaltenes from bitumen is expected to be more susceptible to oxidative addition.

In this study, asphaltenes autoxidation at 190°C – 250°C as a pretreatment method for carbon fiber production was investigated. To allow liquid-phase autoxidation of asphaltenes, the reaction temperature had to be higher than 190°C but also be less than 250°C due to commercialization considerations; heat exchange with steam can be utilized for heating at temperatures ≤250°C but more expensive furnace heating is required for heating at temperatures ≥250°C in commercialized processes[5]. Furthermore, autoxidation by bubbling of air into the bulk material was utilized in this study because a previous analysis[6] on bitumen autoxidation noted bubbling air into the bulk material caused more increase in the viscosity than autoxidation via having an air atmosphere with limited gas-liquid transfer area.

(4.2) Experimental

(4.2.1) Materials

The asphaltenes feed material employed in this work was obtained from CNOOC Ltd. (previously Nexen Energy) from the *n*-pentane solvent deasphalting process at the Long Lake Upgrader in Alberta, Canada. The asphaltenes used in these experiments were obtained from the same barrel as the material utilized in Chapter 3. The characterization of the asphaltenes is shown in Table 3-1.

The cylinder gases used for the autoxidation and control reactions were compressed air and ultra-high purity nitrogen (99.999% mole fraction purity) supplied by Praxair. Silicone oil used for the oil bath was supplied by Beantown Chemical.

(4.2.2) Equipment and Procedure

(4.2.2.1) Autoxidation Procedure

Autoxidation of industrial raw asphaltenes was performed by using the apparatus as shown in Figure 4-1. The setup consists of a PYREX 500 mL three-neck round-bottom flask submerged in a silicone oil bath. The first neck of the flask is connected to an air supply line, the second neck connected to a condenser with the circulating cooling fluid set to 20°C, and finally, the third neck sealed by a rubber stopper to avoid evaporation of volatiles. The air was supplied by the Praxair air cylinder and its flow was adjusted by MTI Corporation Compact Direct Read Flow Meter connected in the inlet line.

Before the reaction, about 50 g of the raw material was loaded to the three-neck round-bottom flask. The flask and the raw asphaltenes was heated to the reaction temperature by the silicone oil bath placed on the Fisherbrand™ Isotemp™ Hot Plate. The selected reaction temperatures were 190°C, 220°C and 250°C. The raw material was preheated to the reaction temperature and when the oil bath reached the reaction temperature, the air supply line was opened, and the reaction time was started. The raw material was magnetically stirred at the stirring speed of 250 rpm by the Fisherbrand™ Isotemp™ Hot Plate Stirrer during the reaction at 220°C and 250°C. On the other hand, autoxidation at 190°C could not be stirred during the reaction due to the high viscosity of the feed material. At the end of the reaction time, the air supply line was shut off and

the product was left in the fume hood to cool. Various reaction times up to 24 hours were investigated. Mettler Model XP1203S analytical balance with the readability of 1 mg and the capacity of 1210 g was used for weighing the materials before and after the reaction.

To check if the heating itself had an effect, control experiments using an inert nitrogen atmosphere were also carried out for the reaction time of 8 hours. For the control experiments, they were carried out in the same way as the autoxidation reactions except there was no air supply line and prior to heating, the flask with the raw material was flushed with nitrogen.

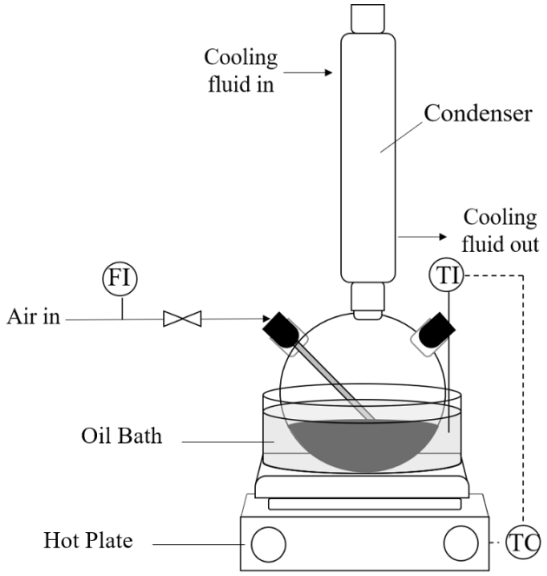

Figure 4-1: Experimental Setup for the Autoxidation of Raw Industrial Asphaltenes

(4.2.2.2) Melt Spinning Procedure

Melt spinning to produce as-spun fibers from the oxidized asphaltenes was completed by using the same procedure and equipment as described in Section 3.2.2.2.

(4.2.3) Analyses

The oxidized products were analyzed by the following techniques and instruments:

(a) Refractive Index

Refractive index measurements were performed using Anton Paar Abbemat 200 refractometer. Since asphaltenes and oxidized products are solid at room temperatures, 100 mg ± 0.5 mg of raw industrial asphaltenes or oxidized products

were mixed with 500 µL of toluene measured with a 1000 µL pipette until the mixture appeared homogeneous. The refractive index of the mixture was measured at 20°C, 30°C, and 40°C using the sodium D-line (589 nm). The range of the instrument is 1.30 to 1.72 nD and the accuracy is ± 0.0001 nD. Ethanol check was completed prior to every measurement to ensure the equipment is working properly and to ensure the measuring cell is completely clean.

In addition, elemental analysis (CHNS), proton nuclear magnetic resonance (^{1}H NMR) spectroscopy, Fourier transform infrared (FTIR) spectroscopy and the penetrometer tests for the oxidized asphaltenes was performed using the same procedure as described in Chapter 3.

(4.3) Results

(4.3.1) Preliminary Autoxidation Experiments at Various Conditions

As outlined in Section 2.6, it is desired to facilitate autoxidation to induce addition reactions without incorporating too much oxygen. In theory, this can be achieved through autoxidation with limited oxygen availability. To find the appropriate air flow rate and the reaction time for autoxidation of asphaltenes, six preliminary autoxidation experiments were completed at various reaction times and air flow rates. The autoxidation conditions summarized in Table 4-1 were investigated.

Table 4-1: Preliminary Autoxidation Experiment Conditions

Reaction Temperature (°C)	Reaction Time (Hours)	Air Flow Rate (mL/min)	Stirred?
190	4	150	No[a]
	8	150	
	4	300	
220	8	450	Yes
	12	300	
	12	450	

[a] Due to the high viscosity of the raw asphaltenes, it could not be stirred using the magnetic stirrer

To see if the studied preliminary autoxidation experiment conditions facilitated cross-linking reactions, refractive index measurements were obtained for the oxidized samples as shown in Table 4-2 and 4-3. Refractive index is the ratio of velocity of the propagation of light in vacuum to that in a given medium[7]. The value increases in the order paraffins < naphthenes < aromatics, and in a given structural series, the value increases with molecular size. It is widely used in the petroleum industry as a quick and useful method to obtain the composition of petroleum[7,8].

As shown in Table 4-2, products from the autoxidation experiments at 190°C showed an increase in the refractive index measurements. However, all products exhibited high standard deviations compared to the raw asphaltenes. On the other hand, the products from autoxidation at 220°C produced oxidized products with comparable standard deviations to the raw asphaltenes. The refractive index values for the oxidized samples at 220°C did not have significant changes from the raw asphaltenes except for the sample oxidized at 220°C, 8 hours at 450 mL/min.

Table 4-2: Refractive Index Results for the Preliminary Autoxidation Experiments at 190°C[a]

Measurement Temperatures (°C)	Refractive Index Measurements (nD)			
	Raw Asphaltenes	190°C, 300 mL/min, 4 h	190°C, 150 mL/min, 4 h	190°C, 150 mL/min, 8 h
20	1.5286 ±0.0006	1.5287 ±0.0017	1.5291 ±0.0018	1.5298 ±0.0015
30	1.5228 ±0.0004	1.5224 ±0.0021	1.5232 ±0.0016	1.5240 ±0.0016
40	1.5176 ±0.0008	1.5164 ±0.0031	1.5175 ±0.0013	1.5183 ±0.0019

[a] Analysis performed in triplicate, values reported as average ± one sample standard deviation

Table 4-3: Refractive Index Results for the Preliminary Autoxidation Experiments at 220°C[a]

Measurement Temperatures (°C)	Refractive Index Measurements (nD)			
	Raw Asphaltenes	220°C, 300 mL/min, 12 h	220°C, 450 mL/min, 8 h	220°C, 450 mL/min, 12 h
20	1.5286 ±0.0006	1.5285 ±0.0003	1.5294 ±0.0005	1.5284 ±0.0004
30	1.5228 ±0.0004	1.5225 ±0.0002	1.5236 ±0.0006	1.5225 ±0.0003
40	1.5176 ±0.0008	1.5174 ±0.0013	1.5187 ±0.0004	1.5178 ±0.0004

[a] Analysis performed in triplicate, values reported as average ± one sample standard deviation

As the autoxidation at 220°C, 450 mL/min, 8 h product showed the most increase in the refractive index values, proton nuclear magnetic resonance (^{1}H NMR) was measured to track if there were any changes to the nature of hydrogen present in the sample. Furthermore, other products from the autoxidation reactions at 220°C were also analyzed. As seen in Table 4-4, all oxidized asphaltenes samples showed a decrease in the aliphatic H present and 220°C, 450 mL/min, 8 h showed the most decrease in the aliphatic H present compared to the raw asphaltenes.

Table 4-4: ^{1}H NMR Results for the Preliminary Autoxidation Experiments at 220°C[a]

Sample	**Aliphatic H (%)**
Raw Asphaltenes	88.6 ± 1.8
220°C, 300 mL/min, 12 h	84.0 ± 0.2
220°C, 450 mL/min, 8 h	83.2 ± 0.2
220°C, 450 mL/min, 12 h	85.5 ± 2.1

[a] Analysis performed in triplicate, values reported as average ± one sample standard deviation

(4.3.2) Autoxidation and Control Experiments for 8 Hours at Temperatures of 190°C – 250°C

From the preliminary autoxidation experiments, 220°C, 450 mL/min, 8 h showed the highest refractive index values and the most decrease in aliphatic H content from the raw asphaltenes, suggesting that it is an autoxidation condition possibly with the most cross-linking reactions.

Hence, further autoxidation experiments for 8-hour reaction time with an air flow rate of 450 mL/min were performed for the reaction temperatures of 190°C, 220°C, and 250°C. In addition, the effect of heating itself at these temperatures was investigated by heating the raw industrial asphaltenes under nitrogen as the control experiment.

(4.3.2.1) Physical Properties of Oxidized Asphaltenes After Autoxidation at 190°C – 250°C for 8 Hours

To assess if there were any changes in the physical properties by autoxidation, penetration values for all oxidized and control products were obtained as presented in Table 4-5. For both products from the oxidation and control experiments, it showed a decrease in the penetration depth with the increasing reaction temperature. Penetration depth decreased from 15.3 mm to as low as 9.6 mm for the oxidized samples and as low as 10.8 mm for the products from the control experiments. A decrease in penetration depth is an indirect indication of an increase in softening point temperature and an increase in viscosity.

The mass changes from both autoxidation and control experiments could not be accurately assessed due to the nature of the experimental procedure using the oil bath as the heating medium. After the reactions, not all oil could be removed from the flask and hence, led to a slight mass increase when the final mass was measured. If there were any mass changes during the autoxidation or control experiments, they were in the margin of error caused by the residual from the oil bath which is in the range of <1-2 wt.% compared to the mass of the initial asphaltenes feed.

Given that there were no significant mass losses during both oxidation and control experiments, the observed decrease in the penetration depth suggests reactions taking place, instead of physical phenomena such as loss of volatiles. What is interesting is that both autoxidation and control experiments created asphaltenes to become more viscous, as suggested by the decrease in penetration. For autoxidation, carbonyl formation and oxidative addition reactions can cause increase in viscosity. On the other hand, for the control experiments, due to the high free radical content of the oilsands-derived asphaltenes, free radical addition reactions are possible and can cause an increase in viscosity. For instance, heating Cold Lake bitumen at 150°C and 200°C

under nitrogen was reported to induce free radical addition reactions to form more viscous products[9]. To further assess which reactions took place during the autoxidation and control experiments, elemental analysis, Fourier transform infrared (FTIR) spectroscopy, proton nuclear magnetic resonance (^{1}H NMR) spectroscopy and refractive index measurements were obtained and is discussed in the next section.

Table 4-5: Penetrometer Results for the Oxidized Asphaltenes and Products from the Control Experiments at 190°C, 220°C, and 250°C for 8 hours [a, b]

Sample	Penetration (mm)[a]
Raw Asphaltenes	15.3 ± 0.4
Oxidized 190°C	12.8 ± 0.6
Oxidized 220°C	-[c]
Oxidized 250°C	9.6 ± 2.6
Control 190°C	17.9 ± 1.0
Control 220°C	13.2 ± 1.4
Control 250°C	10.8 ± 2.8

[a] Analysis performed in triplicate, values reported as average ± one sample standard deviation

[b] Applied load of 100 g for 0.10 s using a Humboldt H-1280 needle at 185 – 190°C

[c] Analysis not performed due to the limited amount of product available

(4.3.2.2) Chemical Composition of Oxidized Asphaltenes After Autoxidation at 190°C – 250°C for 8 Hours

Elemental analysis for the oxidized asphaltenes and the products from the control experiments were completed and the H/C, N/C and S/C atomic ratios were calculated as shown in Table 4-6. Despite the changes in the physical properties, there were no significant differences in the chemical composition compared to the raw asphaltenes. H/C ratio remained the same at 1.17, N/C stayed within the range 0.011 – 0.012 and S/C at the range 0.032 – 0.035, without any notable trends for both products from autoxidation and control experiments. Furthermore, the residual content, which can reflect oxygen content, did not show any significant increases with autoxidation.

Table 4-6: Elemental Analysis for the Oxidized Asphaltenes and Products from the Control Experiments at 190°C, 220°C, and 250°C for 8 hours [a]

	N (wt.%)		C (wt.%)		H (wt.%)		S (wt.%)		Residual [b] (wt.%)		H/C[c]	N/C[c]	S/C[c]
	x	u	x	u	x	u	x	u	x	u			
Raw Asphaltenes	1.07	0.03	82.10	0.17	8.07	0.04	7.61	0.11	1.15	0.26	1.17	0.011	0.035
Oxidized 190°C	1.10	0.01	81.93	0.34	8.09	0.02	7.41	0.42	1.47	0.65	1.17	0.012	0.034
Oxidized 220°C	1.05	0.09	82.05	0.21	8.07	0.01	7.22	0.30	1.62	0.05	1.17	0.011	0.033
Oxidized 250°C	1.11	0.01	82.46	0.34	8.10	0.12	7.05	1.00	1.28	1.22	1.17	0.012	0.032
Control 190°C	1.08	0.01	81.77	0.64	8.03	0.02	7.54	0.21	1.58	0.64	1.17	0.011	0.035
Control 220°C	1.10	0.01	82.26	0.25	8.07	0.04	7.03	0.22	1.53	0.46	1.17	0.011	0.032
Control 250°C	1.12	0.01	82.24	0.57	8.11	0.03	7.45	0.31	1.08	0.86	1.17	0.012	0.034

[a] (x) average and (u) standard deviation due to repeatability of 3 measurements

[b] Calculated by difference

[c] Molar ratio

Oxidized asphaltenes can contain oxygenated functional groups if there were incorporation of oxygen during autoxidation. Table 4-6 did not show any significant increases in the residual content, which can correspond to oxygen. However, other literature that studied autoxidation of oilsands material found significant changes in the FTIR spectra between the feed and oxidized products, even when there were minor differences noted in the elemental compositions or other

properties[4,10]. Hence, FTIR spectra were obtained for the oxidized asphaltenes as illustrated in Figure 4-2.

Interestingly, oxidized asphaltenes and its feed material did not show significant differences in the FTIR spectra. Table 4-7 shows the infrared absorption frequencies of different oxygenate functional groups that can appear in the infrared spectra of oxidized asphaltenes. However, an increase in these peaks were not apparent for the spectra of oxidized asphaltenes, suggesting that oxygen incorporation at these autoxidation conditions is very unlikely; the observed decrease in the penetration values is not due to formation of oxygenated products such as carbonyl formation.

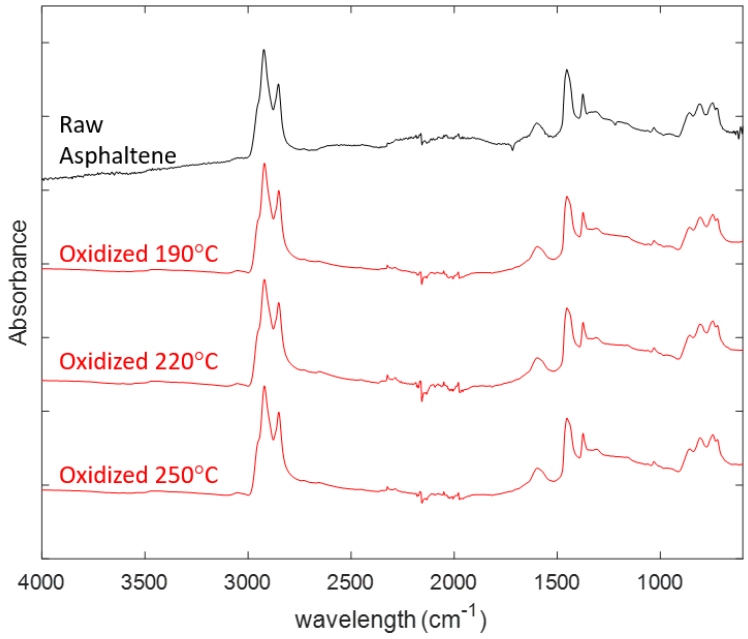

Figure 4-2: FTIR Spectra of Oxidized Asphaltenes at 190°C, 220°C, and 250°C for 8 hours

Table 4-7: Infrared Absorption Frequencies of Different Oxygenate Functional Groups[11]

Compounds	Functional Groups	Frequency ranges (cm^{-1})
Peroxides	C-O-O-H	815-840
	O-O	840-880
	O-H	1000-1040
	O-H	3400-3450
	C-O	1300-1360
Ketones / Esters/ Acids	C=O	1700-1750
Esters	C-O	1200
Alcohol	C-O	1020-1160
	O-H	3620

As previously mentioned, other than carbonyl formation, another reaction that can cause a decrease in the penetration depth is oxidative addition reaction. With limited oxygen availability, oxidative addition reactions without oxygen incorporation can take place to form bulky and bigger molecules. To check this, refractive index measurements were obtained for the oxidized asphaltenes as shown in Table 4-8. Furthermore, the products from the control experiments were also measured and is shown in Table 4-9.

With the increase in the reaction temperature, increase in the refractive index values were observed for all products from both autoxidation and control experiments. The trends are similar for both oxidized and control products for the reaction temperatures 190°C and 220°C. However, the oxidized asphaltenes at 250°C showed insolubility in toluene, which was not observed in the product from the control experiment at 250°C. This suggests that heating itself has a workup on its own and is playing a major role in facilitating free radical addition reactions, but effects of autoxidation are also evident, as shown by presence of toluene insoluble materials in oxidized asphaltenes at 250°C.

On a side note, oxidized asphaltenes at 190°C for 8 hours with an air flow rate of 450 mL/min had no significant increase in the standard deviation in the refractive index values compared to raw asphaltenes. Comparing this to the results from the preliminary experiments as was shown in

Table 4-2, the observed high standard deviations in the preliminary oxidized products at 190°C are likely due to low air flow rates utilized for those experiments. Due to the viscous nature of the asphaltenes at 190°C, it is possible that air flow rate < 300mL/min was too low and had severe mass transport limitations, resulting in high variance within the oxidized sample. However, to make a strong conclusion regarding this statement, more experiments at different conditions or more analysis is required. No additional work at 8 hours reaction time was performed.

Table 4-8: Refractive Index Results for the Oxidized Asphaltenes at 190°C, 220°C, and 250°C for 8 hours [a]

Measurement Temperatures (°C)	**Refractive Index Measurements (nD)**			
	Raw Asphaltenes	Oxidized 190°C	Oxidized 220°C	Oxidized 250°C[b]
20	1.5286 ±0.0006	1.5282 ±0.0002	1.5294 ±0.0005	
30	1.5228 ±0.0004	1.5223 ±0.0002	1.5236 ±0.0006	-
40	1.5176 ±0.0008	1.5167 ±0.0001	1.5187 ±0.0004	

[a] Analysis performed in triplicate, values reported as average ± one sample standard deviation

[b] Sample contains toluene insoluble materials and could not form a homogeneous mixture for refractive index measurements

Table 4-9: Refractive Index Results for the Products from the Control Experiments at 190°C, 220°C, and 250°C for 8 hours [a]

Measurement Temperatures (°C)	**Refractive Index Measurements (nD)**			
	Raw Asphaltenes	Control 190°C	Control 220°C	Control 250°C
20	1.5286 ±0.0006	1.5281 ±0.0001	1.5301 ±0.0005	1.5304 ±0.0004
30	1.5228 ±0.0004	1.5225 ±0.0002	1.5246 ±0.0006	1.5245 ±0.0007
40	1.5176 ±0.0008	1.5172 ±0.0002	1.5197 ±0.0004	1.5193 ±0.0010

[a] Analysis performed in triplicate, values reported as average ± one sample standard deviation

As changes in the penetration depth and the refractive index measurements were observed in the oxidized samples, ^{1}H NMR were also measured to see if there were any changes with the hydrogen distribution. There was a decrease of aliphatic H content noted for both oxidized and control samples at 220°C and 250°C. However, 190°C did not show a significant change in the nature of hydrogens present from the raw asphaltenes, which is similar to the trends noted for the refractive index measurements. This can suggest that at 220°C and 250°C, addition reactions occur for both oxidized and control experiments and addition sites are most likely at the aliphatic groups, as marked by H abstraction from aliphatic groups.

Table 4-10: ^{1}H NMR Results for the Air-blown and the Control Products from Autoxidation of Industrial Raw Asphaltenes [a]

Sample	Aliphatic H (%)
Raw Asphaltenes	88.6 ± 1.8
Oxidized 190°C	87.2 ± 1.7
Oxidized 220°C	83.2 ± 0.2
Oxidized 250°C	85.3 ± 2.4
Control 190°C	88.6 ± 0.8
Control 220°C	84.2 ± 0.8
Control 250°C	84.5 ± 2.0

[a] Analysis performed in triplicate, values reported as average ± one sample standard deviation

(4.3.3) Prolonged Autoxidation for 24 Hours

Autoxidation for 24 hours was studied to see how much asphaltenes hardening can be achieved with 190°C, 220°C, and 250°C autoxidation reaction temperatures at prolonged reaction time. The penetrometer depths for these oxidized samples were obtained and are shown in Table 4-11. There was a notable decrease in the penetration depth observed for all three oxidized samples and they decreased from 15.3 mm to as low as 1.2 mm.

Interestingly, autoxidation at 190°C even for a prolonged oxidation time had the lowest decrease in penetration depth. On the other hand, autoxidation at 220°C and 250°C had more decrease in the penetration depth. This trend was previously observed for the autoxidation at 8 hours in the

penetration depth, refractive index and ^{1}H NMR results as shown in Table 4-5, 4-6 and 4-7. This suggests that there may be a significant change in the rate of autoxidation between 190°C and 220°C. This can be due to a mass transport limitation at 190°C, as raw asphaltenes was observed to be very viscous at 190°C to the point that it does not allow stirring, or due to the reaction rate dependence on the temperature as governed by Arrhenius law. Since oxidized samples at 220°C and 250°C consistently showed comparable results in the various analysis, this observed change can be due to the viscous nature of raw asphaltenes at 190°C.

Table 4-11: Penetrometer Results for the Oxidized Asphaltenes at 190°C, 220°C, and 250°C for 24 hours [a]

Sample	**Penetration (mm)[a]**
Raw Asphaltenes	15.3 ± 0.4
Oxidized 190°C	5.6 ± 1.4
Oxidized 220°C	1.2 ± 0.9
Oxidized 250°C	2.1 ± 1.7

[a] Analysis performed in triplicate, values reported as average ± one sample standard deviation

[b] Applied load of 100 g for 0.10 s using a Humboldt H-1280 needle at 185 – 190°C

Chemical composition changes in the oxidized asphaltenes were examined through elemental analysis and infrared spectra, as illustrated in Table 4-12 and Figure 4-3, respectively. Due to these oxidized samples containing toluene and chloroform insoluble materials, ^{1}H NMR and refractive index measurements could not be obtained.

Even with prolonged autoxidation for 24 hours, it did not result in a significant change in the bulk composition as seen in Table 4-12. Only minor changes were observed, as the H/C for all oxidized products decreased from 1.17 to 1.16 and S/C decreased from 0.035 to 0.034. In addition, decreasing trend in the carbon and sulfur content was noted as it decreased from 82.10 wt.% to as low as 81.45 wt.% and 7.61 wt.% to 7.38 wt.%, respectively with the increasing autoxidation temperatures. Alternatively, residual content showed a slight increasing trend with

the increasing autoxidation temperature as it increased from 1.15 wt.% to 2.16 wt.% with the increasing autoxidation temperatures.

On the other hand, infrared spectra did not show any significant changes with autoxidation. There was no appearance of peaks associated with oxygenated groups, as was presented in Table 4-7, evident in the oxidized products. This suggests that even prolonged autoxidation facilitated oxidative cross-linking reactions without oxygen incorporation.

Table 4-12: Elemental Analysis for the Oxidized Asphaltenes at 190°C, 220°C, and 250°C for 24 hours [a]

	N (wt.%)		**C (wt.%)**		**H (wt.%)**		**S (wt.%)**		**Residual[b] (wt.%)**		**H/C[c]**	**N/C[c]**	**S/C[c]**
	x	**u**	**x**	**u**	**x**	**u**	**x**	**u**	**x**	**u**			
Raw Asphaltenes	1.07	0.03	82.10	0.17	8.07	0.04	7.61	0.11	1.15	0.26	1.17	0.011	0.035
Oxidized 190°C	1.09	0.00	81.83	0.15	7.97	0.04	7.52	0.04	1.59	0.06	1.16	0.011	0.034
Oxidized 220°C	1.09	0.01	81.77	0.07	8.01	0.03	7.49	0.05	1.63	0.08	1.16	0.011	0.034
Oxidized 250°C	1.08	0.01	81.45	0.31	7.93	0.01	7.38	0.11	2.16	0.20	1.16	0.011	0.034

[a] (x) average and (u) standard deviation due to repeatability of 3 measurements

[b] Residual content calculated by difference

[c] Molar ratio

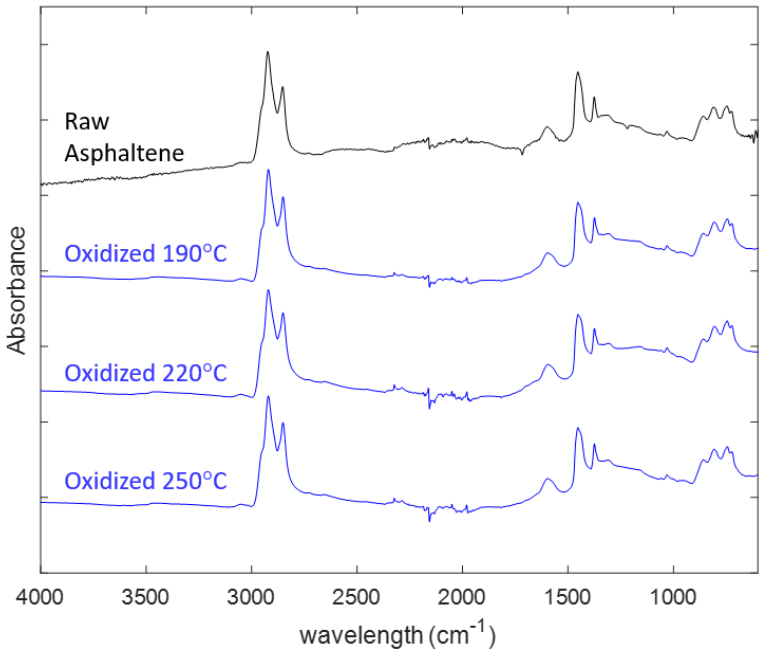

Figure 4-3: FTIR Spectra of Oxidized Asphaltenes at 190°C, 220°C, and 250°C for 24 hours

(4.3.4) Effect of Autoxidation on Melt Spinning Process

The behavior of the oxidized samples during melt spinning were observed and is recorded in Table 4-13. To allow a better comparison, oxidized products obtained from the same reaction temperature of 190°C for 8- and 24-hour autoxidation were selected for melt spinning.

As shown in Table 4-13, autoxidation for 8 hours did not have a significant effect on the melt spinning behavior. The melt spinning temperature stayed relatively similar to the industrial asphaltenes and the maximum melt spinning productivity did not surpass that of the industrial asphaltenes. On the other hand, prolonged oxidation for 24 hours used as a pretreatment method increased the melt spin temperature, as it showed an increase from 195°C to 205°C and corroborated with the penetrometer depth results. The melt spinning performance improved and the productivity increased from 200 rpm (125 m/min) to 600 rpm (378 m/min) by oxidation pretreatment for the duration of 24 hours.

Table 4-13: Maximum Melt Spinning Productivity for Oxidized Asphaltenes Feed Materials

Asphaltenes feed material	Melt Spin Temperature (°C)	Maximum Melt Spinning Productivity
Industrial asphaltenes	195	200 rpm (126 m/min)
Oxidized 190°C, 8 hours	196	200 rpm (126 m/min)
Oxidized 190°C, 24 hours	205	600 rpm (378 m/min)

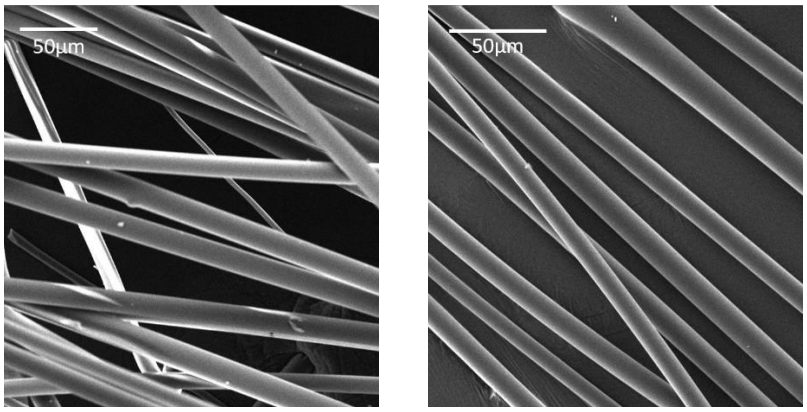

Figure 4-4: As-Spun Fibers from the Oxidized 190°C, 8 hours (left) and Oxidized 190°C, 24 hours (right)

(4.4) Discussion

(4.4.1) Predicted Improvement in Carbon Fiber Quality by Autoxidation of Industrial Asphaltenes

Autoxidation for 8 hours produced oxidized asphaltenes without considerable changes. Hence, the predicted improvement in carbon fiber quality for oxidized asphaltenes for 24 hours will be discussed in this section.

Aside from more consistent fibers with better productivity being produced, autoxidation of asphaltenes is also expected to decrease the stabilization time. The oxidized asphaltenes at 190°C and 24 hours had an increase in the melt spin temperature, as it increased from 195°C to 205°C. Oxidized asphaltenes at 220°C and 250°C is expected to have higher spinning temperature, since it had more significant decrease in the penetration depth. As previously mentioned in Section 2.3.2, increasing the softening point temperature of the precursor can shorten the time and cost intensive stabilization step.

On the other hand, there are some considerations for using autoxidation as a pretreatment method in a commercialized process. Since air is used for oxidation, there is no raw material cost. However, there will be some cost associated with providing enough air pressure during the autoxidation process. To allow a good contact of air with asphaltenes for the autoxidation process, a setup similar to a bubble column, as illustrated in Figure 4-5, is recommended to bubble air into the bulk feed material at elevated temperatures. Then, to allow bubbling of air into the matrix of viscous asphaltenes, sufficient air pressure to exceed the hydrostatic pressure of the liquid in the bubble column reactor will be required.

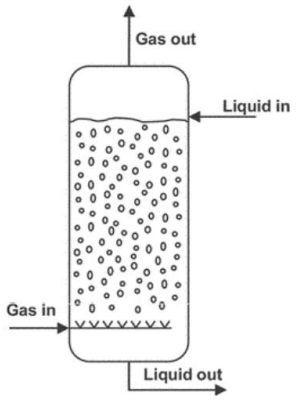

Figure 4-5: Schematic of a Bubble Column[12]

To more properly assess the viability of utilizing autoxidation as a commercialized pretreatment process, more detailed analysis must be completed to quantify the benefits obtained from the autoxidation pretreatment. From the chemical composition analysis, autoxidation seemed to have facilitated oxidative addition reactions without detectable oxygen incorporation; this pretreatment did not unnecessarily increase the heteroatom content in the precursor.

As previously discussed, high heteroatom can lead to defects in the final carbon fibers due to high volatile evolution during carbonization stage. In addition, Kim *et al.*[13] reported pre-treating pitch precursor to form cross-linked long linear compounds were beneficial in producing more homogeneous and better mechanical performance carbon fibers. Thus, autoxidation at these conditions was estimated to be beneficial in terms of final carbon fiber performance. However,

as shown in Appendix B, mechanical properties of the carbon fibers from products from autoxidation did not show improvement compared to the carbon fibers from industrial asphaltenes.

Hence, to evaluate the benefits from using autoxidation as pretreatment method, shortening of the stabilization time needs to be quantified. With this further analysis, a stronger conclusion about using autoxidation as a pretreatment method can be made.

(4.5) Conclusions

Using autoxidation at < 250°C as a pretreatment method for carbon fiber production was evaluated. From this study, the following conclusions were obtained:

a) Effects of autoxidation were more pronounced at autoxidation temperatures at 220°C and 250°C compared to autoxidation at 190°C. This may be oxidation kinetics and/or due to the high viscosity of the feed material at 190°C, leading to mass transport limitations during autoxidation
b) Autoxidation of asphaltenes at a low air flow rate (9 mL/g·min) facilitated oxidative addition reactions without significant oxygen incorporation. No significant increase in the oxygenated groups were evident with autoxidation, as confirmed by elemental analysis and infrared spectra of the oxidized products
c) Thermal treatment of industrial asphaltenes at 220°C and 250°C induced free radical addition reactions to produce more viscous products
d) Autoxidation of industrial asphaltenes had a positive effect on the melt spinning process and produced fibers with more consistent diameters with high melt spin productivity. However, autoxidation of 8 hours was insufficient to induce significant changes to the bulk asphaltenes. Autoxidation at 190 – 250°C for 24 hours produced oxidized products with an increase in the softening point temperature, and improved melt spinning behaviour

(4.6) References

(1) Mallick, R. B.; El-Korchi, T. *Pavement Engineering: Principles and Practice*; 3rd Edition; CRC Press: Boca Raton, Florida, 2013; pp 228.

(2) Babu, D. R.; Cormack, D. E. Effect of Oxidation on the Viscosity of Athabasca Bitumen. *Can. J. Chem. Eng.* **1983**. *61*, 575-580.

(3) Javadli, R.; de Klerk, A. Desulfurization of Heavy Oil - Oxidative Desulfurization (ODS) as Potential Upgrading Pathway for Oil Sands Derived Bitumen. *Energy Fuels* **2012**, *26*, 594–602.

(4) Sanchez, N.; de Klerk, A. Low-Temperature Oxidative Asphaltenes Liquefaction for Petrochemicals: Fact or Fiction? *Appl. Petrochemical Res*. **2016**, *6*, 97–106.

(5) Ulrich, G.; Vasudevan, P. *Chemical Engineering: Process Design and Economics A Practical Guide*, 2nd ed.; Process Publishing, 2004; pp 576.

(6) García Zapata, J. L.; De Klerk, A. Viscosity Changes during Mild Oxidation of Oilsands-Derived Bitumen: Solvent Effects and Selectivity. *Energy Fuels* **2014**. *28*, 6242-6248.

(7) Strausz, O.; Lown, E. M., *The chemistry of Alberta oil sands, bitumens and heavy oil.* Alberta Energy Research Inst., Calgary, AB (Canada): Canada, 2003.

(8) Riazi, M. 2.1.4 Refractive Index. In *Characterization and Properties of Petroleum Fractions*; Riazi, M., Ed.; ASTM International: West Conshohocken, Pennsylvania, 2005; pp 32.

(9) Yañez Jaramillo, L. M. Visbreaking of Oilsands Bitumen Between 150 and 300C. M.S. Thesis, University of Alberta, 2016.

(10) Siddiquee, M. N.; De Klerk, A. Hydrocarbon Addition Reactions during Low-Temperature Autoxidation of Oilsands Bitumen. *Energy Fuels* **2014**. 28 (11), 6848-6859.

(11) Emanuel, Nikolai; Denisov, Evgenii; Maizus, Z. *Liquid-Phase Oxidation of Hydrocarbons*; Plenum Press: New York, 1967; pp.37-39.

(12) de Haan, A. 8.5.4 Bubble Columns. In *Process Technology - An Introduction*; De Gruyter: Berlin/Boston, 2015; pp.174.

(13) Kim, B. J.; Eom, Y.; Kato, O.; Miyawaki, J.; Kim, B. C.; Mochida, I.; Yoon, S. H. Preparation of Carbon Fibers with Excellent Mechanical Properties from Isotropic Pitches. *Carbon* **2014**. *77*, 745-755.

CHAPTER 5:
PRETREATMENT III: HALOGENATION-DEHALOGENATION OF INDUSTRIAL RAW ASPHALTENES

(5.1) Introduction

Similar to autoxidation, halogenation and dehalogenation is capable of causing free radical addition reactions and the removal of hydrogen to decrease the hydrogen-to-carbon ratio. As previously outlined in Section 2.7, the main chemistry of bromination-debromination aims to form olefins, which has been reported to react readily with free radicals to undergo free radical addition reactions. Since oilsands-derived asphaltenes have high free radical content, halogenation-dehalogenation of industrial asphaltenes is expected to result in considerable free radical addition reactions with a lower propensity of carbon elimination than autoxidation. Hence, using halogenation-dehalogenation is expected to achieve similar product to autoxidation without significant decrease in the carbon content.

Halogenation-dehalogenation have been reported in carbon fiber literatures, specifically on using dehalogenation reaction to produce pitch precursor suitable for carbon fiber production. For example, pyrolysis of polyvinylchloride (PVC) at 400°C and 30 minutes in nitrogen was reported to produce pitch made up of carbon and hydrogen, with the formula $C_{62}H_{52}$[1]. In a similar way, a study[2] investigated using PVC as an easily-handled chlorine source for chlorination-dehydrochlorination of ethylene bottom oil to produce higher softening point and molecular weight pitch precursor. In addition, using bromination and dehydrobromination on naphtha-cracked oil as a pretreatment method was reported to produce linear cross-linked molecules with a higher viscosity[3].

In this study, halogenation-dehalogenation of industrial asphaltenes was studied as a pretreatment method by using liquid bromine. Bromine was chosen due to the ease of analysis; raw industrial asphaltenes contain trace amounts of other halogens such as chlorine an iodine but no bromine. Bromination of raw industrial asphaltenes with and without solvent and debromination in both open and closed systems were investigated.

(5.2) Experimental

(5.2.1) Materials

The asphaltenes feed material employed in this work was obtained from CNOOC Ltd. (previously Nexen Energy) from the pentane solvent deasphalting process at the Long Lake Upgrader in Alberta, Canada. The asphaltenes used in these experiments were obtained from the same barrel as the material utilized in Chapter 3 and the characterization of the asphaltenes is shown in Table 3-1. Other chemicals and gases used for the experiments are presented in Table 5-1.

Table 5-1: Chemicals and Gases Used for the Bromination and Debromination Study

Compound	Formula	CASRN [a]	Mass fraction purity [b]	Supplier
Chemicals				
Toluene	C7H8	108-88-3	0.995	Fisher Chemical
Bromine	Br2	7728-95-8	0.995	Alfa Aesar
Heavy Mineral Oil	-	8042-47-5	0.99	Fisher Chemical
Silicone Oil	C16H22O2Si2	68083-14-7	-	Beantown Chemical
Cylinder gases				
Nitrogen	N2	7727-37-9	0.99999 c	Praxair

[a] CASRN = Chemical Abstracts Services Registry Number

[b] This is the purity of the material guaranteed by the supplier; material was not further purified.

[c] Mole fraction purity.

(5.2.2) Equipment and Procedure

(5.2.2.1) Bromination and Debromination Procedure with Solvent

(5.2.2.1.1) Bromination Procedure

Bromination reactions were performed in a Swagelok 316 stainless steel micro-batch reactor (2.1 cm internal diameter, and 14.0 cm long). In a typical experiment, approximately 4 g of industrial asphaltenes and 20 mL of toluene was loaded directly in the micro-batch reactor. Toluene was added so the asphaltenes is dissolved and will remain in a liquid state during the reaction. Then, with a 10µL micropipette, 13 µL of bromine, which is about 1 wt.% relative to the mass of asphaltenes, was added to the asphaltenes and toluene mixture. The reactor was leak tested before

being pressurized with nitrogen to an initial pressure of 2 MPa gauge. The weight of the reactor before and after pressurization was recorded.

The pressurized reactor was then submerged in a preheated oil bath placed on the heating plate. The reaction time was started the moment the reactor was submerged in the oil bath and in a typical experiment, reaction time was set to 24 hours. The heavy mineral oil bath was placed on the Fisherbrand™ Isotemp™ Hot Plate and the temperature of the oil bath was set to 100°C and was regulated through the temperature sensor attached to the Hot Plate, which was submerged into the oil bath during the reaction. A schematic of the experimental setup is illustrated in Figure 5-1.

After the reaction, the reactor was removed from the oil bath and left to be cooled down. The final pressure of the reactor after cooling was typically at 2 MPa gauge. The reactor was depressurized by releasing the gases in the fume hood and it was weighed before and after depressurization.

Following the depressurization, solids from the reaction products were removed through vacuum filtration. 0.22 μm Micropore filter paper was used to remove the solids. The solids were left in the fume hood for 48 hours to evaporate the solvents. The dried products were weighed and the previously weighed membrane filter and the aluminum cup were subtracted to obtain the weight of the solids. Mettler Model XP1203S analytical balance with the readability of 1 mg and the capacity of 1210 g was used for weighing the materials.

The solid-free liquid products were subjected to the rotary evaporation process to remove toluene. Heidolph Hei-VAP rotary evaporator was used at 50°C and 77 kPa to facilitate toluene evaporation. The remaining solid products were collected and washed with distilled water, then left in the fume hood for 48 hours to evaporate the water from the solids. The dried solids were transferred into a vial and presence of bromine in these samples were confirmed by Energy Dispersive X-Ray (EDX) Analysis.

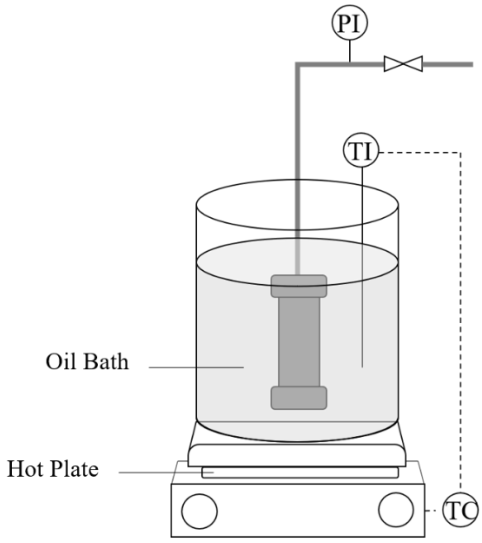

Figure 5-1: Experimental Setup for the Bromination Reaction

(5.2.2.1.2) Debromination Procedure

Debromination was completed by heating the brominated asphaltenes products on an aluminum cup and watch glass, which was placed on a Fisherbrand™ Isotemp™ Hot Plate. In a typical debromination experiment, the temperature of the aluminum cup or watch glass was set to 200°C and was regulated through the temperature sensor attached to the Hot Plate as shown in Figure 5-2. On the pre-heated aluminum cup or watch glass, about 1 g of brominated asphaltenes was loaded. The heating took place inside the fumehood in an open atmosphere for upto 6 hours. Subsamples were taken at debromination reaction time of 3 and 4 hours for further analysis.

To test the effect of heating on a watch glass itself, control experiments were also conducted using raw industrial asphaltenes. The experimental setup for the control experiments were the same as debromination experiments and two control experiments – one in an open system and one with flowing nitrogen – were completed. The heating took place for upto 4 hours with the subsample taken at the reaction time of 3 hours for further analysis.

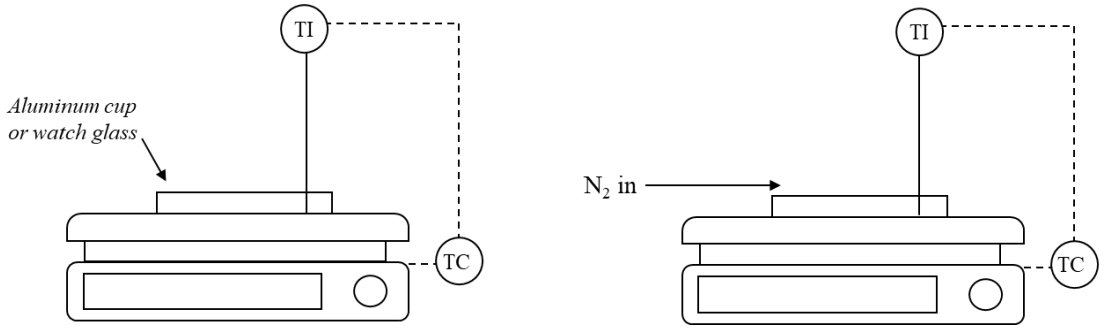

Figure 5-2: Experimental Setup for the Debromination (left) and Control Experiments (left and right)

(5.2.2.2) Bromination and Debromination Procedure without Solvent

(5.2.2.2.1) Bromination Procedure

Bromination reactions without solvent were performed in a Swagelok 316 stainless steel micro-batch reactor (2.1 cm internal diameter, and 14.0 cm long) with a glass insert. 8 g of asphaltenes was pre-weighed and was divided into four-quarters. For each quarter of asphaltenes loaded, it was layered with 10 µL bromine, and this was repeated until 8 g of asphaltenes and 30 µL of bromine, which is about 1.2 wt.% relative to asphaltenes, was loaded into the glass insert. The glass insert was then put into the reactor and then was leak tested before being pressurized with nitrogen to an initial pressure of 3 MPa gauge. The weight of the reactor before and after pressurization was recorded.

The pressurized reactor was then submerged in a preheated oil bath placed on the heating plate. Higher temperature of 150 – 170°C was used to facilitate the reaction at the temperatures when the asphaltenes is softened. The reaction time was started the moment the reactor was submerged in the oil bath and in a typical experiment, reaction time was set to 24 hours. The silicone oil bath was placed on the Fisherbrand^{TM} Isotemp^{TM} Hot Plate and the temperature of the oil bath was regulated through the temperature sensor attached to the Hot Plate, which was submerged into the oil bath during the reaction. A schematic of the experimental setup is illustrated in Figure 5-1, i.e. the same as employed for bromination with a solvent.

After the reaction, the reactor was removed from the oil bath and left to be cooled down. The final pressure of the reactor after cooling was typically at 3 MPa gauge. The reactor was

depressurized by releasing the gases in the fume hood and it was weighed before and after depressurization. The products from the reaction were collected into a vial to be stored in dark. Small subsample of the brominated products was washed with distilled water to remove the residual bromine, then left in the fume hood for 48 hours to evaporate the water from the solids. The water washed subsamples were checked by Energy Dispersive X-Ray (EDX) Analysis to confirm the presence of bromine in the products.

(5.2.2.2.2) Debromination Procedure

Debromination was completed in the same Swagelok 316 stainless steel micro-batch reactor as the bromination experiments (2.1 cm internal diameter, and 14.0 cm long) with a glass insert. About 6 g of brominated asphaltenes was pre-weighed and was loaded into the glass insert. The glass insert was then put into the reactor and then was leak tested before being pressurized with nitrogen to an initial pressure of 1 MPa gauge. The weight of the reactor before and after pressurization was recorded.

The pressurized reactor was then submerged in a 200°C preheated silicone oil bath placed on the heating plate. The reaction time was started the moment the reactor was submerged in the oil bath and in a typical experiment, reaction time was set to 4 hours. The silicone oil bath was placed on the Fisherbrand^{TM} Isotemp^{TM} Hot Plate and the temperature of the oil bath was regulated through the temperature sensor attached to the Hot Plate, which was submerged into the oil bath during the reaction as illustrated in Figure 5-1.

After the reaction, the reactor was removed from the oil bath and left to be cooled down. The final pressure of the reactor after cooling was typically at 1 MPa gauge. The reactor was depressurized by releasing the gases in the fume hood and it was weighed before and after depressurization. The products from the reaction were collected into a vial for further analysis.

(5.2.2.3) Melt Spinning Procedure

Melt spinning to produce as-spun fibers from the debrominated asphaltenes was completed by using the same procedure and equipment as described in Section 3.2.2.2.

(5.2.3) Analyses

(a) Energy Dispersive X-Ray (EDX) Analysis

Presence of bromine in the samples were confirmed by field emission scanning electron microscopy (ZEISS Sigma 300 VP-FESEM), using energy dispersive X-ray (EDX) analysis. An accelerating voltage of 30 kV was used.

(b) Gas Chromatography with Mass Spectrometry (GC-MS)

Identifying bromination reaction products was completed by using Gas Chromatography with Mass Spectrometry. The instrument used was an Agilent 7820 with 5977E mass spectrometer. Separation was performed on an HP-5 column (30 m×0.25mm×0.25 μm), using helium as a carrier gas.

(c) Gas Chromatography with Flame Ionization Detector (GC-FID)

Quantification of brominated toluene was completed by using Gas Chromatography with Flame Ionization Detector (GC-FID). An Agilent GC-FID (Agilent 7890A GC system) equipped with DB-5MS column (30 m × 0.25 mm × 0.25 μm) was employed for this purpose. The samples were prepared using pentane as solvent.

In addition, elemental analysis (CHNS) and the penetrometer tests for the debrominated asphaltenes was performed using the same procedure as described in Chapter 3.

(5.3) Results

(5.3.1) Bromination and Debromination with Solvent

(5.3.1.1) Bromination with Solvent

Bromination of raw industrial asphaltenes was completed with toluene employed as the solvent to perform bromination when asphaltenes is in a dissolved liquid state. One run of reference experiment was completed in the same setup as the outlined bromination experiment but without bromine. Gas and solids produced from the bromination and the reference reaction were calculated and are shown in Table 5-2.

As shown in Table 5-2, there were no significant changes noted to the gas and solid produced during the bromination reaction compared to the reference experiment. On the other hand, the products from the bromination experiments showed presence of bromine from the energy dispersive X-ray (EDX) analysis, whereas the product from the reference experiment showed no bromine content. Consequently, these products were assumed to be brominated and were advanced to debromination, which was facilitated in an open system at 200°C on an aluminum cup and watch glass.

Table 5-2: Gas and Solids Produced from Bromination of Industrial Asphaltenes with Solvent at 100°C and the EDX Results on the Brominated Products

	Number of Runs					
	1	**2**	**3**	**4**	**5**	**Ref.**
Asphaltenes Feed (g)	4.00	4.02	4.05	4.00	4.02	4.05
Gas Produced (g)	0.0	0.0	0.0	0.0	0.0	-0.2
Solids Produced (g)	0.012	0.031	0.010	0.024	0.017	0.012
Presence of Br [a]	Yes	Yes	Yes	-[b]	-[b]	No

[a] Checked by EDX analysis

[b] EDX analysis not completed on these samples

(5.3.1.2) Two Debromination Methods

Elemental analysis for the debrominated asphaltenes for the two debromination methods were completed and the H/C, N/C and S/C atomic ratios were calculated as shown in Table 5-3. During debromination, subsamples were obtained at debromination time of 3 and 4 hours to see the changes in the composition with debromination time upto 6 hours.

As seen in the table, both debromination methods had a significant effect on the product composition, and the H/C ratio decreased from 1.17 to as low as 1.12 – 1.14 and 0.94 – 0.97 for debromination with aluminum cup and watch glass, respectively. On the other hand, N/C and S/C ratio remained relatively the same as the raw asphaltenes throughout the debromination reactions. Furthermore, increase in the residual content (elements other than CHNS) was noted

for both debromination methods, as the residual content around 1 wt.% increased upto 2.96 wt.% and 5.92 wt.% for debromination with aluminum cup and watch glass, respectively.

Table 5-3: Elemental Analysis of Debrominated Products from Bromination of Industrial Raw Asphaltenes at 100°C with Solvent[a]

Sample		Run #	N (wt.%)	C (wt.%)	H (wt.%)	S (wt.%)	Resd.[a] (wt.%)	H/C[b]	N/C[b]	S/C[b]
Raw Asphaltenes		1	1.11	82.14	8.07	7.51	1.17	1.17	0.012	0.034
		2	1.05	82.25	8.10	7.72	0.88	1.17	0.011	0.035
		3	1.05	81.92	8.03	7.61	1.39	1.16	0.011	0.035
Aluminum Cup	3 h	1	1.05	81.22	7.87	7.38	2.47	1.15	0.011	0.034
		2	1.08	81.82	8.03	7.61	1.47	1.17	0.011	0.035
	4 h	1	1.06	81.38	7.86	7.32	2.38	1.15	0.011	0.034
		2	1.06	81.28	7.85	7.38	2.43	1.15	0.011	0.034
	6 h	1	1.06	80.84	7.64	7.50	2.96	1.12	0.011	0.035
		2	1.10	81.02	7.78	7.62	2.48	1.14	0.012	0.035
Watch Glass	3 h	1	1.09	80.49	7.17	7.13	4.12	1.06	0.012	0.033
		2	1.08	80.79	7.34	7.13	3.65	1.08	0.012	0.033
	4 h	1	1.15	82.02	6.95	6.55	3.33	1.01	0.012	0.030
		2	1.11	76.24	5.52	8.53	8.60	0.86	0.013	0.042
	6 h	1	1.09	79.77	6.54	6.68	5.92	0.97	0.012	0.031
		2	1.14	80.56	6.36	6.85	5.09	0.94	0.012	0.032

[a] Residual content calculated by difference, i.e. non-CHNS content

[b] Molar ratio

As H/C and residual content had the most changes with the progress of debromination reactions, they were plotted as shown in Figure 5-3 as a function of debromination time to see their changes throughout debromination. Reaction time 0 h represents H/C and residual content for raw industrial asphaltenes. As illustrated, with an increase in debromination time, H/C ratio decreased, and residual content increased for debromination using both aluminum cup and watch

glass. The decrease in H/C and increase in residual content is more pronounced for debromination using watch glass.

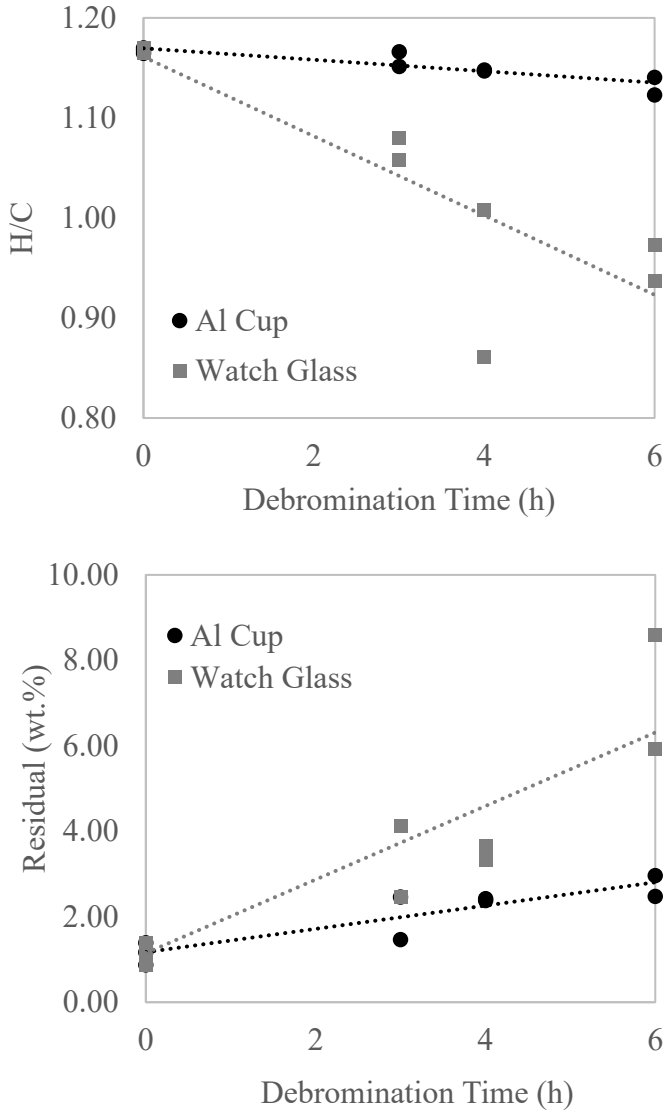

Figure 5-3: Change in H/C and Residual Content with Debromination of Industrial Raw Asphaltenes with Aluminum Cup and Watch Glass. Lines indicate general trends only and do not imply a specific correlation.

(5.3.1.3) Debromination Control Experiments

With the progression of debromination, there were notable changes in the H/C and residual content. On the other hand, since debromination reactions were facilitated in an open system,

there is a possibility of autoxidation, which also has a capacity to decrease H/C and increase residual content. Furthermore, due to the high free radical content in oilsands-derived asphaltenes, there is also possibility of free radical addition reactions occurring from heating alone.

Hence, control experiments with industrial raw asphaltenes on watch glass were conducted in an open system and under nitrogen environment to verify if the observed compositional changes are from debromination. Elemental analysis on the products from the control experiments were performed and are shown in Table 5-4.

Interestingly, both control experiments showed a decrease in H/C with the increase in the reaction time. As well, there was a slight increase in N/C for debromination with watch glass as it increased from 0.011 up to 0.013, and products from the control experiment in an open atmosphere increased up to 0.015. On the other hand, control experiment with nitrogen did not exhibit a significant increase in N/C.

Table 5-4: Elemental Analysis of Debrominated Products from Bromination of Industrial Raw Asphaltenes at 100°C with Solvent and Products from Control Experiments

Sample		Run #	N (wt.%)	C (wt.%)	H (wt.%)	S (wt.%)	Resd. (wt.%)	H/C[a]	N/C[a]	S/C[a]
Raw Asphaltenes[b]		1	1.11	82.14	8.07	7.51	1.17	1.17	0.012	0.034
		2	1.05	82.25	8.10	7.72	0.88	1.17	0.011	0.035
		3	1.05	81.92	8.03	7.61	1.39	1.16	0.011	0.035
Watch Glass	3h[b]	1	1.09	80.49	7.17	7.13	4.12	1.06	0.012	0.033
		2	1.08	80.79	7.34	7.13	3.65	1.08	0.012	0.033
	4h[b]	1	1.15	82.02	6.95	6.55	3.33	1.01	0.012	0.030
		2	1.11	76.24	5.52	8.53	8.60	0.86	0.013	0.042
Control, Open[c]	3h	1	1.06	81.94	7.89	6.43	2.68	1.14	0.011	0.029
		2	1.07	81.99	7.93	7.09	1.92	1.15	0.011	0.032
	4h	1	1.44	81.33	5.58	7.40	4.24	0.82	0.015	0.034
		2	1.32	80.76	5.53	7.12	5.27	0.81	0.014	0.033
Control, N_2[d]	3h	1	1.13	81.07	7.54	7.60	2.67	1.11	0.012	0.035
		2	-[e]							
	4h	1	1.14	81.39	7.66	7.42	2.39	1.12	0.012	0.034
		2	1.13	81.18	7.64	7.43	2.63	1.12	0.012	0.034

[a] Molar ratio

[b] Repeated from Table 5-1 for the ease of comparison

[c] Heated industrial asphaltenes on watch glass in air atmosphere

[d] Heated industrial asphaltenes on watch glass in nitrogen atmosphere

[e] Analysis completed once

With a significant decrease in H/C noted, H/C ratio as a function of reaction time was plotted as shown in Figure 5-4. As illustrated, the decrease in H/C for the debrominated samples fall in between the two control experiments. The decrease in H/C was more pronounced with control experiment in an open atmosphere, as it showed a decrease in H/C to 0.81 – 0.82, and control experiment under nitrogen showed a decrease as low as 1.12 in 4 hours of reaction time. The debrominated products at 4 hours of reaction time showed H/C ratio of 1.01 and 0.86. Furthermore, the products from debromination with watch glass and from control experiments in

open atmosphere showed more significant increase in the residual content. Hence, it seems that the effect of heating as well as oxidation were the driving factors of the observed decrease in H/C for the debrominated products.

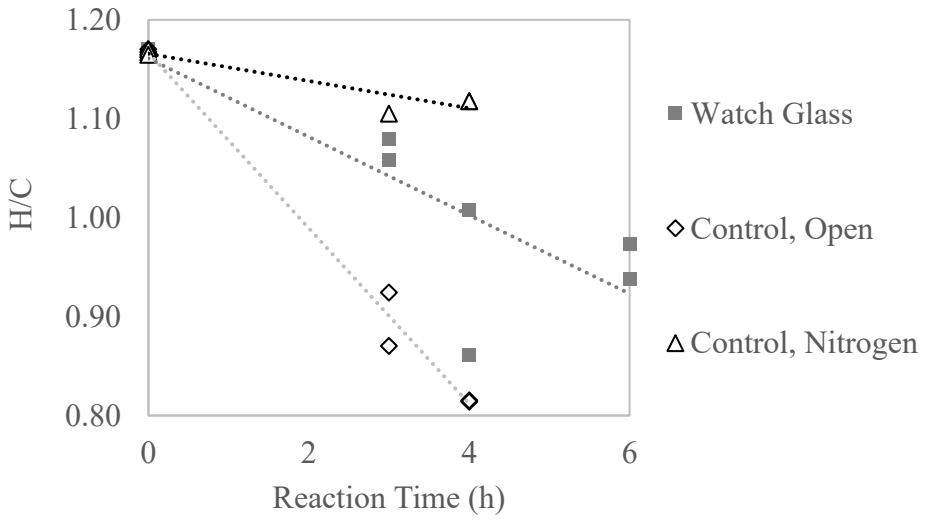

Figure 5-4: Changes in H/C with the Debromination Reaction Time for Debromination and Control Experiments for Industrial Raw Asphaltenes with Watch Glass. Lines indicate general trends only and do not imply a specific correlation.

(5.3.1.4) Does Toluene and Bromine React?

The results from the control experiments suggested that the observed decrease in H/C is not from debromination but an effect from autoxidation. One of the reasons why debromination effects were not observed can be that there was little bromination of asphaltenes in the first place. This is possible if toluene, which was assumed to be inert during the bromination reaction, reacted with bromine instead of asphaltenes. Some of the potential products from bromination of toluene include benzyl bromide (bromination of alkyl) and bromo-toluene (bromination of aromatic ring), and both products have higher boiling point than toluene. When facilitating toluene removal after bromination, these products could have been retained and hence, were picked up by EDX analysis.

To check if bromine and toluene reacts, these two reactants were heated in a micro-batch reactor at the studied bromination conditions (100°C, 2MPa for 24 hours) and the products were

characterized with gas chromatography mass spectrometry. The results indicated that bromine and toluene reacted to be converted into bromo-toluene at the studied bromination conditions. Hence, the reaction products were further analyzed by using a gas chromatograph with a flame ionization detector. Assuming that the response factor for brominated toluene is the same as chlorobenzene, conversion of toluene to bromo-toluene was calculated and shown in Table 5-5.

As illustrated, concentration of brominated toluene in the reaction products were 3.8 mol.%. Comparing this to the concentration of brominated toluene at 100% conversion of bromine, 12.2 mol.%, about 31% of bromine reacted with toluene to form brominated toluene. Since this value was obtained by using the response factor for chlorobenzene, not brominated toluene, the real conversion of toluene to brominated toluene is most likely to be higher. Nevertheless, the results clearly indicate toluene is not inert during the bromination reaction, and hence, possibly led to lack of asphaltenes bromination.

Table 5-5: Conversion of Toluene to Brominated Toluene at the Studied Bromination Conditions (100°C, 24 h, 2 MPa)

Run # [a]	Concentration of brominated toluene (mol.%) [b]	Concentration of brominated toluene at 100% Br_2 conversion (mol.%)	Conversion (%)
1	3.8	12.2	31
2	3.8		31

[a] Subsamples from the same reaction

[b] Calculated using the response factor for chlorobenzene as the response factor for brominated toluene was not available

(5.3.2) Bromination and Debromination Without Solvent

Since toluene and bromine react during the studied outlined bromination conditions to hamper interpretation, bromination without toluene was studied. The feed material, industrially precipitated asphaltenes, was previously observed to start softening around 150 – 160°C and become viscous liquid around 190°C. Hence, bromination was completed by using higher temperatures – 150°C, 160°C and 170°C – where the industrial raw asphaltenes soften, and using

higher pressure, 3 MPa, to avoid vaporization of bromine during the reaction. The products were checked by EDX to confirm presence of bromine, then were debrominated in a closed system. There were no significant mass changes noted for bromination and debromination reactions, and the cumulative mass change during both bromination and debromination were in < 0.5 wt.%.

(5.3.2.1) Bromination and Debromination Without Solvent

To see if there were any significant changes in the physical properties by bromination and debromination, penetration values were obtained the debrominated products as shown in Table 5-6. For all products, they showed a decrease in the penetration depth, as it decreased from 15.3 mm to penetration depths ranging in 7.8 – 8.9 mm. On the other hand, there were no notable trends noted with the increase in the bromination temperatures.

Table 5-6: Penetrometer Results for the Debrominated Products for Bromination at 150°C, 160°C, and 170°C [a]

Sample	Penetration (mm)[a]
Raw Asphaltenes	15.3 ± 0.4
Bromination 150°C	8.3 ± 2.4
Bromination 160°C	7.8 ± 1.2
Bromination 170°C	8.9 ± 1.4

[a] Analysis performed in triplicate, values reported as average ± one sample standard deviation

[b] Applied load of 100 g for 0.10 s using a Humboldt H-1280 needle at 185 – 190°C

(5.3.2.2) Chemical Composition Changes

As seen in Table 5-7, little change in the bulk composition was observed for the debrominated asphaltenes. There were no significant changes to H/C molar ratio and the N/C and S/C molar ratio of the debrominated products remained constant as the starting material and stayed at 0.011 and 0.033 – 0.034, respectively. On the other hand, there was an increase in the residual content noted for all debrominated products, as it increased from 1.15 wt.% to the range of 2.50 – 3.92 wt.%. Since only 1 wt.% bromine was used for bromination, it is unlikely that the observed increase in the residual mass is entirely from bromine. Overall, the elemental data did not

suggest significant composition changes with bromination and debromination of industrial asphaltenes.

Table 5-7: Elemental Analysis Results for the Debrominated Products for Bromination of Industrial Asphaltenes Without Solvent at 150°C, 160°C, and 170°C

Sample	Run #	N (wt.%)	C (wt.%)	H (wt.%)	S (wt.%)	Resd. (wt.%)	H/C[a]	N/C[a]	S/C[a]
Raw Asphaltenes [b]	1	1.11	82.14	8.07	7.51	1.17	1.17	0.012	0.034
	2	1.05	82.25	8.10	7.72	0.88	1.17	0.011	0.035
	3	1.05	81.92	8.03	7.61	1.39	1.16	0.011	0.035
Bromination 150°C	1	1.05	80.09	7.99	6.94	3.92	1.19	0.011	0.033
	2	1.10	81.33	7.98	7.10	2.50	1.17	0.012	0.033
Bromination 160°C	1	1.08	80.54	7.95	7.39	3.03	1.17	0.012	0.034
	2	1.05	81.00	7.97	7.35	2.62	1.17	0.011	0.034
Bromination 170°C	1	1.07	80.40	7.87	7.16	3.50	1.16	0.011	0.033
	2	1.06	81.00	7.91	6.91	3.13	1.16	0.011	0.032

[a] Molar ratio

[b] Repeated from Table 5-1 for the ease of comparison

The hardening caused by debromination is suspected to have similar reaction chemistry as autoxidation and hence, refractive index measurements were to be performed to check if there are any evidence cross-linking reactions. However, all debrominated products were incompletely soluble in toluene and hence, refractive index measurements could not be performed. Then again, the products exhibiting insolubility in toluene itself reveal physical changes in the bulk material.

(5.3.3) Effect of Bromination-Debromination on the Melt Spinning Process

Debrominated asphaltenes from bromination with solvent was melt spun and the results showed improved melt spin productivity without a significant change to the melt spin temperature. In the previous analyses, debromination with watch glass was seen to facilitate autoxidation to decrease H/C ratio and increase insolubility in toluene. Although these indicate hardening of the material, the melt spin temperature of this product rather decreased slightly compared to the industrial

asphaltenes. This can be due to some brominated toluene that is still present in the bulk material. For example, Sanchez and de Klerk[4] observed almost 30% decrease in bitumen viscosity with an addition of 1 wt.% of solvent such as butylbenzene or *n*-decane. Small amount of brominated toluene present in the bulk material can easily reduce the viscosity and hence, the melt spin temperature.

On the other hand, debrominated asphaltenes from bromination without solvent was melt spun and there was a slight improvement in the maximum melt spin productivity as it increased from 200 rpm (126 m/min) to 300 rpm (189 m/min). Despite the decrease in penetration depth after bromination-debromination compared to the industrial asphaltenes feed, the melt spin temperature of the debrominated asphaltenes was the same.

Table 5-8: Maximum Melt Spinning Productivity for Debrominated Products

Asphaltenes feed material	**Melt Spin Temperature (°C)**	**Maximum Melt Spinning Productivity**
Industrial asphaltenes	195	200 rpm (126 m/min)
Debrominated Watch Glass, 4 hours (w/ solvent)	193	800 rpm (504 m/min)
Debrominated, 4 hours (w/o solvent)	195	300 rpm (189 m/min)

[a] Not measured

(5.4) Discussion

(5.4.1) What is Happening During Debromination in an Open and Closed System?

Debromination in an open system under air and closed system under nitrogen were investigated. Facilitation of debromination by heating at 200°C in presence of air seems to have facilitated autoxidation reactions. There was a pronounced decrease in the H/C atomic ratios for debromination with a watch glass in an open system (Table 5-4), where no significant changes in the H/C ratio was observed (Table 5-7) for debromination in a closed system under nitrogen.

According to the proposed reaction chemistry of bromination-debromination reactions as was shown in Section 2.7, significant bulk composition changes are not expected with the low amounts of bromine used. The major chemical composition change expected from bromination-debromination reactions occur in Reaction (2.7.3), as Br is eliminated as HBr with debromination. Hence, the major expected composition change is decreased H content.

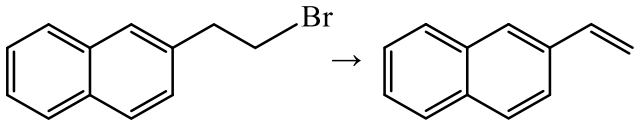

(2.7.3)

Then, assuming 100% of the added Br_2 reacts with asphaltenes and 100% of incorporated Br is eliminated as HBr during debromination, H eliminated from asphaltenes is 1.2×10^{-3} g and the calculations are shown in Appendix A. Then, with 1.2×10^{-3} g of H eliminated from the raw asphaltenes through debromination, the new H/C ratio from this change is 1.17, which is the same as H/C ratio for the raw asphaltenes. From the debromination alone, small changes to H/C ratio is expected when using 1.2 wt.% Br_2. As such, no significant changes in H/C were observed as shown in Table 5-7 for debromination in a closed system under nitrogen.

This strongly suggests that the observed H/C in the debrominated products from heating in air environment is primarily due to autoxidation reaction with air. This is further strengthened by the slight increase in N/C for debromination with watch glass, as it increased from 0.011 up to 0.013, and products from the control experiment in an open atmosphere increased up to 0.015 as previously shown in Table 5-4. As increase in nitrogen content in asphaltenes in these conditions

are unlikely, the observed increase in N/C is most likely due to the decrease in carbon content. This can allude to evolution of volatiles, such as CO and CO_2, which are products from autoxidation.

On the other hand, effect of debromination was evident from the physical changes for the products from debromination in a closed system under nitrogen. The decrease in penetrometer depth and insolubility in toluene reveal physical changes that can be due to addition reactions facilitated by bromination-debromination reactions. Through addition reactions, bulkier molecules are formed, which can increase the softening point and reduce solubility in toluene.

(5.4.2) Predicted Improvement in Carbon Fiber Quality by Bromination-Debromination of Industrial Asphaltenes

Since toluene, which was utilized as the solvent during bromination, was seen to react with bromine during the bromination conditions, commercialization considerations and predicted improvement in carbon fiber quality for bromination-debromination without the use of solvent will be discussed in this section.

Some of the major considerations for using bromination-debromination as a pretreatment method in a commercialized process include use of halogens. To make the scale-up more practical, use and recovery of hydrogen halides are considered for bromination and debromination of asphaltenes. However, hydrogen halides are acidic gases and scale-up involving hydrogen halides require proper safeguards in place due to their negative impact on the environment and health. Furthermore, use of more specialized materials of construction need to be considered as common construction materials such as carbon steel, alloy steel, stainless steel, and aluminum, copper and nickel alloys are not recommended to use with hydrogen halides[5].

To more properly assess the viability of utilizing bromination-debromination as a commercialized pretreatment process, more detailed analysis must be completed to quantify the benefits obtained from the halogenation-dehalogenation pretreatment. From the chemical composition analysis, bromination-debromination seem to have facilitated addition reactions without significant loss of materials. Previously, Kim *et al.*[3] reported bromination and

subsequent dehydrobromination of naphtha-cracked oil produced cross-linked long linear compounds, and this pretreatment was beneficial in producing more homogeneous and better mechanical performance carbon fibers. Therefore, bromination-debromination of industrial asphaltenes is expected to be beneficial in terms of final carbon fiber performance. Hence, there may be some improved mechanical properties of the produced carbon fibers, and further experiments should be performed to verify these predictions. On the other hand, the softening point temperature did not seem to increase significantly and hence, little or no benefits from shortening of the stabilization time is expected. With the further analysis on the mechanical properties, stronger conclusions about using bromination and debromination as a pretreatment method can be made. Using the present data only, there is insufficient benefit compared to autoxidation (Chapter 4) to indicate that bromination is a competitive alternative.

(5.5) Conclusions

Using bromination-debromination as a pretreatment method for carbon fiber production was evaluated. From this study, the following conclusions were obtained:

a) Bromination – debromination as a pretreatment method resulted in asphaltenes hardening without significant loss of carbon content
b) Toluene and bromine react under bromination conditions and hence, use of toluene for asphaltenes bromination is not recommended
c) Debromination at 200°C in the presence of air can facilitate autoxidation reactions. Due to high surface area open to the atmosphere, considerable autoxidation can be induced to significantly decrease the H/C atomic ratio

(5.6) References

(1) Otani, S. On the Carbon Fiber from the Molten Pyrolysis Products. *Carbon* **1965**. *3*, 35-38.

(2) Liu, J.; Shimanoe, H.; Nakabayashi, K.; Miyawaki, J.; Ko, S.; Jeon, Y. P.; Yoon, S. H. Preparation of Isotropic Pitch Precursor for Pitch-Based Carbon Fiber through the Co-Carbonization of Ethylene Bottom Oil and Polyvinyl Chloride. *J. Ind. Eng. Chem*. **2018**. *67*, 276-283.

(3) Kim, B. J.; Eom, Y.; Kato, O.; Miyawaki, J.; Kim, B. C.; Mochida, I.; Yoon, S. H. Preparation of Carbon Fibers with Excellent Mechanical Properties from Isotropic Pitches. *Carbon* **2014**. *77*, 745-755.

(4) Sanchez, N.; de Klerk, A. Viscosity Mixing Rules for Bitumen at 1-10 wt.% Solvent Dilution When Only Viscosity and Density Are Known. *Energy Fuels* **2020**, *34*, 8227–8238.

(5) Ulrich, G.; Vasudevan, P. *Chemical Engineering: Process Design and Economics A Practical Guide*, 2nd ed.; Process Publishing, 2004; pp 98.

CHAPTER 6:
CONCLUSIONS AND RECOMMENDATIONS

(6.1) Introduction

The objective of this study was to investigate pretreatment methods for industrially precipitated asphaltenes from Canadian oilsands bitumen to increase its viscosity and softening point temperature for melt spinning to produce carbon fibers. This was to render the as-spun fibers from asphaltenes, which has a softening point temperature <200°C, infusible during the subsequent oxidative stabilization step that occurs at temperatures 200 – 300°C, as well as to shorten the overall time required in the costly and time-consuming stabilization step.

To increase the softening point temperatures, three pretreatment methods were studied, and they were: (1) Solvent Deasphalting/ Solvent Extraction (physical pretreatment) (2) Autoxidation (conventional reactive pretreatment) (3) Halogenation/ Dehalogenation (newly suggested pretreatment).

(6.2) Major Conclusions

The following major conclusions could be drawn from the experimental investigation on the three asphaltenes pretreatment methods:

- All three pretreatment methods were successful in obtaining more viscous products, as noted by the decreased penetration depth.

- Removing the *n*-heptane soluble materials by rigorous solvent deasphalting at 40:1 solvent-to-feed ratio resulted in the most pronounced decrease in the penetration depth and increase in softening point of all pretreatment methods evaluated. However, it resulted in material with a low melt spinning productivity.

- Second best pretreatment performance, with a comparable decrease in penetration depth and increase in softening point were obtained by removing *n*-pentane soluble materials by

rigorous solvent deasphalting at 40:1 solvent-to-feed ratio, and by autoxidation for 24 hours at 220 and 250 °C.

- Removing the *n*-pentane soluble materials from the industrially precipitated asphaltenes from a C_5 deasphalting process improved the melt spinning productivity of the material. Melt spinning productivity could also be increased at some of the autoxidation and halogenation-dehalogenation conditions that were tested compared to the untreated raw asphaltenes.

- Autoxidation of industrially precipitated asphaltenes at 190 – 250°C with an air flow rate of 9 mL/g·min facilitated free radical addition reactions without significant oxygen incorporation. At these conditions, autoxidation for 8 hours did not result in a considerable change in the asphaltenes viscosity and only at autoxidation for 24 hours, more notable increase in the viscosity was noted, as seen by the increased melt-spin temperatures and decrease in penetration depth. The observations were consistent with a description of the conversion in terms of oxidation facilitating free radical addition.

- Halogenation-dehalogenation with 1 wt.% liquid bromine also seems to facilitate free radical addition reactions without significant effect on the product yield.

(6.3) Suggested Future Work

From the observations from this study, potential opportunities for future investigation were identified:

- Perform autoxidation and halogenation-dehalogenation pretreatments together. Through halogenation of asphaltenes followed by dehalogenation in an air environment, more free radical addition reactions are expected to be facilitated. Through presence of air, more free radical species should be produced in the bulk asphaltenes to react with the olefins formed by debromination reactions.

Furthermore, through performing the following work, better conclusion can be achieved to quantify the benefits of the pretreatment methods on the overall carbon fiber production process:

- Quantify shortening of the oxidative stabilization time to measure the benefits of increased softening point temperature for the each pretreated asphaltenes.

BIBLIOGRAPHY

Alberta Energy Regulator. Crude Bitumen Production https://www.aer.ca/providing-information/data-and-reports/statistical-reports/st98/crude-bitumen/production (accessed Dec 23, 2020).

Alcañiz-Monge, J.; Cazorla-Amorós, D.; Linares-Solano, A.; Oya, A.; Sakamoto, A.; Hosm, K., Preparation of general purpose carbon fibers from coal tar pitches with low softening point. *Carbon* **1997**, *35 (8),* 1079-1087.

Ancheyta, J.; Centeno, G.; Trejo, F.; Marroquín, G.; García, J. A.; Tenorio, E.; Torres, A. Extraction and Characterization of Asphaltenes from Different Crude Oils and Solvents. *Energy Fuels* **2002**, 16 (5), 1121–1127.

ASTM D2007-19: Standard Test Method for Characteristic Groups in Rubber Extender 29 and Processing Oils and Other Petroleum-Derived Oils by the Clay-Gel Absorption Chromatographic Method. ASTM International. 2019, pp 1–9

Babu, D. R.; Cormack, D. E. Effect of Low-Temperature Oxidation on the Composition of Athabasca Bitumen. *Fuel* **1984**, *64*, 858-861.

Babu, D. R.; Cormack, D. E. Effect of Oxidation on the Viscosity of Athabasca Bitumen. *Can. J. Chem. Eng.* **1983**. *61*, 575-580.

Bahl, O. P.; Shen, Z.; Lavin, J. G.; Ross, R. A., *Carbon Fibers* Third Edition, Revised and Expanded. Marcel Dekker: New York, 1998.

Barr, J. B.; Lewis, I. C., Chemical changes during the mild air oxidation of pitch. *Carbon* **1978**, *16 (6),* 439-444.

Barton, A. F. M., *CRC Handbook of Solubility Parameters and Other Cohesion Parameters*. Routledge as part of the Taylor and Francis group: New York, 2017.

Berrueco, C.; Álvarez, P.; Díez, N.; Granda, M.; Menéndez, R.; Blanco, C.; Santamaria, R.; Millan, M., Characterisation and feasibility as carbon fibre precursors of isotropic pitches derived from anthracene oil. *Fuel* **2012**, *101*, 9-15.

Bhat, G., *Structure and Properties of High-Performance Fibers*. Matthew Deans: Duxford, UK, Cambridge, MA, Kidlington, UK, 2017; Vol. 187, p 438.

Blanco, C.; Santamaría, R.; Bermejo, J.; Menéndez, R., A comparative study of air-blown and thermally treated coal-tar pitches. *Carbon* **2000**, *38 (4),* 517-523.

Buckley, J. D.; Edie, D. D., *Carbon-Carbon Materials and Composites*. William Andrew: 1993; p 294.

Burnsell, A. R., *Fibre Reinforcements for Composite Materials*. Elsevier Science Publishers: Amsterdam, Nethernalnds, 1988; Vol. 2.

Chawla, K., *Fibrous Materials*. 2nd ed.; Cambridge University Press: Cambridge, 2016.

Chmielewski, A. G.; Haji-Saeid, M.; Ahmed, S., Progress in radiation processing of polymers. *Nucl. Instrum. Methods Phys. Res., Sect. B* **2005,** *236*, 44-54.

Choi, D.; Kil, H.-S.; Lee, S., Fabrication of low-cost carbon fibers using economical precursors and advanced processing technologies. *Carbon* **2019**, *142*, 610-649.

Chung, D. D. L., *Carbon Fiber Composites*. Butterworth-Heinemann: Newton, MA, 1994; p 215.

Clough, R. L., High-energy radiation and polymers: A review of commercial processes and emerging applications. *Nucl. Instrum. Methods Phys. Res., Sect. B* **2001**, *185*, 8.
de Haan, A. 8.5.4 Bubble Columns. In *Process Technology - An Introduction*; De Gruyter: Berlin/Boston, 2015; pp.174.

de Klerk, A. *Fischer-Tropsch Refining*; 1st ed. Wiley VCH: Weinheim, 2011.

Derbyshire, F.; Andrews, R.; Jacques, D.; Jagtoyen, M.; Kimber, G.; Rantell, T., Synthesis of isotropic carbon fibers and activated carbon fibers from pitch precursors. *Fuel* **2001**, *80 (3),* 345-356.

Dhami, T. L.; Manocha, L. M.; Bahl, O. P., Oxidation behaviour of pitch based carbon fibers. *Carbon* **1991**, *29 (1),* 51-60.

Dietrich, J.; Hirt, P.; Herlinger, H., Electron-beam-induced cyclisation to obtain C-fibre precursors from polyacrylonitrile homopolymers. *Eur. Polym. J.* **1996**, *32 (5)*, 617-623.

Dumanlı, A. G.; Windle, A. H., Carbon fibres from cellulosic precursors: a review. *J. Mater. Sci.* **2012**, *47 (10)*, 4236-4250.

Emanuel, Nikolai; Denisov, Evgenii; Maizus, Z. *Liquid-Phase Oxidation of Hydrocarbons*; Plenum Press: New York, 1967; pp 37-39.

Fernández, J. J.; Figueiras, A.; Granda, M.; Bermejo, J.; Menéndez, R., Modification of coal-tar pitch by air-blowing — I. Variation of pitch composition and properties. *Carbon* **1995**, *33 (3),* 295-307.

Fernández, J. J.; Figueiras, A.; Granda, M.; Bermejo, J.; Parra, J. B.; Menéndez, R., Modification of coal-tar pitch by air-blowing II. Influence on coke structure and properties. *Carbon* **1995**, *33 (9),* 1235-1245.

Frank, E.; Hermanutz, F.; Buchmeiser, M. R., Carbon Fibers: Precursors, Manufacturing, and Properties. *Macromol. Mater. Eng.* **2012**, *297 (6),* 493-501.

Freeman, D. H.; Swahn, I. D.; Hambright, P. Spectrophotometry and Solubility Properties of Nickel and Vanadyl Porphyrin Complexes. *Energy Fuels* **1990**, 4 (6), 699–704.

García Zapata, J. L.; De Klerk, A. Viscosity Changes during Mild Oxidation of Oilsands-Derived Bitumen: Solvent Effects and Selectivity. *Energy Fuels* **2014**. *28*, 6242-6248.

Gray, M. R., *Upgrading Oilsands Bitumen and Heavy Oil*. University of Alberta Press: 2015.

Gupta, A. K.; Paliwal, D. K.; Bajaj, P., Acrylic Precursors for Carbon Fibers. *JMS, Polym. Rev.*, Part C **1991**, *31 (1)*, 1-89.

Hansen, C., *Hansen Solubility Parameters: A User's Handbook*, 2nd Ed. CRC Press: Boca Raton, 2012; p 546.

Harding, K. *Bitumen Beyond Combustion- Phase 2 Report*; Stantec: 2018; p 112.

Harland, W.; King, M.; Phillips, L. Improvements in or Relating to Fibrous Materials. 1,431,883, 1976.

Huang, X., Fabrication and Properties of Carbon Fibers. *Materials* **2009***, 2 (4),* 2369-2403.

Huson, M. G., *High-performance pitch-based carbon fibers*. 2017; pp 31-78.

Hutchenson, K. W.; Roebers, J. R.; Thies, M. C., Fractionation of petroleum pitch by supercritical fluid extraction. *Carbon* **1991**, *29 (2),* 215-223.

Javadli, R.; de Klerk, A. Desulfurization of Heavy Oil - Oxidative Desulfurization (ODS) as Potential Upgrading Pathway for Oil Sands Derived Bitumen. *Energy Fuels* **2012**, *26*, 594–602.

Kett, I. *Asphalt Materials and Mix Design Manual*; Noyes Publications: New Jersey, 1998; pp 8.

Kim, B. J.; Eom, Y.; Kato, O.; Miyawaki, J.; Kim, B. C.; Mochida, I.; Yoon, S. H. Preparation of Carbon Fibers with Excellent Mechanical Properties from Isotropic Pitches. *Carbon* **2014**. *77*, 745-755.

Kim, B.-J.; Kotegawa, T.; Eom, Y.; An, J.; Hong, I.-P.; Kato, O.; Nakabayashi, K.; Miyawaki, J.; Kim, B. C.; Mochida, I.; Yoon, S.-H., Enhancing the tensile strength of isotropic pitch-based carbon fibers by improving the stabilization and carbonization properties of precursor pitch. *Carbon* **2016**, *99*, 649-657.

Lee, J. M.; Shin, S.; Ahn, S.; Chun, J. H.; lee, K. B.; Mun, S.; Jeon, S. G.; Na, J. G.; Nho, N. S., Separation of solvent and deasphalted oil for solvent deasphalting process. *Fuel Processing Technology* **2014**, *119*, 7.

Lewis, I. C., Thermal polymerization of aromatic hydrocarbons. *Carbon* **1980**, *18 (3),* 191-196.

Li, X.; Ashida, R.; Miura, K. Preparation of High-Grade Carbonaceous Materials Having Similar Chemical and Physical Properties from Various Low-Rank Coals by Degradative Solvent Extraction. *Energy Fuels* **2012**, *26(11)*, 6897-6904.

Li, X.; Zhu, X. Q.; Okuda, K.; Zhang, Z.; Ashida, R.; Yao, H.; Miura, K. Preparation of Carbon Fibers from Low-Molecular-Weight Compounds Obtained from Low-Rank Coal and Biomass by Solvent Extraction. *New Carbon Mater.* **2017**, *32(1)*, 41-47.

Li, X.; Zhu, X. Q.; Xiao, L.; Ryuichi, A.; Kouichi, M.; Luo, G. Q.; Yao, H. Degradative Solvent Extraction of Demineralized and Ion-Exchanged Low-Rank Coals. *J. Fuel Chem. Technol. (Beijing, China).* **2014**, *42(8)*, 897-904.

Liu, J.; Shimanoe, H.; Nakabayashi, K.; Miyawaki, J.; Ko, S.; Jeon, Y. P.; Yoon, S. H. Preparation of Isotropic Pitch Precursor for Pitch-Based Carbon Fiber through the Co-Carbonization of Ethylene Bottom Oil and Polyvinyl Chloride. *J. Ind. Eng. Chem.* **2018**. *67*, 276-283.

Long, R., Concept of Asphaltenes. In *Chemistry of Asphaltenes*; Division of Petroleum Chemistry. Bunger, J., Li, N., Eds.; American Chemical Society, 1982.

Luo, P.; Wang, X.; Gu, Y., Characterization of Asphaltenes Precipitated with Three Light Alkanes under Different Experimental Conditions. *Fluid Phase Equilib* **2010**, 291 (2), 103–110.

Maeda, T.; Ming Zeng, S.; Tokumitsu, K.; mondori, J.; Mochida, I., Preparation of isotropic pitch precursors for general purpose carbon fibers (GPCF) by air blowing—I. Preparation of spinnable isotropic pitch precursor from coal tar by air blowing. *Carbon* **1993**, *31 (3)*, 407-412.

Maghe, M.; Creighton, C.; Henderson, L. C.; Huson, M. G.; Nunna, S.; Atkiss, S.; Byrne, N.; Fox, B. L., Using ionic liquids to reduce energy consumption for carbon fibre production. *J. Mater. Chem. A* **2016**, *4 (42),* 16619-16626.

Mallick, R. B.; El-Korchi, T. *Pavement Engineering: Principles and Practice*; 3rd Edition; CRC Press: Boca Raton, Florida, 2013; pp 228.

Mannistu, K. D.; Yarranton, H. W.; Masliyah, J. H., Solubility Modeling of Asphaltenes in Organic Solvents. *Energy Fuels* **1997**, *11 (3),* 615-622.

Matsumoto, T.; Mochida, I., A structural study on oxidative stabilization of mesophase pitch fibers derived from coaltar. *Carbon* **1992**, *30 (7),* 1041-1046.

McHugh, M.; Krukonis, V., *Supercritical Fluid Extraction*, 2nd Ed. Elsevier: Butterworth-Heinemann, 2013; p 608.

Meisen, A. *Bitumen Beyond Combusion (BBC) Project Phase 1 Report*; Alberta Innovates: 2017; p 112.

Mittal, J.; Mathur, R. B.; Bahl, O. P., Post spinning modification of PAN fibres — a review. *Carbon* **1997**, *35 (12),* 1713-1721.

Molnár, Á.; Olah, G. A.; Prakash, G. K. S. *Hydrocarbon Chemistry, Two Volume Set*, 3rd Ed.; Hoboken, New Jersey, 2017; pp 593 – 691.

Morgan, P., *Carbon Fibers and Their Composites*. 1st ed.; CRC Press: Boca Raton, 2005.

Mortensen, A., *Concise Encyclopedia of Composite Materials*. 2nd ed.; Elsevier: Oxford, UK, 2007.

Moschopedis, S. E.; Speight, J. G. The Halogenation of Athabasca Asphaltenes with Elemental Halogen. *Fuel* **1971**. *50 (1)*, 58-64

Murzin, D. Chapter 8: Halogenation. In *Chemical Reaction Technology*, 1st Ed.; De Gruyter: Finland, 2015; pp 197-203.

Niizuma, S.; Steele, C. T.; Gunning, H. E.; Strausz, O. P. Electron Spin Resonance Study of Free Radicals in Athabasca Asphaltene. *Fuel* **1977**. *56(3)*, 249-256.

Otani, S. On the Carbon Fiber from the Molten Pyrolysis Products. *Carbon* **1965**. *3*, 35-38.

Park, S.; Yoo, S. H.; Kang, H. R.; Jo, S. M.; Joh, H.-I.; Lee, S. Comprehensive stabilization mechanism of electron-beam irradiated polyacrylonitrile fibers to shorten the conventional thermal treatment *Scientific reports* [Online], 2016, p. 27330. PubMed. https://doi.org/10.1038/srep27330

Park, S.-J., *Carbon Fibers*. Springer Nature Pte Ltd. : Incheon, Korea (Republic of), 2018; Vol. 210, p 366.

Prado, G. H. C.; De Klerk, A. Halogenation of Oilsands Bitumen, Maltenes, and Asphaltenes. *Energy Fuels* **2014**. *28 (7)*, 4458-4468.

Prado, G. H. C.; De Klerk, A. Origin of Penetration Hardness Due to Mild Halogenation: A Model Compound Study. *Energy and Fuels* **2015**. *29(11)*, 6935–6947.

Qiao, W. M.; Yoon, S. H.; Korai, Y.; Mochida, I.; Inoue, S.; Sakurai, T.; Shimohara, T. Preparation of Activated Carbon Fibers from Polyvinyl Chloride. *Carbon* **2004**. *42*, 1327-1331.

Ramírez-Corredores, M. M., *The science and technology of unconventional oils: finding refining opportunities*. Academic Press: London, 2017.

Riazi, M. 2.1.4 Refractive Index. In *Characterization and Properties of Petroleum Fractions*; Riazi, M., Ed.; ASTM International: West Conshohocken, Pennsylvania, 2005; pp 32.

Sanchez, N.; de Klerk, A. Low-Temperature Oxidative Asphaltenes Liquefaction for Petrochemicals: Fact or Fiction? *Appl. Petrochemical Res*. **2016**, *6*, 97–106.

Sanchez, N.; de Klerk, A. Viscosity Mixing Rules for Bitumen at 1-10 wt.% Solvent Dilution When Only Viscosity and Density Are Known. *Energy Fuels* **2020**, *34*, 8227–8238.

Saruyama, H.; Yamazaki, K. Production of Precursor Yarn for Producing Carbon Yarn. 63135510, 1988.

Sawran, W.; Turrill, F.; Newman, J.; Hall, N.; Ward, C. Process for the Manufacture of Carbon Fibers and Feedstock Therefor. 4,671,864, 1987.

Senda, T.; Yamada, Y.; Morimoto, M.; Nono, N.; Sogabe, T.; Kubo, S.; Sato, S., Analyses of oxidation process for isotropic pitch-based carbon fibers using model compounds. *Carbon* **2019**, *142*, 311-326.

Siddiquee, M. N.; De Klerk, A. Heterocyclic Addition Reactions during Low Temperature Autoxidation. *Energy Fuels* **2015**. *29(7)*, 4236-4244.

Siddiquee, M. N.; De Klerk, A. Hydrocarbon Addition Reactions during Low-Temperature Autoxidation of Oilsands Bitumen. *Energy and Fuels* **2014**. 28 (11), 6848-6859.

Speight, J. G. Chemical and Physical Studies of Petroleum Asphaltenes. *Dev. Pet. Sci.* **1994**, 40 (PA), 7–65.

Speight, J. G., *Fouling in refineries*. 2015; p 1-538.

Speight, J. G.; Long, R. B.; Trowbridge, T. D. Factors Influencing the Separation of Asphaltenes from Heavy Petroleum Feedstocks. *Fuel* **1984**, *63(5)*, 616-620.

Speight, J., Petroleum Asphaltenes - Part 1: Asphaltenes, Resins and the Structure of Petroleum. *Oil & Gas Science and Technology-revue De L Institut Francais Du Petrole - OIL GAS SCI TECHNOL* **2004**, *59*, 467-477.

Strausz, O.; Lown, E. M.*, The chemistry of Alberta oil sands, bitumens and heavy oil.* Alberta Energy Research Inst., Calgary, AB (Canada): Canada, 2003.

Turuga, A. S. S. Effect of Solvent Deasphalting Process on the Properties of Deasphalted Oil and Asphaltenes From Bitumen. M.S. Thesis, University of Alberta, 2017.

Ulrich, G.; Vasudevan, P. *Chemical Engineering: Process Design and Economics A Practical Guide*, 2nd ed.; Process Publishing, 2004; pp 98, 576.

Yamazaki, K.; Yamane, S.; Fukuhara, M. Production of Acrylic Precursor Fiber Bundle. 6183373, 1986.

Yañez Jaramillo, L. M. Visbreaking of Oilsands Bitumen Between 150 and 300C. M.S. Thesis, University of Alberta, 2016.

Yang, J.; Nakabayashi, K.; Miyawaki, J.; Yoon, S.-H., Preparation of pitch based carbon fibers using Hyper-coal as a raw material. *Carbon* **2016**, *106*, 28-36.

Yoo, S. H.; Park, S.; Park, Y.; Lee, D.; Joh, H.-I.; Shin, I.; Lee, S., Facile method to fabricate carbon fibers from textile-grade polyacrylonitrile fibers based on electron-beam irradiation and its effect on the subsequent thermal stabilization process. *Carbon* **2017**, *118*, 106-113.

Yuan, G.; Li, X.; Xiong, X.; Dong, Z.; Westwood, A.; Li, B.; Ye, C.; Ma, G.; Cui, Z.; Cong, Y.; Zhang, J.; Li, Y., A comprehensive study on the oxidative stabilization of mesophase pitch-based tape-shaped thick fibers with oxygen. *Carbon* **2017**, *115*, 59-76.

Yusof, N.; Ismail, A. F., Post spinning and pyrolysis processes of polyacrylonitrile (PAN)-based carbon fiber and activated carbon fiber: A review. *J. Anal. Appl. Pyrolysis* **2012**, *93*, 1-13.

Zeng, S. M.; Maeda, T.; Tokumitsu, K.; Mondori, J.; Mochida, I., Preparation of isotropic pitch precursors for general purpose carbon fibers (GPCF) by air blowing—II. Air blowing of coal tar, hydrogenated coal tar, and petroleum pitches. *Carbon* **1993**, *31 (3),* 413-419.

Zeng, S. M.; Maeda, T.; Mondori, J.; Tokumitsu, K.; Mochida, I., Preparation of isotropic pitch precursors for general purpose carbon fibers (GPCF) by air blowing—III. Air blowing of isotropic naphthalene and hydrogenated coal tar pitches with addition of 1,8-dinitronaphthalene. *Carbon* **1993**, *31 (3),* 421-426.

APPENDIX A: RELEVANT CALCULATIONS

This appendix presents the calculations for the expected H/C atomic ratio for bromination and debromination of industrially precipitated asphaltenes using 1.2 wt.% bromine as discussed in Section 5.4.1. According to the bromination-debromination reactions as was shown in Section 2.7, the most significant composition change occurs in Reaction (2.7.3), as Br is eliminated from the bulk material as HBr. Using this reaction, the calculation of the expected H.C atomic ratio with H eliminated as HBr was conducted.

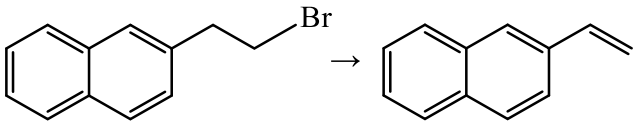

(2.7.3)

For this calculation, the following assumptions were made:

- 100% of the added Br_2 reacts with asphaltenes
- 100% of incorporated Br is eliminated as HBr during debromination

Then, since for every 1 mole of Br_2 that is added to this system, 2 H is eliminated to form 2 HBr as illustrated below,

$$Br_2 + 2\ H\ (\text{from asphaltenes}) \rightarrow 2HBr$$

The amount of H eliminated can be calculated using these relationships:

$$m\ [g] = n\ [mol] \cdot M\ [g/mol]$$

$$m_{H\ eliminated} = \frac{m_{Br_2}}{M_{Br_2}} \times \frac{2mol_H}{1mol_{Br_2}} \times M_{H\ eliminated}$$

For the studied bromination-debromination reactions, 8.0 g of industrial asphaltene and 1.2 wt.% liquid bromine, which is 0.096 g, was used. Then, amount of H eliminated with bromine during debromination can be calculated as follows:

$$m_{H\ eliminated} = \frac{0.096\ g}{159.81 g/mol_{Br_2}} \times \frac{2mol_H}{1mol_{Br_2}} \times 1.01 \frac{g}{mol_H} = 0.0012\ g$$

Then, the H/C atomic ratio of the debrominated asphaltene with 0.0012 g of H removed from the bulk composition can be calculated as:

$$\frac{H}{C} = \frac{n_H}{n_C} = \frac{m_H}{M_H} \times \frac{M_C}{m_C}$$

Mass of H and C in the 8.0 g of debrominated asphaltene can be estimated using the average C and H wt.% data of industrially precipitated asphaltene as was shown in Table 3-1.

$$\frac{H}{C} = \frac{\left(8.0\ g_{Asphaltene}\right) \times (8.07\ wt.\%_H) - (0.0012\ g_H)}{1.01 \frac{g}{mol}} \times \frac{12.01 \frac{g}{mol}}{\left(8.0\ g_{Asphaltene}\right) \times (82.10\ wt.\%_C)}$$

$$\frac{H}{C} = 1.17$$

Hence, bromination-debromination of industrial asphaltene with 1.2 wt.% Br_2 will lead to the total of 0.0012 g of H eliminated in the form of HBr, leading to the H/C atomic ratio to be 1.17.

APPENDIX B: MECHANICAL STRENGTH RESULTS

The precursor fibers prepared from materials obtained by different pretreatment procedures were subjected to oxidative stabilization and carbonization. Oxidative stabilization process was completed by immersing the precursor fibers into 20 vol.% HNO_3 acid solution for 10 minutes, then heating in the air environment in a tubular furnace. The acid-treated fibers were heated to 300°C with a heating rate of 0.5 °C/min then was heated at 300 °C for 1 hour under an air flow of 400 mL/min supplied by Praxair. Following, carbonization was completed by heating the stabilized fibers via tubular furnace under nitrogen flow. The stabilized fibers were heated to 1500°C with a heating rate of 3°C/min then was heated at 1500°C for 2 hours under the nitrogen flow of 400 mL/min.

The mechanical properties of the carbonized carbon fibers were measured. The tensile strength values are shown in relation to fiber diameter and in the same way the Young's modulus values are shown in relation to fiber diameter, as illustrated in Figures B-1 and B-2.

Due to the difficulty in spinning and its broad diameter distribution, strength tests were not completed for fibers from C7 (40:1) insoluble material.

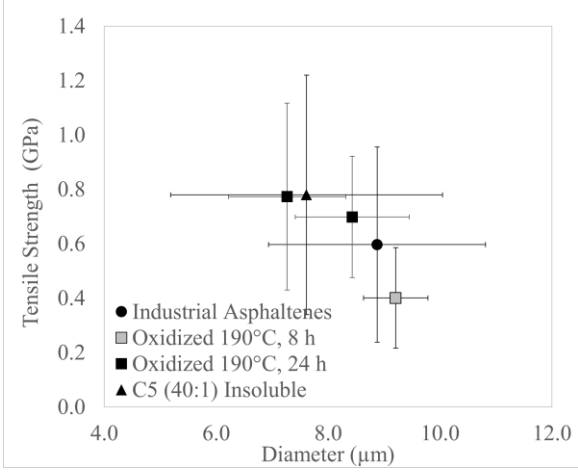

Figure B-1: Tensile strength for carbonized fibers from pretreated asphaltenes precursor. Error bars indicate one sample standard deviation from ten measurements.

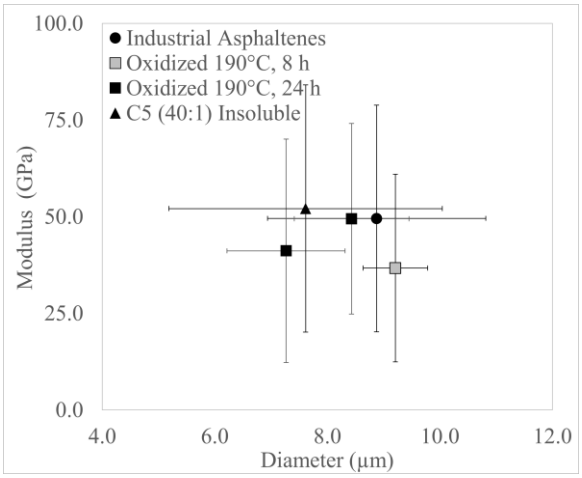

Figure B-2: Modulus for carbonized fibers from pretreated asphaltenes precursor. Error bars indicate one sample standard deviation from ten measurements.

The data obtained from the other pretreatment methods and the industrial asphaltenes feed that was not pretreated, indicated diameter had a more significant effect on the tensile strength than the method of pretreatment. On the other hand, there was no clear trend observed for the modulus of the fibers in relation to either the pretreatment method, or the diameter.